Response to Reviewers' Comments to Manuscript acp-2019-964 "Observations of speciated isoprene nitrates in Beijing: implications for isoprene chemistry" by Reeves et al.

Reviewers' comments are in black upright font.

Our response is in blue italic font.

Referee #1

This data set is likely interesting.

We believe the data are very interesting and our view is supported by reviewer #3 who says "This makes this a highly unique and useful data set for chemically coupled species, and does indeed represent a great opportunity for testing the mechanism for isoprene photooxidation, and studying the impact of isoprene chemistry on the fate of NOx, and for production of ozone and particulate matter.".

However, this paper is long, data rich and is not succinct in its analysis. It is very hard to tell which conclusions are unambiguously supported by the observations and which depend on assumptions about transmission and sensitivity.

On reflection, we agree that the paper is too long and not succinct in analysis and more clarity is required regarding which conclusions are unambiguously supported by the observations.

We have created a much-shortened revised version, in part by removing the simple model analysis completely and section 6.6. We have added uncertainties, and we have rewritten the abstract and conclusions to highlight the key findings.

It is not currently accessible to a general reader of ACP. I recommend it be rejected. Only the most determined reader will be able to wade through this and find the important information and three years from now, no one will be able to identify key ideas that should stand the test of time from ideas that are momentary arguments about different rates constants in a version of MCM and W2018. Today, no one not deeply steeped in the isoprene chemistry will be able to read it and recognize the ideas being tested.

There are many papers published on isoprene chemistry, demonstrating widespread interest in the subject. Many of these papers are themselves very detailed including several published in ACP. This paper identifies areas of uncertainty in mechanisms that can then be addressed through further research. Publishing these results are an important way to advance science.

In shortening the revised version, we have also aimed to make it more accessible to the general ACP reader.

It would greatly benefit from editing in collaboration with someone who is not as engaged in the details. I recommend it be rewritten with many fewer figures. The figures that remain should be chosen to demonstrate how the observations test competing ideas for the behavior of these nitrates.

In shortening the revised version, we have reduced the number of figures from 21 to 9. We have done this combining some figures, reducing the number of things plotted, removing some plots altogether and moving others to the Supplementary Information. We believe key scientific points are now more clearly illustrated.

In addition, the sections on MCM should be more clearly motivated–are there choices MCM has made that are in conflict with W2018. If so is there a logic to them or is MCM just not updated to be consistent with W2018 yet?

The MCM is a widely used chemical mechanism. There is a logic to the choices made, which for isoprene are primarily described in Jenkin et al (2015). Wennberg et al (2018) does consider some more recent findings, but both mechanisms are based on many assumptions, often with few constraining observations. We, therefore, believe it is important to test both against new observations.

Referee #3

The paper by Reeves et al. describes measurements of speciated organic nitrates that are produced from both OH and NO_3 reaction with isoprene. Using a GC/MS approach, they were able to identify and quantify seven different “isoprene nitrates”, specifically, two ïA¸c´-hydroxy nitrates, four ïA¸d’-carbonyl nitrates, and propanone nitrate, in Beijing during the winter of 2016 and summer of 2017. Isomers were generally (not always) identified by injections of samples of the individual synthesized isomers, and quantified with reasonable time resolution (it appears to be hourly, but that is not stated clearly in the manuscript; that should be clarified). What resulted was a highly unique data set for these compounds, in an isoprene-impacted urban environment, with very good supporting chemical measurements, including isoprene, NOx, HOx, RO_2, NO_3, HONO, and HCHO. Many of these measurements are highly challenging. This makes this a highly unique and useful data set for chemically coupled species, and does indeed represent a great opportunity for testing the mechanism for isoprene photooxidation, and studying the impact of isoprene chemistry on the fate of NOx, and for production of ozone and particulate matter. This paper then should be published, and will be high impact, I believe, ……

We appreciate the reviewer recognising the importance of this data set and its value in testing the isoprene photooxidation mechanisms and potential for high impact.

The measurements were made approximately hourly. We have clarified this in the revised manuscript.

…… once one major flaw in the paper is repaired. Specifically, while the data are compared to simulations using MCM chemistry, for both absolute concentrations and ratios of coupled species, these comparisons are extremely difficult to interpret because there is no uncertainty analysis done for these seven compounds. And that lack of detailed uncertainty analysis is a problem in this case because of all the assumptions made, e.g. that sensitivities are the same for the 4,3-IN and the 1,2-IN, and because of issues related to losses of the compounds, e.g. on valves and other surfaces, that clearly have an impact, and these impacts can be different for different isomers, as the authors recognize. So, while they discuss that looking at ratios of isomer concentrations can remove the complexities of boundary layer dynamics, dilution, and ventilation, there is no discussion of the uncertainties of the ratios presented in the various analysis, discussed at length for figures 5, 6, 10, 13, 14, and 15. So, it is possible that the analyses of the these ratios and comparisons to the models are meaningful, but also possible that they contain systematic errors that make the comparison problematic. With no error bars on any of the data, it is impossible to know if the discussions and conclusions are meaningful. Given the likely very large (impressive!) effort in acquiring these data, this is an unfortunate oversight, and needs to be repaired before this paper is published. I recommend a section that does a detailed error analysis for measurements of each isomer, and presents a calculated uncertainty (which could be concentration-dependent) for each one, and also calculates the uncertainty for the ratios that are compared to MCM. The figures could include representative error bars, either on some points, or use shading to reflect the uncertainties, or some other approach. With this added information, this can be a great paper. I note that the last sentence in the paper says “Our interpretation is limited by the uncertainties in our measurements and relatively small data set, but highlights areas of the isoprene chemistry that warrant further study, in particular the NO_3 initiated isoprene degradation chemistry.” This is good to recognize, but the reader has no idea what are the uncertainties in the measurements.

We accept these criticisms.

In the revised manuscript we have included a detailed uncertainty analysis (section 3.3), providing uncertainties for both concentrations and ratios, and included errors bars in the figures. We have modified the discussions and conclusions of the comparison with the model to reflect these uncertainties.

Other comments and relatively minor issues are listed below, in the order they arose in the paper. Comments/issues, in order

Abstract – line 32 could say isoprene-derived organic nitrates (the first time)?

Added

Line 43 – The observed relationship. . .

Corrected.

Line 53 – should say “from” the observed.

Corrected.

Line 92 – This key issue should be explained mechanistically, e.g. showing an example of an alkoxy radical that can decompose, releasing NO_2.

The Wennberg et al (2018) paper is cited and more information is given already in the Supplementary Information (section S1.3), so in the interest in shortening the paper, we decided not to add further explanation here.

Line 167 – sentence needs a period.

Corrected.

Section 3.2 – what do you know about the desorption efficiency from the Tenax trap? Since INs are olefinic, and there is lots of O_3, what do you know about ozonolysis during sampling?

The reviewer is correct to point out that olefinic compounds can be affected by trapping with oxidants, however in our instrument paper (Mills et al 2016, Atmos. Meas.Tech., 9, 4533-4545, doi: 10.5194/amt-9-4533-2016, 2016.) we have demonstrated that our trapping methods are unaffected by ozone or NO_2.

Is the metal valve the only surface on which INs can be (differentially) lost? How do (will) all these things affect your calculated analytical uncertainties? When you knew you had some loss on the valve, did you apply any correction for this? If not, do you have asymmetric error bars?

Regarding differential losses, the inlet and column are not substantially different from the analytical columns and conditions used by CalTech (e.g. Vasquez et al, Atmos. Meas. Tech., doi: 10.5194/amt-11-6815-2018, 2018) so any differential losses in these parts of our system are likely to be similar and very small, consistent with the Caltech group not reporting any such losses. Only the trap and metal valve are significantly different. The metal valve clearly had significant differential losses and we have stated in our experimental section that we have indeed applied corrections for these losses. We have included the uncertainties for these corrections in our uncertainty analysis.

It is possible that the glass sample trap may cause differential losses. For the IHNs we measured in Mills et al (2016), these are accounted for in the overall sensitivity from calibrations of single isomer samples, however we could not do this for the ICN. We used two different sample traps and fittings towards the end of the campaign (with the plastic valve in place), and did not notice any obvious changes in the nature of the data, but this was in a period when we were doing calibrations etc and so there was a period of many hours between the air samples on the two different traps. As far as desorption from the Tenax trap, that is also covered in the Mills et al (2016). Whilst we do not know the exact desorption efficiency or losses, they must be consistent and vary little as the instrument linearity and precision demonstrated in that paper are good and there is no observable carry-over to a subsequent blank.

Lines 204 – 208 – how do these assumptions impact your calculated uncertainties?

The assumptions the reviewer refers to here are regarding ion counts for IN that we were unable to directly calibrate for. We have included these in our measurement uncertainty analysis (section 3.3).

Line 278 – what exactly is the “large uncertainty”? Without these estimates, comparing to model results is an empty exercise.

We have now provided an uncertainty analysis and adjusted the text of this section accordingly.

Line 295 – should be “of” the summer campaign.

Corrected.

Line 322 – since you mention the “appreciable concentrations of OH at night”, and there is a lot of interest in that subject, can you include some representative error bars in Figure 7? The same goes for NO_3; I would like to repeat that there is some really lovely data in this paper, but it would help the reader to know things like LODs and uncertainties.

We have added information on the uncertainties of the supporting data in the Supplementary Information. Measurement uncertainties for OH have been added as error bars to Fig. S2 (old Fig. 3) and shaded areas representing ±1 s.d. in the variability of values for each hour of the day have been added to Fig. 4 (old Fig. 7).

Line 357 – the ratio E-1,4 to E-4,1 is not in Figure 6.

Yes, this was an error in the text. Corrected.

Line 365 – yes, but we don’t know what the uncertainties are!

Addressed in the revised manuscript with the addition of the uncertainty analysis.

Line 400 – I’ll just note that alpha is not known to even two significant figures.

Whilst we agree with the reviewers comment this value is taken from MCM which is given to 3 significant figures. However, we have removed the simple model analysis, so this has been deleted anyway.

Line 415 – Is it known that the -OH group has no impact? What is the uncertainty here?

We use the photolysis rates in the MCM. Without measurements of the photolysis rates of some of the larger VOCs, the MCM uses measured rates for some of the smaller VOCS to represent those of the larger VOCs following the protocols set out in Jenkin et al (1997) and Saunders et al (2003). Jenkin et al (2015) updated the degradation scheme for isoprene, and although the photolysis rates of the higher generation nitrates with carbonyl groups were revised on the basis of work by Muller et al (2014; 2015), no changes were made to the photolysis rates of the hydroxy nitrates. Whilst we accept that the -OH group may have some impact, we believe that the MCM represents the state-of-the-art in terms of scientific understanding and so it is appropriate to use these rates.

Line 417 – how does 4x10-5 s-1 compare to the magnitude of the calculated chemical reaction loss? (since you assume here that all the loss is uptake)

We have removed the simple model analysis and focussed the paper on the MCM model. This has therefore been removed.

Line 443 – Is the upwind environment chemically comparable on a timescale relevant to the lifetimes of these species? If not, there could be significant advective dilution.

We have removed the simple model analysis and focussed the paper on the MCM model. This has therefore been removed.

Line 460 and Figure 10. Consider that the difference between the simple model and the adjusted model is about 25%. Is the uncertainty in the measured ratio smaller than that? If not then this would not be a useful exercise.

We have removed the simple model analysis and focussed the paper on the MCM model. This has therefore been removed.

Line 472 – I am not sure that your analytical system materials are a good proxy for vegetation or urban materials like pavement. And, at night, is the dominant deposition resistance the aerodynamic resistance? If so, we would expect more or less identical deposition rates for these isomers.

Our analytical system materials may not be a good proxy for vegetation or urban materials, but the evidence that exists (i.e. difficulty of getting (1-OH, 2-ONO_2)-IHN through an analytical system and its fast rate of hydrolysis (W2018)) suggest that, if anything, (1-OH, 2-ONO_2)-IHN is more likely to have a faster deposition than that of (4-OH, 3-ONO_2)-IHN.

Line 504 – doesn't this imply that the glyoxal chemistry is very well known? Are there aromatic hydrocarbons present? Other glyoxal precursors? What is your confidence in the model production chemistry for glyoxal?

A range of aromatic species were measured (including benzene, toluene, ethyl benzene, xylenes and tri-methyl benzenes) and used to constrain the model as well as acetylene which is another important glyoxal precursor. As a further check on the physical loss rate imposed, however, the model was run unconstrained to HCHO using the same deposition rates and was found to reproduce the observed HCHO concentrations that were observed during the daytime, but under-predicted the concentrations at night.

Line 552 – delete "the" before "using".

Corrected.

Line 573 – is there a statistically meaningful diel pattern for the observed ratio? It doesn't look like it to me.

No, there is not. The text here is referring to the modelled rather than observed ratio.

We have clarified this in the text.

Line 638 – it would be good to recognize that in chemically reactive environments, NO_3 chemistry can be equally important in the daytime, if the NO_3 production rate is greater in the daytime.

We do not fully understand the point being made by the reviewer. Equally important to what? Night-time chemistry? OH chemistry? We do say "the production of δ-ICN in the model is mostly during the daytime, despite NO_3 usually being considered to be more important at night.". We think this is a clear message as to the importance of NO_3 chemistry during the daytime, based on looking at the modelled source of the δ-ICN.

Line 647 – please recognize that the dilution term depends on the concentration of the species in the diluent air.

Yes, this is an important point and we have added this to the discussion here.

Figure 19 – this makes it clear that given the broad diel cycle, a lot of propanone nitrat arises from transport, and so likely can't be simulated well.

Whilst transport may play a part, the broad diel cycle may also be due to there being both daytime and night-time sources. The chemical lifetime of propanone nitrate does mean that transport is important making it difficult to simulate the observations with a box model, but it is still useful to gain an insight into the dominant chemical production and loss processes.

Line 703 – is it really mostly nighttime and unimportant? What do you know about the propene concentrations and their diel cycle?

Yes, the source of propanone nitrate produced following the NO_3 addition to propene acts predominantly at night-time. Overall, the model results suggest this to be a relatively small source, however, looking at the fluxes again we can see that at night it is often calculated to be the dominant source, and so some of the night-time peaks in propanone nitrate may not come from isoprene.

The text has been changed to reflect this.

Line 733 – why do you believe it to be anthropogenic? I think Section 6.6 could be dropped.

This section has been dropped.

Conclusions – this section is entirely a summary. Instead of restating what is in the paper, can you draw conclusions about what we don't know that we should work on? What are the areas that warrant further study (your important last line)?

The Conclusions sections has been rewritten highlighting what we do not know and areas for further study as suggested.

Observations of speciated isoprene nitrates in Beijing: implications for isoprene chemistry

Claire E. Reeves[1], Graham P. Mills[1], Lisa K. Whalley[2], W. Joe F. Acton[3], William J. Bloss[4], Leigh R. Crilley[4,5], Sue Grimmond[6], Dwayne E. Heard[7], C. Nicholas Hewitt[3], James R. Hopkins[8], Simone Kotthaus[6,9], Louisa J. Kramer[4], Roderic L. Jones[10], James D. Lee[8], Yanhui Liu[1], Bin Ouyang[10], Eloise Slater[7], Freya Squires[11], Xinming Wang[12], Robert Woodward-Massey[13], and Chunxiang Ye[13]

[1]Centre for Ocean and Atmospheric Sciences, School of Environmental Sciences, University of East Anglia, UK
[2]National Centre for Atmospheric Science, School of Chemistry, University of Leeds, UK
[3]Lancaster Environment Centre, Lancaster University, Lancaster, UK
[4]School of Geography, Earth and Environmental Sciences, the University of Birmingham, Birmingham, B15 2TT, UK
[5]now at Department of Chemistry, York University, Toronto, Canada.
[6]Department of Meteorology, University of Reading, Reading, UK
[7]School of Chemistry, University of Leeds, UK
[8]National Centre for Atmospheric Science, Wolfson Atmospheric Chemistry Laboratories, Department of Chemistry, University of York, UK
[9]Institut Pierre Simon Laplace, Ecole Polytechnique, France
[10]Department of Chemistry, University of Cambridge, UK
[11]Wolfson Atmospheric Chemistry Laboratories, Department of Chemistry, University of York, UK
[12]Guangzhou Institute of Geochemistry, Chinese Academy of Sciences, Guangzhou, China
[13]Beijing Innovation Center for Engineering Science and Advanced Technology, State Key Joint Laboratory for Environmental Simulation and Pollution Control, Center for Environment and Health, College of Environmental Sciences and Engineering, Peking University, Beijing, 100871, China

Correspondence to: Claire E. Reeves (c.reeves@uea.ac.uk)

Abstract. Isoprene is the most important biogenic volatile organic compound in the atmosphere. Its calculated impact on ozone (O_3) is critically dependent on the model isoprene oxidation chemical scheme, in particular the way the isoprene-derived organic nitrates (IN) are treated. By combining gas chromatography with mass spectrometry, we have developed a system capable of separating, and unambiguously measuring, individual IN isomers. In this paper we report measurements from its first field deployment, which took place in Beijing as part of the Atmospheric Pollution and Human Health in a Chinese Megacity (APHH-Beijing) programme. Seven individual isoprene nitrates were identified and quantified during the summer campaign: two β-isoprene hydroxy nitrates (IHN); four δ isoprene carbonyl nitrates (ICN); and propanone nitrate. Box model simulations using the Master Chemical Mechanism (MCM) (v.3.3.1) were made to assess the key processes affecting the production and loss of the IN.

The observed mixing ratios of the two β-IHN are well correlated with an R^2 value of 0.85. The mean for their ratio ((1-OH, 2-ONO_2)-IHN : (4-OH, 3-ONO_2)-IHN) is 3.4 (the numbers in the names indicate the carbon (C) atom in the isoprene chain to which the radical is added). This observed ratio tends to increase with decreasing mixing ratios of nitric oxide (NO),

Deleted: , along with b

Deleted: ¶
¶
Seven individual isoprene nitrates were identified and quantified during the summer campaign: two β-isoprene hydroxy nitrates (IHN); four δ isoprene carbonyl nitrates (ICN); and propanone nitrate. Whilst we had previously demonstrated that the system can measure the four δ-IHN, we found no evidence of them in Beijing.¶

Moved down [5]: Whilst we had previously demonstrated that the the four δ-IHN, we found no evidence of them in Beijing.¶

Deleted: mixing ratios

Deleted: and exhibits no clear diel cycle

although the relationship is weak due to there being only a few data points. Examining this relationship in a box model demonstrates that it is largely a reflection of the respective β-IHN precursor peroxy radicals which, at NO mixing ratios of less than 1 part per billion (ppb), shift towards those of (1-OH, 2-ONO_2)-IHN. The model, however, tends to simulate lower ratios than observed.

Of the δ-ICN, the two *trans* (E) isomers are observed to have the highest mixing ratios and the mean isomer ratio (E-(4-ONO_2, 1-CO)-ICN to E-(1-ONO_2, 4-CO)-ICN)) is 1.4, which is considerably lower than the expected ratio of 6 for addition of NO_3 in the C1 and C4 carbon positions in the isoprene chain. The model produces far more δ-ICN than observed, particularly at night and it also simulates an increase in the daytime δ-ICN that greatly exceeds that seen in the observations. Interestingly, the modelled source of δ-ICN is predominantly during the daytime, due to the presence in Beijing of appreciable daytime amounts of NO_3 along with isoprene. δ-ICN is modelled to be the main precursor for propanone nitrate, but their modelled ratio is very different from the observed. The model also simulated large enhancements of (1-OH, 4-ONO_2)-IHN and δ-ICN on some nights, but we did not observe these enhancements in δ-ICN and, despite the modelled mixing rations of (1-OH, 4-ONO_2)-IHN being above our detection limit, we did not detect it.

This study demonstrates the value of speciated IN measurements to test our understanding of the isoprene degradation chemistry. Our interpretation is limited by the uncertainties in our measurements and relatively small data set, but highlights areas of the isoprene chemistry that warrant further study, in particular the impact of NO on the formation of the β-IHN, and the NO_3 initiated isoprene degradation chemistry.

1 Introduction

Isoprene is the most important biogenic volatile organic compound (BVOC) in the atmosphere, with its emissions accounting for around 500 Tg yr^{-1}, about half of the global biogenic non-methane VOC emissions (Guenther et al., 2012). It is emitted by vegetation primarily during the daytime as a function of temperature and solar radiation and is readily oxidised by the hydroxyl (OH) and nitrate (NO_3) radicals and ozone (O_3). Through its degradation chemistry, isoprene impacts O_3 and the formation of secondary organic aerosols (SOA), which together impact the oxidising capacity of the atmosphere and radiative forcing. Global and regional model studies show that the calculated impact of isoprene on O_3 is critically dependent on the model isoprene oxidation chemical scheme, in particular the way the isoprene-derived nitrates (IN) are treated (e.g. Emmerson and Evans, 2009; Fiore et al., 2005; Squire et al., 2015; von Kuhlman et al., 2004; Wu et al., 2007; Bates and Jacob, 2019; Schwantes et al., 2020). Much of the uncertainty in this chemistry is related to the yield and fate of IN, in particular whether NO_X (nitrogen oxides) and radicals, which are tied up in the nitrates, are later recycled or lost from the atmosphere.

Deleted: its sensitivity to nitric oxide (NO), with lower NO mixing ratios favouring (1-OH, 2-ONO_2)-IHN over (4-OH, 3-ONO_2)-IHN. Thisthat it

Deleted: modelled ratios of their

Deleted: ,

Deleted: increase substantially with decreasing NO

Deleted: Interestingly, this ratio in the peroxy radicals still exceeds the kinetic ratio (i.e. their initial ratio based on the yields of the adducts from OH addition to isoprene and the rates of reaction of the adducts with oxygen (O_2)) even at NO mixing ratios as high as 100 ppb. The relationship of the observed β-IHN ratio with NO is much weaker than modelled, partly due to far fewer data points, but it agrees with the model simulation in so far as there tend to be larger ratios at sub 1 ppb amounts of NO.¶

Deleted: ¶

Deleted: MCM

Deleted: The modelled ratios of

Deleted: to

Deleted: are

Deleted: to

Formatted: Subscript

Formatted: Subscript

Moved (insertion) [5]

Deleted: Whilst we had previously demonstrated that the system can measure the four δ-IHN, we found no evidence of them in…

Deleted: Beijing

First generation IN are formed following oxidation of isoprene by either OH or NO_3 (Wennberg et al., 2018) (Fig. 1). On oxidation by OH, peroxy radicals are formed which when they react with nitric oxide (NO) can lead to the formation of hydroxy nitrates (IHN), with a yield of around 4-15 % (e.g. Chen et al., 1998; Chuong and Stevens, 2002). These are dominated by β-IHN, but some δ-IHN are also formed. Although NO_3 is mostly present at night, isoprene oxidation by NO_3 can be important, particularly in the early evening (Brown et al., 2009) and, due to the larger organic nitrate yield of ~65-80 % (Kwan et al., 2012; Perring et al., 2009b, Rollins et al., 2009; Schwantes et al., 2015), can be responsible for a considerable proportion (~40-50 %) of the IN (Horowitz et al., 2007; von Kuhlmann et al., 2004; Paulot et al., 2012; Xie et al., 2013). Depending on the fate of the peroxy radicals formed following NO_3 addition, a variety of IN can be produced: isoprene hydroperoxy nitrates (IPN); isoprene dinitrates (IDN); isoprene carbonyl nitrates (ICN); as well as IHN.

The fate of first generation IN is poorly understood and until recently understanding was based on theoretical calculations, with most observational constraints based on measurements of either groups of nitrates as totals, or degradation products that come from more than one reaction and precursor species (Giacopelli et al., 2005; Paulot et al., 2009; Rollins et al., 2009). Much advancement in recent years has been made through new laboratory studies following the synthesis of some of the IN (Jacobs et al., 2014; Lee et al., 2014; Lockwood, et al., 2010; Teng et al., 2017; Xiong et al., 2016), but these are still limited to specific IN isomers (six IHN and one ICN) and reaction rates for others are based on extrapolation and structural activity relationships. The IN are lost via reaction with OH, O_3 and NO_3 (Wennberg et al., 2018) and by photolysis (Xiong et al., 2016; Müller et al., 2014) and deposition (Nguyen et al., 2015), and have lifetimes of the order of a few hours.

One of the key issues is whether NO_X and radicals are returned to the system or whether they remain tied up in second generation nitrates. In the case of the IHN and ICN reactions with OH can lead to the formation of carbonyls and release of NO_2 or the formation of shorter chained nitrates such as methyl vinyl ketone nitrate, methacrolein nitrate, propanone nitrate (acetone nitrate) and ethanal nitrate, with the ratio between these two pathways differing for specific IN isomers (Wennberg et al., 2018). Critically the β-IHN and δ-IHN have different lifetimes and return different fractions of NO_2 (Paulot et al., 2012). As the yields of the IHN from the β and δ peroxy radicals are fairly similar (Teng et al., 2017), a key factor in the amount of NO_X recycled is the relative yields of the β and δ peroxy radicals from OH oxidation of isoprene.

Over the last decade or so there has been a considerable effort to improve understanding of isoprene oxidation mechanisms, with the latest understanding detailed in Wennberg et al. (2018) (hereafter referred to as W2018). More details of the chemistry of IN are given in Sect. 1 of the Supplementary Information (Supp. Info.).

The implications of this chemistry have been subject to several model studies (Fiore et al., 2005; Wu et al., 2007; Emmerson and Evans, 2009; Paulot et al., 2012; Xie et al, 2013; Squire et al., 2015; Bates and Jacob, 2019; Schwantes et al., 2020), although it should be noted that several of these studies predate many of the recent advancements in understanding of the

Deleted: The OH reaction dominates accounting for around 85 % of the reactive fate of isoprene largely due to concurrent daytime presence of isoprene and OH. On oxidation b

Deleted: (lifetimes ~3-10 h at 0.04 parts per trillion (ppt) of OH)

Deleted: (lifetimes ~10 -1000 h at 40 ppb of O_3)

Deleted: lifetimes ~100 -400 h at 1 ppt of NO_3) (lifetimes calculated for 298K and 993 hPa based on rate recommendations in

Deleted: (

Deleted:)

detailed isoprene nitrate chemistry outlined above. However, the key findings are that the yield of the IN and the rate at which NO_X is recycled are important in determining the overall impact of isoprene on O_3 and the distribution of O_3 production.

The results of the model studies need to be evaluated against field data of IN. Some of the early field measurements used gas chromatography (GC) to separate the IHN (Werner et al., 1999; Giacopelli et al., 2005; Grossenbacher et al., 2001; 2004), but without synthesised samples of the IN, the identity of the specific isomers could not be confirmed. Several studies (e.g. Horowitz et al., 2007; Perring et al., 2009a; Mao et al., 2013; Xie et al., 2013; Zare et al., 2018) have used thermal dissociation laser-induced fluorescence spectroscopy (TD-LIF) measurements of the sum of alkyl and multifunctional nitrates (∑ANs) as observational constraints, but whilst this includes IN, it also includes other organic nitrates, and there is no separation of individual IN. Field studies using chemical ionisation mass spectrometry (CIMS) (e.g. Beaver et al., 2012; Xiong et al., 2015; Fisher et al., 2016; Lee et al., 2016; Lee et al., 2018) were able to provide further insight through partial separation of different types of IN, including first generation and second generation IN, but were not able to distinguish between different isomers (e.g. of IHN).

By combining GC with mass spectrometry (MS), we (Bew et al., 2016; Mills et al., 2016), Vasquez et al. (2018) and Li et al. (2019) have developed systems capable of separating, and unambiguously measuring, individual IN isomers in the field. We used negative ion (NI) MS, whilst Vasquez et al. (2018) used CIMS and Li et al. (2019) EI-MS.

In this study we deploy our system in the field for the first time, allowing us to quantify the concentrations of several of the individual IHN and ICN, along with propanone nitrate during a major field campaign in Beijing as described in Sect. 3. In Sect. 4 we present the observed time series of the measured IN, examine their ratios and diel patterns. We a chemical box model to examine the ratio of the β-IHN isomers and how their ratio changes with NO, and to assess the key processes affecting the production and loss of all the IN measured (Sect. 5).

2 Nomenclature

In this paper when naming the IN we have followed the nomenclature described by Wennberg et al. (2018). We assign numbers to the carbons of isoprene based on the conjugated butadiene backbone being comprised of carbons 1−4, with the methyl substituent (carbon 5) connected to carbon 2. We refer to these carbons as "C#" without subscripts (e.g., "C2"). For functionalized isoprene oxidation products, we drop the "C" when describing substituent positions; for example, (1-OH, 2-ONO_2)-isoprene hydroxy nitrate (IHN) has a hydroxy group at C1 and a nitrooxy group at C2. This is different to the way

Deleted: Wu et al. (2007) found that increasing the yield of the IHN from 4 % to 12 % led to a significant decrease in the global production rate of O_3. They also found that the production rate of O_3 saturated above a certain threshold of VOC emissions due to NO_X being efficiently lost from the atmosphere via the IN. Fiore et al. (2005) calculated that increasing the yield of IHN from 8 % to 12 %, and assuming NO_X is permanently lost via the IHN, led to decreases in surface O_3 concentrations by 4-12 ppb in the South Eastern U.S. In a regional model of the same area Xie et al. (2013) found that uncertainties in the IN chemistry can impact O_3 production by 10 % and OH concentrations by 6 %, the main uncertainty being in the efficiency of NO_X recycling rather than IN yield or dry deposition rate. This is consistent with a similar conclusion regarding the importance of the removal, recycling and export of NO_X by IN on tropical O_3 (Paulot et al., 2012). Emmerson and Evans (2009), in a comparison of chemistry schemes, showed that even the sign (positive or negative) of the impact of isoprene on O_3 varied between schemes. They identified the treatment of IN as the dominant cause of these discrepancies. Similarly Squire et al. (2015) assessed how four different reduced isoprene schemes in a global model respond to climate, isoprene emission, anthropogenic emission and land-use change. They noted the importance of the yield of the IN and how this also affected the distribution of O_3 production, with more produced locally and less further away when the IN yields are lower. ¶ ¶

Deleted: and

Deleted: In our case w

Deleted:

Deleted: along with some of the

Deleted: and

Deleted: use

Deleted: simple

Deleted: (Sect. 5) and a more detailed chemical box model to investigate how their ratio changes with NO

Deleted: 6

Deleted: who state:

Deleted: 'w

Deleted: as follows:

Deleted: carbons 1−4 comprise

Deleted: of the backbone

Deleted: Throughout the text, w

Deleted: ;

Deleted: subscripted numbers (e.g., "C_2") are used instead to refer to the total number of carbon atoms in a molecule. In the names of…

Deleted: '

we named the IN in Mills et al. (2016) in which the IHN naming followed that of Lockwood et al. (2010) and the ICN were named similarly to the equivalent IHN, except they have "–al" as a suffix. We referred to acetone nitrate as NOA in Mills et al. (2016) whereas here we refer to it as propanone nitrate.

Deleted: where the oxygen atom and nitrate are in the same position in the molecule…

Deleted: also

3 Field campaigns and instrumentation

3.1 Field campaigns

The GC-NI-MS system was deployed in Beijing as part of the Atmospheric Pollution and Human Health in a Chinese Megacity (APHH-Beijing) programme (Shi et al., 2019) during two campaigns at the Institute of Atmospheric Physics (IAP), Chinese Academy of Sciences. IAP is located at 39.97° N, 116.38° E in a residential area between the 3rd and 4th North ring roads of Beijing. The site contained small trees and grass, with roads 150 m away. The first campaign was in winter (10th November to 10th December 2016) and the second in the summer (21st May to 22nd June 2017). For reasons discussed below we shall focus on the summer campaign.

Details of the isoprene nitrate measurement technique are provided below, whilst details of instrumentation used for the supporting data are provided in the Supp. Info.

3.2 Isoprene nitrate measurements

This was the first deployment of a GC-NI-MS system in the field to measure speciated isoprene nitrates. Measurements were made approximately hourly. Air was drawn at 10 L min^{-1} down a 2.5 m heated inlet (3/8" PFA and 45 °C) mounted on the roof (a height of approximately 3 m above the ground) of a mobile laboratory. During the summer campaign three different instrument setups were employed: (1) From the start of the measurements to 31 May, samples of 500 ml were taken off the inlet line down a 0.3 m length of 0.53 mm ID MxT-200 transfer line held at 50 °C and preconcentrated on a Tenax adsorption trap at 35 °C and 50 ml min^{-1}, and injected onto the column via a metal six port Valco valve by heating to 150 °C (Mills et al. 2016). A 30.5 m, 0.32 mm (internal diameter (ID)) combination column was used which was comprised of 28 m of Rtx-200 followed by 2.5 m of Rtx-1701 column. The GC oven was temperature profiled from 40 °C to 200 °C, with a constant column flow of 4.5 ml min^{-1} of helium; (2) Between 10th June and 16th June, the system was operated without a trap but instead direct injection of a 3 ml sample through a plastic Valco Cheminert valve connected to a short 0.32 mm ID

combination column (2.5 m of Rtx-200 joined to 0.5 m of Rtx-1701). The GC oven was temperature programmed from 10 °C to 200 °C and cooled with carbon dioxide (CO_2). A constant flow of 6.5 ml min^{-1} of helium was used as the carrier gas; (3) From 18th June to the end, the system again used the 30 m column and Tenax trapping as described above but the metal valve was replaced with the Cheminert valve that was used for the direct injections.

Of the compounds reported here, all but those of (1-OH, 2-ONO_2)-IHN and E-(1-ONO_2, 4-CO)-ICN were confirmed by injection of known isomers (Mills et al. 2016) post campaign. (1-OH, 2-ONO_2)-IHN was identified based on its expected elution just before (4-OH, 3-ONO_2)-IHN (Nguyen et al., 2014) and the similarity of the observed ions to those of (4-OH, 3-ONO_2)-IHN. The E-(1-ONO_2, 4-CO)-ICN peak was identified by its relative elution position compared to the other ICN (Schwantes et al., 2015), its expected retention time estimated from the relative retention times of known δ-IHN on this system and their aldehydic equivalents, and the similarity of observed ions to the other ICN.

During several comparisons of samples measured immediately before and after the valve was changed from metal to plastic and vice versa (1 h between samples), it was evident that the (4-OH, 3-ONO_2)-IHN and the ICN were lost to varying degrees on the metal valve as suggested by Crounse (J. D. Crounse, personal communication 2016), while simple alkyl nitrates were not. To account for this, all data obtained with the metal valve were scaled by the ratio of peak areas from the samples on either side of the valve changes to give results equivalent to those obtained when using the Cheminert valve.

Calibrations for (4-OH, 3-ONO_2)-IHN and propanone nitrate were derived from the relative sensitivity of the compound to that of n-butyl nitrate (Mills et al., 2016) corrected for the relative ion abundances of the specific measurement ions used for each compound (m/z 71 and 73, respectively). M/z 73 is a relatively minor ion for propanone nitrate, but we were unable to use a more major ion due to interferences from other compounds. N-butyl nitrate calibrations were performed every few days by attaching the transfer line to the standard in place of the inlet. We were unable to measure the relative sensitivities of (1-OH, 2-ONO_2)-IHN and the ICNs to n-butyl nitrate directly. To obtain an estimate, we have assumed that the ICN and propanone nitrate all have the same total ion yields compared to those of n-butyl nitrate and scaled this relative total ion yield by the fraction of the ion yield that the measurement ion represents. Similarly we have assumed that the total ion yields of (1-OH, 2-ONO_2)-IHN and (4-OH, 3-ONO_2)-IHN are the same (and thus the n-butyl nitrate m/z 71: total IN ion ratio) and scaled this to reflect the proportion of the total ions that m/z 101 represents for (1-OH, 2-ONO_2)-IHN.

3.3 Isoprene nitrate measurement uncertainties

We had previously determined the uncertainty for the measurement of the INs in laboratory (including the GCMS precision and calibration uncertainties) to be ±14 % (Mill et al, 2016), which includes an uncertainty of 5% for the GCMS precision. For determination of propanone nitrate in the field, we had to use a minor ion, and, with much smaller peaks, the precision

was worse than it had been in the laboratory using more abundant ions. Based on the signal to noise on a peak, we estimate that the precision was 10% rather than the 5%. We obtained ion counts per ppt of NO_Y for three isoprene nitrates: (4-OH, 3-ONO_2)-IHN (2030), propanone nitrate (2202) Z-(4-OH, 1-ONO_2)-IHN (2365). Using this range, we assume an additional uncertainty of 17% for the electron capture / ionisation efficiency of (1-OH, 2-ONO_2)-IHN and the ICN. During the campaign, we swapped between a metal and plastic valve twice. Using the peak areas for the last sample with the old valve and first sample with the new valve we calculated loss correction factors as well as the uncertainties in these correction factors of: (4-OH, 3-ONO_2)-IHN (±5.2%), propanone nitrate (±6.4%), E-(1-ONO_2, 4-CO)-ICN (±14.8%), E-(4-ONO_2, 1-CO)-ICN (±9.0%), Z-(1-ONO_2, 4-CO)-ICN (±7.5%) and Z-(4-ONO_2, 1-CO)-ICN (±9.2%). Loss corrections were applied to the data collected with the metal valve, and these additional uncertainties included in the overall uncertainties calculated for the periods when the metal valve was used. Based on Mills et al (2016) the detection limit (DL) of our system with the column and trap is 0.1 ppt, but this increased to 1 ppt when run with direct injection. Combining these uncertainties, we get overall uncertainties for the measurements of the IN as shown in Table 1.

When determining the uncertainties in the ratios between IN, we first calculated the uncertainties for each individual IN measurement excluding the calibration uncertainties that were common to both. We then combined the uncertainties in these to derive overall uncertainties in the ratios. We only assessed the ratios of 4-OH, 3-ONO_2)-IHN : (1-OH, 2-ONO_2)-IHN in period 2, when we the used the plastic valve and direct injection. I.e. for the ratio (4-OH, 3-ONO_2)-IHN : (1-OH, 2-ONO_2)-IHN, we considered the GCMS precision of 5% for each β-IHN and the additional 17% uncertainty for the electron capture / ionisation efficiency of (1-OH, 2-ONO_2)-IHN, plus the 1 ppt for the DL. We only assessed the ICN ratio in period 3 when we the used the plastic valve, along with column and trap. I.e. we considered the GCMS precision of 5% and the additional 17% uncertainty for the electron capture / ionisation efficiency for each of the ICN and 0.1 ppt for the DL.

4 Field observations

4.1 Overview of air quality conditions

During the winter campaign air quality was very poor with several haze events and average concentrations of $PM_{2.5}$ of ~90 μg m^{-3}, and average mixing ratios of NO_2 of 40 ppb, CO of 1300 ppb and O_3 of ~8 ppb (Shi et al., 2019). During the summer campaign air quality was also poor, but the mix of pollutants differed, with higher amounts of O_3 and lower amounts of $PM_{2.5}$, NO_2 and CO. i.e. average concentrations of $PM_{2.5}$ of ~30 μg m^{-3} and average mixing ratios of NO_2 of 15 ppb, CO of 450 ppb and O_3 of ~45 ppb (Shi et al., 2019).

Deleted: 3.3 Other measurements¶

¶

A large suite of meteorological and chemical measurements was made during the campaigns (Shi et al., 2019). Here we describe briefly only those used in this paper. Isoprene was measured using a dual channel GC with a flame ionisation detector (DC-GC-FID) (Hopkins et al. (2011). A Thermo Environmental Instruments (TEI) 49i UV absorption analyser was used to measure O_3. Measurements of OH, HO_2 and RO_2 were obtained using the fluorescence assay by gas expansion (FAGE) technique equipped with a scavenger inlet for OH, with the OH chem method used to obtain the background OH signal (Whalley et al., 2010; Whalley et al., 2018; Woodward-Massey et al., 2019). NO was measured using a TEI 42i, NO_2 by a Teledyne cavity attenuated phase shift (CAPS) instrument and HONO by long path absorption photometer (LOPAP) (Crilley et al., 2016). NO_3 and glyoxal were measured using broadband cavity enhanced absorption spectroscopy (Kennedy et al., 2011). SO_2 was measured by TEI 43i and CO by a sensor box (Smith et al., 2017). A proton transfer reaction-time of flight-mass spectrometer (PTR-ToF-MS) was used to measure multi-functional aromatics and monoterpenes, whilst HCHO was measured by LIF (Cryer, 2016). The mixed layer height was determined from the attenuated backscatter measured with a Vaisala CL31 ceilometer (Kotthaus and Grimmond (2018), and photolysis rates from spectral radiometer measurements (Bohn et al., 2016).¶

¶

4.2 Isoprene nitrate observations

4.2.1 Time series

The winter campaign was the first field deployment of the GC-NI-MS system for measuring isoprene nitrates. With the very poor air quality the air was loaded with nitrated species which led to many unidentifiable peaks in the chromatograms and, with low temperature and sunlight, biogenic emissions of isoprene were low and no IN were identified. We shall therefore limit our presentation of results to the summer campaign.

Seven individual isoprene nitrates were identified and quantified during the summer campaign (Fig. 1): two β-IHN ((1-OH, 2-ONO_2)-IHN, (4-OH, 3-ONO_2)-IHN); four ICN (E-(1-ONO_2, 4-CO)-ICN, Z-(1-ONO_2, 4-CO)-ICN, E-(4-ONO_2, 1-CO)-ICN, Z-(4-ONO_2, 1-CO)-ICN); and propanone nitrate.

Whilst we had previously demonstrated that the system can measure the four δ-IHN (Mills et al., 2016), we found no evidence of them in Beijing. This may not be so surprising given that Xiong et al. (2015) calculated the sum of the δ-IHN to have made up only a few percent of the total IHN during Southern Oxidant and Aerosol Study (SOAS) in the United States in 2013. Jenkin et al. (2015), using the Master Chemical Mechanism (MCMv3.3.1) (http:/mcm.york.ac.uk), calculated that the molar faction of IHN yield that would be made up of δ-IHN would increase with increasing NO such that for NO mixing ratios of 5-40 ppb typical of peak daytime values in Beijing this would be around 5-15% but less than 5% for mean daytime NO values of ~2.5 ppb. Note the isomer distribution will also be affected by loss processes and the δ-IHN have shorter lifetimes than the β-IHN (W2018).

The IN follow broadly similar temporal patterns with elevated mixing ratios for the first five days, followed by a period of five days of lower values before rising again (Fig. S1 in Supp. Info.). There were then breaks in data and a period of seven days whilst the GC-NI-MS was run in direct injection mode enabling the measurement of (1-OH, 2-ONO_2)-IHN along with (4-OH, 3-ONO_2)-IHN. During this period, these two β-IHN followed similar patterns (Fig. 2). There was then a final period when the trap was reinstalled when the other IN were measured again (Fig. S1).

The general trend in IN mixing ratios does not appear to be related to a similar trend in isoprene mixing ratios (Fig. S2). The isoprene time series exhibits a number of spikes in mixing ratios, several of which occurred at night. These are likely from very local sources, probably anthropogenic given the time of day, and injected into a shallow nocturnal mixed layer. The

Deleted: , however the campaign allowed useful tests of the field operation procedures. We shall therefore limit our presentation of

Deleted: 2

Deleted: ¶
Figures 3 and 4 show the time series of the IN and other relevant chemical species during the summer campaign. All measured IN follow similar patterns with elevated mixing ratios for the f

Deleted: (Fig. 3)

Deleted: broadly followed similar patterns

Deleted: 4

highest mixing ratios of IN appear not to be related to polluted periods, but rather coincide with low NO mixing ratios when the NO_2:NO ratios were high (Figs. S1 and S2).

For the few days with measurements of both (1-OH, 2-ONO_2)-IHN and (4-OH, 3-ONO_2)-IHN available, the sum of the β-IHN show daily maxima of around 40-120 ppt with night-time values of around 10-30 ppt (Fig. 2). This is broadly similar to the sum of IHN reported for SOAS (Xiong et al., 2015; Schwantes et al., 2016). Likewise, our observed sum of the δ-ICN also exhibited night-time peaks of around 30-70 ppt (Figs. S1 and 3) which are broadly similar to those reported for SOAS (Schwantes et al., 2016). Our measurements of propanone nitrate often exceeded 50 ppt (Figs. S1 and 3) making them generally higher than those observed in SOAS, which rarely exceeded 40 ppt (Schwantes et al., 2016).

4.2.2 IN ratios

The two β-IHN are well correlated, with an R^2 value of 0.85. The mean for the ratio (1-OH, 2-ONO_2)-IHN : (4-OH, 3-ONO_2)-IHN is 3.4 (standard deviation of 1.7) and exhibits no clear diel cycle (Fig. 2). This compares with the average daytime ratios of ~2.6 and ~1.4 obtained by Vasquez et al. (2018) in Michigan during the PROPHET campaign and at Pasadena California, respectively. Xiong et al. (2015) calculate a ratio ranging from 2.6 to 6.0 based on the conditions experienced in SOAS. Jenkin et al. (2015), using the MCMv3.3.1, calculated that the ratio of (1-OH, 2-ONO_2)-IHN to (4-OH, 3-ONO_2)-IHN varies between about 1.5 and 2.5, decreasing with increasing NO and is around 2 for NO mixing ratios typical of the daytime values observed in Beijing (Fig. 4). It should be noted that the ratio we obtain from our measurements is not based on an independent calibration for (1-OH, 2-ONO_2)-IHN, but based on the assumption that the analytical system has the same sensitivity to (1-OH, 2-ONO_2)-IHN as it does to (4-OH, 3-ONO_2)-IHN. We have tried to account for this in the uncertainty calculations by assuming that the error in this sensitivity is equal to the percentage range of sensitivities that we observed for the other IN (see section 3.3). It is possible that this is an underestimate. The β-IHN ratio we obtain is broadly consistent with the studies described above and is examined in more detail with a model in Sect. 5.

Of the δ-ICN, the two *trans* (E) isomers have the highest mixing ratios with E-(1-ONO_2, 4-CO)-ICN being the most abundant (Fig. S1). Focusing on the last four days (three nights) of the summer campaign (Fig. 3), when we have most confidence in the data (i.e. when the plastic valve was used (Sect. 3.2)), we see that the observed ICN C1:C4 isomer ratio exhibits a diel cycle with higher values at night (mean of 2.0, standard deviation (s.d.) of 0.3) and an overall mean of 1.4 (s.d. of 0.6). These values are considerably lower than would be expected based solely on the addition of NO_3 to isoprene occurring in the C1 and C4 positions in a ratio of 6 (C1:C4) (W2018). Our observed ratios are more comparable to the C1:C4 isomer ratio of 2.8 reported in Schwantes et al. (2016) for their environmental chamber. In their experiment the ICN mostly came from RO_2 + RO_2 reactions (see Sect. S1.2) because the NO and NO_3 concentrations were low. Although, we

Deleted: 4

Deleted: , which suggests that the air was more photochemically aged.

Deleted: 5

Deleted: the

Deleted: There is a large uncertainty in our calibration for propanone nitrate since we were only able to use a minor ion for detection during the field campaign (Sect. 3.2).…

Deleted: 5

Formatted: Not Highlight

Deleted: es

Formatted: Not Highlight

Deleted: peak

Deleted: Nevertheless, t

Deleted: it

Deleted: s

Deleted: and Sect. 6

Deleted: 3

Deleted: if

Deleted: 6

Deleted: ratios of the ICN showed similar values each day. There are some diel variations in these ratios, particularly those involving E-(1-ONO_2, 4-CO)-ICN, which shall be discussed further below.¶ ¶ The mean

Deleted: is 1.4

Deleted: (i.e. E/Z-(1-ONO_2, 4-CO)-ICN : E/Z-(4-ONO_2, 1-CO)-ICN). Th

Deleted: is

Deleted: is

Deleted: (74:26)

Deleted: It should be noted that i

Deleted: whereas

had relatively higher NOx concentrations in Beijing, the afternoon mixing ratios of NO were often below 1 ppb (Fig. 4). Turning to the E:Z ratios, we observed the E-ICN isomers to dominate over the Z-ICN isomers. The (1-ONO_2, 4-CO)-ICN isomers exhibit a mean night-time E:Z ratio of 8 (s.d. of 1.4), whilst the (4-ONO_2, 1-CO)-ICN isomers exhibit a mean night-time E:Z ratio of 11 (s.d. of 1.5), giving an overall mean night-time E:Z ratio of 9 (s.d. of 1.0). These values are far greater than the *trans*:*cis* ratio of 1 presumed by W2018 for the reaction of NO_3 addition to isoprene, based on the OH addition to C1 of isoprene calculated by Peeters et al. (2009). However, it should be noted that the peroxy radicals formed from the reaction of the adducts with O_2 may be in a different ratio as these reactions are reversible, similar to those for peroxy radicals formed following OH addition to isoprene, as discussed in Sect. S1.1.

4.2.3 Diel patterns

In this section we examine the diel patterns of the IN and other trace gases by considering the means for each hour of the day (Fig. 4. Shaded areas represent ±1 s.d. in the variability of the measurements for each hour of the day). The isoprene mixing ratios exhibit a typical diel pattern with the highest values (~1 ppb) around midday, which are maintained through the afternoon before declining in the evening to near zero values at night. Much of the variability in the values, particularly at night, is caused by the high spikes shown in Fig. S1. O_3 mixing ratios build up gradually through the daytime, peaking mid to late afternoon and then slowly declining to minimum values around sunrise. Remarkably the mean diel peak value of O_3 was very high at around 100 ppb, demonstrating the considerable amount of photochemical pollution during the campaign. OH concentrations also exhibited a typical diel cycle peaking around midday at just below 1 x 10^7 molecules cm^{-3}. Evidence was found of low, but appreciable concentrations of OH at night, along with peroxy radicals, signifying the presence of nocturnal radical chemistry. NO peaked just after sunrise at around 7 ppb, and dropped below 1 ppb in the mid-afternoon.

The β-IHN, as illustrated by (4-OH, 3-ONO_2)-IHN, exhibit diel patterns (Fig. 4) that are consistent with formation from OH oxidation of isoprene (Sect.S1.2). They peak around midday and these levels are maintained until around sunset when they decline to reach minimum values just after sunrise. This pattern is broadly similar to that observed during SOAS for total IHN with a daytime peak of around 70 ppt and a minimum around sunset of around 10 ppt (Xiong et al., 2015). However, the SOAS IHN peaked earlier in the day at 10:00 Central Daylight Time, i.e. prior to the daytime maxima in OH and isoprene. Xiong et al. (2015) attribute this to competition between the different peroxy radical (ISOPOO) reactions, with the relative importance switching from reaction with NO to reaction with HO_2. Whilst NO mixing ratios peaked in the morning in Beijing, similar to those in SOAS, they are of greater magnitude and remain above 1 ppb until mid-afternoon (Fig. 4)), thus favouring IHN production for longer. Xiong et al. (2015) also suggest that mixing down of IHN from the residual layer may contribute to the morning increase in IHN mixing ratios. We will explore the diel pattern in (4-OH, 3-ONO_2)-IHN in more detail with a model in Sect. 5.

Deleted: 5
Deleted: 7
Deleted: medians
Deleted: 7
Deleted: Some
Deleted: 4
Deleted: median
Deleted: 7
Deleted: so
Deleted: into the
Deleted: (e.g. the median value only goes below 1 ppb in the mid-afternoon (Fig.
Deleted: 7
Deleted: simple

Conversely, the δ-ICN, as illustrated by E-(4-ONO_2, 1-CO)-ICN, exhibit nocturnal peaks, with maximum values in the early night and minimum values during the daytime (Fig. 4), which is consistent with formation from NO_3 addition to isoprene (Sect. S1.2) in the evening and a lifetime of the order of a few hours or less. The mean mixing ratio increases in the evening at a rate of 3 ppt h^{-1} from around 2 to 8 ppt in 2 hours. We calculated the concentrations of NO_3 required to produce such an increase by considering its loss via reactions with OH, O_3 and NO_3, and its production from NO_3 addition to isoprene with an assumed yield of ~5 %. We use bimolecular rate coefficients given in W2018 and number densities of the reactants from the observations (Fig. 4). This calculation assumes that the rate limiting step in the production of (4-ONO_2, 1-CO)-ICN is the reaction of isoprene with NO_3 and that deposition is negligible. The 5 % yield is based on Schwantes et al. (2015) chamber experiments results, whereby we assume a 20 % yield of ICN from NO_3 addition to isoprene, of which 25 % is E-(4-ONO_2, 1-CO)-ICN. We calculate that ~3 ppt of NO_3 is required to produce the observed evening increase in E-(4-ONO_2, 1-CO)-ICN, which is consistent with the observed NO_3 mixing ratios (mean values rise from 2 ppt to 8 ppt from 18:00 to 20:00) (Fig. 4).

Interestingly, ~1-2 ppt of E-(4-ONO_2, 1-CO)-ICN persists during the daytime. We performed a similar calculation to the above, but this time assuming steady state and a photolysis rate based on Xiong et al. (2016) (i.e. a value of 4.6 x 10^{-4} s^{-1} for a solar zenith angle of 0° and adjusting for latitude, time of year and time of day). We find that around 1-2 ppt of NO_3 is required to produce the observed E-(4-ONO_2, 1-CO)-ICN. Whilst we observe this amount during the afternoon, mean values in the morning are ~0.2-0.5 ppt (Fig. 4). This might suggest mixing down of ICN into the mixed layer in the morning but would require considerable production of ICN in the residual layer during the previous evening/night.

As noted above, the ratios of C1-ICN to C4-ICN ratios exhibit diel patterns (Fig. 3). The ratios are higher at night and lower in the daytime. The evening ratios are driven by the preferential addition of NO_3 to the C1 position as discussed above in Sect. 4.2.2. The decrease in this ratio during the morning could be explained if the lifetime of C1-ICN were shorter than for the other isomers. However, the rate coefficients for reaction with OH recommended by W2018 are about 20 % slower for C1-ICN than for C4-ICN. Photolysis is expected to be the largest daytime sink, but Xiong et al (2016) only determined this for E-(4-ONO_2, 1-CO)-ICN. There is a hint of a diel pattern in the ratio of the E and Z isomers of (1-ONO_2, 4-CO)-ICN, with larger values at night, but during the daytime the Z isomers are at or below our detection limit of 0.1 ppt leading to large uncertainties in the calculated ratios.

Propanone nitrate shows no clear diel cycle. The pattern can change from day to day, sometimes peaking during the daytime and sometimes at night-time. This is illustrated in Fig. 3 which shows the temporal variation of propanone nitrate, along with (4-OH, 3-ONO_2)-IHN and (4-ONO_2, 1-CO)-ICN for the last four days of the campaign. Propanone nitrate peaks on the night of the 19/06/2017 coincident with the ICN. This is followed by two peaks, one in the night of the 20-21/06/2017, again

Deleted: 7
Deleted: median
Deleted: .0
Deleted: .6
Deleted: 7.6
Deleted: 7
Deleted: 2.5
Deleted: median
Deleted: 5
Deleted: 7
Deleted: then
Deleted: median
Deleted: 1
Deleted: 3
Deleted: 7
Deleted: E-(1-ONO_2, 4-CO)-ICN with both E-(4-ONO_2, 1-CO)-ICN and Z-(1-ONO_2, 4-CO)-ICN …
Deleted: 6
Deleted: of E-(1-ONO_2, 4-CO)-ICN to E-(4-ONO_2, 1-CO)-ICN
Deleted: E-(1-ONO_2, 4-CO)-ICN
Deleted: (1-ONO_2, 4-CO)
Deleted: (4-ONO_2, 1-CO)-
Deleted: It is not clear why there is such a strong
Deleted: during the daytime when the mixing ratios are close to our detection limit the ratios will be very sensitive to uncertainties in the measurements.d
Deleted: 8
Deleted: five
Deleted: suggesting formation from NO_3 oxidation of isoprene (Sect. S1.2)…

coincident with the ICN, and then a second peak during the daytime of the 21/06/2017 when (4-OH, 3-ONO_2)-IHN maximises. Schwantes et al. (2016) noted that on some days during the SOAS campaign propanone nitrate increased after sunrise following the presence of ICN the night before, while on other occasions night-time ICN was not followed by increases in propanone nitrate, or propanone nitrate appeared during the day when ICN had not been present the night before. They suggest that as well as photooxidation of the ICN, boundary layer dynamics may have played a role as propanone nitrate may have been formed aloft in a residual layer at night and was then mixed down to the surface in the morning. We investigate the night-time and daytime sources of propanone nitrate during the Beijing campaign further in Sect. 5.5 using a model.

5 MCM Box modelling

5.1 MCM model set up

A zero dimensional box model, utilising a subset of the chemistry described within the Master Chemical Mechanism, MCMv3.3.1 (Jenkin et al., 2015), was used to calculate the concentration of the various isoprene nitrates for comparison with those measured. The MCMv3.3.1 includes an update of the isoprene degradation chemistry to reflect findings of recent laboratory and theoretical studies.

The model was constrained by measured values of water vapour, temperature, pressure, NO, NO_2, NO_3, O_3, CO, SO_2, HONO and HCHO. Speciated VOC measurements of alcohols, alkanes, alkenes, dialkenes (including isoprene), multi-functional aromatics, carbonyls and monoterpenes were included as further model constraints. The concentrations of H_2 and CH_4 were held constant at 500 ppb and 1.8 ppm, respectively. The photolysis rates for j(O^1D), j(NO_2) and j(HONO), calculated from the measured actinic flux and published absorption cross sections and quantum yields, were included as model inputs. Other photolysis frequencies used in the model were calculated. For UV-active species, such as HCHO and CH_3CHO, photolysis rates were calculated by scaling to the ratio of clear-sky j(O^1D) to observed j(O^1D) to account for clouds. For species able to photolyse further into the visible the ratio of clear-sky j(NO_2) to observed j(NO_2) was used. The variation of the clear-sky photolysis rates (j) with solar zenith angle (χ) was calculated within the model using the following expression:

$$j = l\cos(\chi)^m \times e^{-n\sec(\chi)} \quad (3)$$

with the parameters l, m and n optimised for each photolysis frequency (see Table 2 in Saunders et al. (2003)).

Deleted: 6

Deleted: through the use of

Deleted: **5 Simple Box Modelling of the β-IHN**¶

¶

A simple model was constructed to calculate the diurnal cycle of the β-IHN. The production of the β-IHN used the equation of Xiong et al. (2015):¶

¶

$P = k_{ISOP+OH}[OH][ISOP] \times \varphi \times \gamma \times \alpha$ (1)¶

¶

where $k_{ISOP+OH}$ is the rate constant for the reaction of isoprene with OH, [OH] and [ISOP] are the number densities of OH and isoprene. φ is the yield of ISOPOO following OH addition to isoprene that is available to react with NO, HO_2 and RO_2. I.e., it takes account of the redistribution of the ISOPOO isomers as a result of the reversibility of the reactions of the OH adducts with O_2 and formation of hydroperoxyaldeyhyde (HPALD) following Z-δ-ISOPOO isomerisation (see Sect. S1.1). Xiong et al. (2015) calculates a value for φ of around 0.8 for β-ISOPOO when their lifetimes are around 1 to 35 s so we adopt that value for φ. As we consider the β-IHN separately we then need to assume a distribution of the β-ISOPOO so we assume this is the same as the kinetic ratio of the β-ISOPOO yields recommended by W2018 (65:35) giving values of φ of 0.52 and 0.28 for (1-OH, 2-OO)-ISOPOO and (4-OH, 3-OO)-ISOPOO, respectively, which given their short lifetimes in the high NO_X environment is reasonable. γ is the fraction of ISOPOO that reacts with NO, as opposed to reacting with HO_2, RO_2 or NO_3. Isomerisation is assumed to be negligible for β-ISOPOO loss. Due to the high NO_X environment, γ was calculated to be very close to 1 throughout the whole day, ranging from 1.00 in the morning for both β-ISOPOO to 0.95 in the later afternoon / early evening for (4-OH, 3-OO)-ISOPOO and 0.97 for (1-OH, 2-OO)-ISOPOO. The higher value for (1-OH, 2-OO)-ISOPOO is due to its reaction with RO_2 being about 3.5 times slower than for (4-OH, 3-OO)-ISOPOO. α is the branching ratio of the reaction of ISOPOO with NO that forms the IHN, which is set at 0.104 for both β-IHN based on the MCMv3.3.1 (Jenkin et al., 2015). Reaction rate constants are taken from the MCMv3.3.1 (Jenkin et al., 2015) and the number densities are the hour of day medians from the observations.¶

¶

To calculate the diel variation in the mixing ratios of the β-IHN, we used the equation for the solution of the chemical continuity equation:¶

¶

$C_{(t+\Delta t)} = \frac{P}{k'} + \left(C_t - \frac{P}{k'}\right)e^{-k'\Delta t}$ (2)¶

¶

C_t is the concentration of each IHN at time t, P is the production calculated using Eq. (1), k' is the loss rate constant for each IHN and Δt the time step. $C_{t+\Delta t}$ was calculated for each hour using median concentrations of the reactants for that hour. ¶

¶

For the loss rate constants of the β-IHN, we consider the reactions with OH, O_3 and NO_3, taking the recommended rate constants from W2018 and use the observed median number densities of the reactants for the hour of day. We calculate the photolysis rates as a function of solar zenith angle using the parameterisation in the MCM, which assumes the rates for (1-OH, 2-ONO_2)-IHN and (4-OH, 3-ONO_2)-IHN are equivalent to those of tert-butyl nitrate and iso-propyl nitrate, respectively. Based on the observed decrease in (4-OH, 3-ONO_2)-IHN between midnight and 6 in the morning, we ...

Deleted: 6

The model was run for the entirety of the campaign (21st May 2017 – 25th June 2017) in overlapping 7 day segments, with the model constraints updated every 15 minutes. By this method, a model time-series was produced which could be directly compared with observations and, from which, diel averages were generated. There was a spike of very high concentrations of isoprene in the early hours of the morning of 16th June 2017, which led to extremely high concentrations of modelled ICN, propanone nitrate and (4-OH, 1-ONO_2)-IHN. These have been removed from the diel averages presented in this paper. Fluxes through each reaction were calculated for every 15 minute period to allow an analysis of the production and loss terms of the chemical species.

The loss due to mixing of all non-constrained, model generated species, including the speciated isoprene nitrates, was parametrised and evaluated by comparing the model-predicted glyoxal concentration with the observed glyoxal concentration. Applying a loss rate proportional to the observationally-derived mixed layer height (Fig. 4), the model was able to reproduce glyoxal observations reasonably well. As a result of this first order loss process, the partial lifetime of the model generated species was ~2 h at night, then decreased rapidly to a lifetime of <30 min in the morning as the mixed layer grew, effectively simulating ventilation of the model box. With the collapse of the mixed layer in the late afternoon the model lifetime with respect to ventilation of glyoxal (and other model generated species) increased. However, the model has a tendency to underestimate glyoxal concentrations between 4 pm and midnight. This underestimation suggests that either the lifetime with respect to ventilation should be even longer or that the model is underestimating oxidation processes that lead to glyoxal production at these times.

5.2 β-IHN

Figs. S3 and 5 compare the measured and modelled β-IHN. The shaded areas in Fig. 5 represent ±1 s.d. in the data for each hour of the day and illustrate the large day-to-day variability in the mixing ratios of β -IHN. Note that for (1-OH, 2-ONO_2)-IHN there are only 6 days of data, hence why the average diel patterns are strongly affected by the day-to-day variability. This is particularly the case for the measurements where three of the hourly bins contain just one measurement, and the rest have between three and eight measurements.

The MCM simulates (1-OH, 2-ONO_2)-IHN daytime mixing ratios very similar to those observed. The modelled evening mixing ratios are lower than observed. Like glyoxal, this underestimation suggests the lifetime with respect to ventilation might be longer than 2 hours.

Deleted: 7

Deleted: 6

Deleted: peak

Deleted: for the few days with measurements available (Figs. 11 and 12)…

Deleted: night-time

Deleted: that either

Deleted: should

Deleted: or that the model is underestimating production of the (1-OH, 2-ONO_2)-IHN, the only modelled pathway being reaction of NO with (1-OH, 2-OO)-ISOPOO.

During the daytime the (4-OH, 3-ONO_2)-IHN modelled by the MCM tends to give larger mean mixing ratios and greater day-to-day variability than observed. This is partially the result of a few days when the model calculates high mixing ratios of (4-OH, 3-ONO_2)-IHN that are not observed (Fig. S3). Like the modelled (1-OH, 2-ONO_2)-IHN, the concentrations of (4-OH, 3-ONO_2)-IHN decline more rapidly in the evening than observed, suggesting that its lifetime with respect to ventilation might be longer than 2 hours.

To limit the impact of mixing on the comparison between the model and observations, Figs. 2 and 6 compare the ratios of (1-OH, 2-ONO_2)-IHN to (4-OH, 3-ONO_2)-IHN. When looking at the times series (Fig. 2) of this ratio the model and measurements often agree within the measurement uncertainties, although there are times when the modelled values are less that observed. The shaded areas in Fig. 6 represent ±1 s.d. in the data for each hour of the day. The large variability in the observed data are caused by some hours having very few data points, sometimes affected by a single high value (Fig. 2). The MCM simulates mean ratios that, are generally lower than the observed mean, although they are sometimes within the uncertainty of the measured ratio and often within the day-to-day variability.

There are four main factors that determine the ratio of the β-IHN: 1) the yields of their respective peroxy radicals (ISOPOO) following oxidation of isoprene by OH addition (φ); 2) the fraction of the respective ISOPOO that reacts with NO (γ); 3) the branching ratios for the formation of the IHN from the reaction of NO with the ISOPOO (α); and 4) the relative loss rates of the β-IHN, including via deposition.

For the first two factors, the concentration of NO is largely the determining influence. NO is often present in large amounts (Figs 4 and S2) so that reaction with it is the dominant loss process for the ISOPOO. NO is the major factor determining the lifetime of the ISOPOO and therefore the extent of the redistribution of the ISOPOO from a kinetic ratio towards a thermodynamic equilibrium. The adducts formed from OH addition to a specific C in isoprene can form a β-ISOPOO and either a *trans* or *cis* δ-ISOPOO. These reactions are reversible and occur at different rates which along with the rapid 1,6 H atom shift isomerisation of the Z-δ-ISOPOO means that the longer the lifetime of the ISOPOO the more the ratio of the β-ISOPOO shifts towards (1-OH, 2-OO)-ISOPOO. Consequently, at lower NO mixing ratios the ratio of φ-(1-OH, 2-ONO_2)-IHN to φ-(4-OH, 3-ONO_2)-IHN becomes larger. This is illustrated in Fig. 7a, which shows the modelled ratio of the values of φ. For mixing ratios of NO greater than ~2 ppb the ratio of the values of φ decreases approximately linearly from around 2 to about 1.7 at 100 ppb of NO. The ratio of the kinetic yields in the MCM is 1.58, which is the ratio of the values of φ that we get if we switch off the reverse pathway of the O_2 reactions. This implies that even at 100 ppb of NO, the ratio of the yields of the (1-OH, 2-OO)-ISOPOO to (4-OH, 3-OO)-ISOPOO is shifted to values slightly greater than the kinetic ratio. At NO mixing ratios less than ~2 ppb the ratio of the values of φ increase greatly with decreasing NO, such that at a few 10s of ppt of NO the ratio is typically between 2.5 and 4.

Deleted:
Deleted: For
Deleted: ,
Deleted: during the daytime but lower than observed from early evening to midnight (Figs. 11 and 12). Again, like glyoxal, this night-time underestimation suggests that that the…
Deleted: Whilst increasing the production of the (4-OH, 3-ONO_2)-IHN, the only modelled pathway being the reaction of NO with the (4-OH, 3-OO)-ISOPOO, would improve the comparison of the model with the night-time measurements it would worsen it during the daytime.¶
Deleted: The production rates calculated for both β-IHN using the MCM (Fig. 12) are very similar to those calculated using the simp…
Formatted: Font: 10 pt
Deleted: 10
Deleted: s
Deleted: diel pattern of the
Formatted: Font: 10 pt
Deleted: from the observations and as calculated by the MCM …
Deleted: Throughout much of the day the
Deleted: very similar
Deleted:
Deleted: to that calculated by the simple model and are
Deleted: ratio
Formatted: Font: 10 pt, Not Highlight
Formatted: Font: 10 pt
Deleted:
Deleted: represented by
Deleted: in the simple model
Deleted: represented by
Deleted: in the simple model
Deleted: 3
Deleted: ; and 4) the branching ratios for the formation of the IH…
Deleted: It should be noted that deposition
Deleted: is not included in the MCM model but, as discussed fo…
Deleted:
Deleted: 13
Deleted: (each calculated as the net production of the specific …
Deleted: The values of φ that we used for the simple model hav…
Deleted: MCM
Deleted: uses slightly different
Deleted: giving a ratio of

The rates at which the ISOPOO are assumed to be lost via the reactions with NO, HO_2 and NO_3 are the same for both β-ISOPOO. However, the rate of reaction for (1-OH, 2-OO)-ISOPOO with RO_2 and its rate of isomerisation are slower than for (4-OH, 3-OO)-ISOPOO. At lower NO mixing ratios, these reactions become relatively more important and so the value of γ is lower for (4-OH, 3-OO)-ISOPOO than for (1-OH, 2-OO)-ISOPOO, therefore the ratio of γ-(1-OH, 2-OO)-ISOPOO to γ-(4-OH, 3-OO)-ISOPOO is larger (Fig. 7b). This is further enhanced as the concentrations of RO_2 can also be much greater at the lower NO concentrations, particularly below 1 ppb of NO (Fig. 7c), which leads to the ratio in the γ values being considerably greater than 1 at NO concentrations below a few 10s of ppt.

It should be noted that the MCM model underestimates the measured RO_2 mixing ratios. This will lead to underestimation of the ratio of γ-(1-OH, 2-OO)-ISOPOO to γ-(4-OH, 3-OO)-ISOPOO, primarily at mixing ratios of NO below ~2 ppb. This might explain some of the differences between the MCM modelled and observed β-IHN ratios.

The net effect of these relationships is that the ratio of (1-OH, 2-OO)-ISOPOO to (4-OH, 3-OO)-ISOPOO increases with decreasing NO (Fig. 7d), i.e. for NO mixing ratios greater than 2 ppb the ratio is around 1.7-2.0, but at NO mixing ratios less than 2 ppb the ratio increases up towards a value of around 4. The ratio of the rate of production of (1-OH, 2-ONO_2)-IHN to (4-OH, 3-ONO_2)-IHN will have the same relationship with NO as the ratio of their precursor ISOPOO since the MCM assumes that the branching ratios for the formation of the two β-IHN from the reaction of NO with the ISOPOO (i.e. α, third factor) are the same. However, there are still considerable uncertainties in these branching ratios (Sect. S1.1).

As for the loss processes of the β-IHN (fourth factor), the dominant loss in the model is the mixing term which is set at the same rate for both β-IHN. Photolysis is assumed to be faster for (1-OH, 2-ONO_2)-IHN than for (4-OH, 3-ONO_2)-IHN in the MCM, but is only a minor loss process. However, (1-OH, 2-ONO_2)-IHN reacts with both OH and O_3 more slowly than does (4-OH, 3-ONO_2)-IHN and since the dominant chemical loss process for the β-IHN are by far their reactions with OH, the net effect of these loss processes is to increase the ratio of (1-OH, 2-ONO_2)-IHN to (4-OH, 3-ONO_2)-IHN above their production ratio. The diel pattern in OH (Fig. 4) will tend to increase the ratio of 1-OH, 2-ONO_2)-IHN to (4-OH, 3-ONO_2)-IHN during the daytime.

Regarding deposition, it is not included in the MCM model. We expect (1-OH, 2-ONO_2)-IHN to be lost more efficiently than (4-OH, 3-ONO_2)-IHN given the fast rate of hydrolysis reported for (1-OH, 2-ONO_2)-IHN (W2018) (Sect. S1.3.5) and the greater difficulty we have getting (1-OH, 2-ONO_2)-IHN through our analytical system indicating a greater loss of this isomer on to surfaces. However, including a greater deposition rate for (1-OH, 2-ONO_2)-IHN would reduce the agreement with the observed β-IHN ratios.

Deleted: 14

Deleted: extenuated

Deleted: 14

Deleted: 13

Deleted: .

Deleted: The diel pattern of the median hourly NO mixing ratios (Fig. 7) illustrates that whilst NO mixing ratios were typically above 2 ppb between 06:00 and 12:00 local time, they were mostly below this value in the afternoon when production rates of the β-IHN were also high (Fig. 12). This explains some of the diel pattern in the ratio of the β-IHN shown in Fig. 10.¶
¶

Deleted: one

Deleted: 7

Deleted: (Fig. 10)

Deleted: Interestingly, the MCM simulation is closer to the simple model which uses the rate coefficients for the reactions of the β-IHN with OH recommended by W2018, rather than the simple model run in which they are set to those in the MCM (Fig. 10). …

Deleted: It should be noted that the MCM model underestimates the measured RO_2 mixing ratios. This will lead to underestimation of the ratio of γ-(1-OH, 2-OO)-ISOPOO to γ-(4-OH, 3-OO)-ISOPOO and consequently the ratio of (1-OH, 2-ONO_2)-IHN to (4-OH, 3-ONO_2)-IHN, primarily at mixing ratios of NO below ~2 ppb. This might explain some of the differences between the MCM modelled and observed β-IHN ratios and why the MCM ratios are lower than those of the simple model run that used the MCM rate coefficients for the reactions of OH with the β-IHN (the simple model was constrained by observed RO_2 concentrations).¶

Overall, this means that the modelled ratio of (1-OH, 2-ONO_2)-IHN to (4-OH, 3-ONO_2)-IHN increases with decreasing NO mixing ratios (Fig. 7e) (as also seen by Jenkin et al. (2015) in a box model using the MCM), and generally does not drop below the ratio of the β-ISOPOO (Fig. 7d). In the conditions modelled for Beijing, at NO mixing ratios above ~30 ppb it remains between 1.75 and 2.0. At NO mixing ratios between 1 ppb and ~30 ppb it is mostly around 2.0 but is sometimes up to 3. At NO mixing ratios below 1 ppb, it is typically between 2 and 3, but sometimes up to 4. There are several cases at these low NO mixing ratios when the ratio of the β-IHN is below the ratio of the β-ISOPOO, but these occur at night when the production rates and the mixing ratios of the β-IHN are very small.

Newland et al., (2020) point out that during the campaign a high NO_X environment existed in the morning that then switched to a low NO_X environment in the afternoon. The mean hourly NO mixing ratios were typically above 2 ppb between 06:00 and 12:00 local time, but mostly below this value in the afternoon (Fig. 4) when production rates of the β-IHN were also high. This largely explains why the modelled ratio of the β-IHN (Fig. 6), is ~2 between about 06:00 and 09:00 and then rises up to around 2.5 in the afternoon. The modelled variability in this ratio is very small between 06:00 and 09:00 as the ratio of 2 relates to a wide range of NO mixing ratios (~2-30 ppb) (Fig. 7e).

In comparison, the observed ratios of (1-OH, 2-ONO_2)-IHN to (4-OH, 3-ONO_2)-IHN show a much weaker relationship with NO (Fig. 7f). This may be due to there being far fewer data points and uncertainties in the measurements. The observed ratios tend to be higher than modelled. At times they drop below the kinetic ratio for φ (but with the uncertainty range of the measurements). Despite far more scatter, including 2 outliers with large uncertainties, there is a tendency for higher values of the observed ratio at NO mixing ratios of less than 1 ppb, as simulated by the model.

Vasquez et al. (2018) reported lower daytime values for the ratio of (1-OH, 2-ONO_2)-IHN to (4-OH, 3-ONO_2)-IHN in PROPHET campaign (~2.6) and in Pasadena (~1.4) compared to our observations of ~3.4, but their data show a similar pattern to ours in that the ratio is higher in the low NO_X environment of PROPHET compared to the high NO_X environment in Pasadena. On average our modelled results are close to the ratios observed in PROPHET. We cannot rule out calibration differences affecting this comparison and like us Vasquez et al (2018) relied on relative calibrations estimates. Also, differences in the observed β-IHN ratios may be due to the amount and reactivity of the peroxy radicals present in the different studies. However, the ratio of 1.4 observed for Pasadena is lower than the value of around 1.75 that we calculate for NO mixing ratios of 100 ppb, and furthermore, it is also lower than the kinetic φ ratios of 1.58 and 1.85 based on MCM and W2018 kinetic yields, respectively.

5.3 δ-ICN

Deleted: ¶
We have also assumed that the branching ratios for the formation of the two β-IHN from the reaction of NO with the ISOPOO are the same. However, there are still considerable uncertainties in these branching ratios (Sect. S1.1).¶
¶

Deleted: 13

Deleted: , which sets a baseline value

Deleted: 13

Deleted: does not fall below 1.95,

Deleted: ,

Deleted: 15

Deleted: , although a

Deleted: Although

Deleted: there is clearly

Deleted: The field observations reported by Vasquez et al. (2018) are consistent with our results in that they obtained higher average daytime values for the ratio of (1-OH, 2-ONO_2)-IHN to (4-OH, 3-ONO_2)-IHN in the low NO_X environment of the PROPHET campaign compared to the high NO_X environment in Pasadena (i.e. ratios of ~2.6 and ~1.4, respectively). On the other hand, the ratio of ~3.4 that we observed in the very high NO_X environment of Beijing is higher than for the two US studies. On average our modelled

Deleted: (both with the simple model and the MCM)

Deleted: , despite Beijing often being a high NO_X environment

Deleted: 6

The δ-ICN time series (Fig. S4) shows that the MCM often produces far more δ-ICN than observed, particularly at night. This is further illustrated by the diel patterns (Fig. 8), which shows both higher modelled mixing ratios and greater day-to-day variability at night compared to the observations. Moreover, the model simulates an increase in the daytime δ-ICN that far exceeds that seen in the observations. We are unable to assess the ratios of the different δ-ICN isomers using the model as the MCM assumes all of the δ-ICN formed can be represented by a single species, (1-ONO_2, 4-CO)-ICN, called NC4CHO in the MCM.

The source of δ-ICN is via the addition of NO_3 to isoprene followed by addition of O_2. This produces δ-nitroxy peroxy radicals (INO_2) (NISOPO2 in the MCM) and, in the conditions simulated for Beijing, the major loss of NISOPO2 is reaction with NO to form NO_2 and a δ-nitroxy alkoxy radical (NISOPO in the MCM), which then reacts rapidly with O_2 to form the δ-ICN (NC4CHO). Other production pathways for NC4CHO exist in the MCM, but the reaction of NISOPO with NO is by far the dominant source of δ-ICN in our simulations. There are some nights when there are large sources of NISOPO2, but typically the production of NISOPO2 maximises in the mid-afternoon when isoprene concentrations are still high and mean NO_3 mixing ratios were observed to be around 2 ppt (Fig. 4). Consequently, the production of δ-ICN in the model is mostly during the daytime, despite NO_3 usually being considered to be more important at night. Comparison of the modelled and observed mixing ratios of the δ-ICNs suggest that this source might be too fast even during the daytime, despite the model being constrained by observed concentrations of isoprene and NO_3.

Alternatively, the loss processes could be too slow. The dominant loss in the model is the mixing term, which is greatest during the daytime when the mixed layer is fully developed. The same loss process has been applied to all model generated species (Sect. 5.1). For glyoxal, (1-OH, 2-ONO_2)-IHN and (4-OH, 3-ONO_2)-IHN, the model tends to overestimate the decrease in concentrations from late afternoon onwards suggesting that the lifetime with respect to mixing should be longer at these times. Increasing the lifetime of all the model intermediates would lead to a further overestimation of δ-ICN. Applying the same loss term to all model species is of course an approximation, not least because the dilution term depends on the concentration of the species in the diluent air.

The next most important loss processes for δ-ICN are simulated to be photolysis and reaction with OH, which are also both predominantly daytime losses. The net effect of the production and loss terms is that the modelled δ-ICN maximise during the night-time as obsdeved (Fig. 8).

The MCM uses a photolysis frequency for δ-ICN based on that measured for propanone nitrate, which is equivalent to 3.16 x 10^{-4} s^{-1} for a solar zenith angle of 0°. Xiong et al. (2016) determined a rate of 4.6 x 10^{-4} s^{-1} for (4-ONO_2, 1-CO)-ICN for a solar zenith angle of 0°. Reaction with OH constitutes a similar size loss for δ-ICN as photolysis in the model. Whilst these are both predominantly daytime sinks, increasing them would not only reduce the daytime increase in δ-ICN but would also

Deleted: 16

Deleted:

Deleted: as

Deleted: 17

Deleted: Note that an event in which the modelled mixing ratios of the δ-ICN reached nearly 10 ppb in the early hours of the 16th June 2017 (Sect. 6.6) skewed the night-time 15 minute mean values. Removing this event from the modelled means gives night-time values that are much lower but still higher than the observed values.

Deleted: MCM

Deleted: (reactions of OH with isoprene hydroperoxy nitrate and with isoprene dinitrate, and reaction of NISOPO2 with RO_2)…

Deleted: median

Deleted: 7

Deleted: 6

Deleted: underestimate

Deleted: observed

Deleted: Alternatively, this potentially suggests that a

Deleted: not necessarily appropriate

Deleted: Overestimation of the dilution due to the growing mixed layer depth at around 7 am might explain why the modelled mixing ratios are lower than observed at that time.¶

Deleted: 17

reduce the amount of modelled δ-ICN that would persist into the night. The MCM treats all the δ-ICN as (1-ONO_2, 4-CO,)-ICN and uses a rate coefficient for reaction with OH of 4.1 x 10^{-11} cm^3 s^{-1}. However, W2018 suggests a lower rate coefficient for reaction of OH with (4-ONO_2, 1-CO)-ICN than for (1-ONO_2, 4-CO,)-ICN (3.4 x 10^{-11} cm^3 s^{-1} versus 4.1 x 10^{-11} cm^3 s^{-1}). Therefore, treating the two separately in the model would, overall, reduce the loss of δ-ICN with respect to OH, increasing discrepancy with the model.

Night-time losses of δ-ICN are reaction with O_3 and NO_3. The MCM uses a rate coefficient of 2.4 x 10^{-17} cm^3 s^{-1} for the reaction of δ-ICN with O_3, which is 5 times faster than the rate of 4.4 x 10^{-18} cm^3 s^{-1} recommended by W2018, giving a partial lifetime on the order of 12 hours for an O_3 mixing ratio of 40 ppb. On the other hand, the MCM uses a rate for the reaction of δ-ICN with NO_3 which is 10 times slower than the rate recommended by W2018, but even so the lifetime of δ-ICN with respect to reaction with NO_3 as estimated by W2018 is of the order of 4 days, so this loss pathway would have to be much faster to reduce the modelled night-time δ-ICN to close to that observed.

5.4 Propanone nitrate

Figures S4 and 8 show the time series and diel patterns of the measured and modelled propanone nitrate. The observed mixing ratios are generally higher than the modelled values. As discussed above, elevated propanone nitrate mixing ratios are observed both during the daytime and night-time, leading to a weak bimodal pattern in the mean, but there is large day-to-day variability. This is consistent with both daytime and night-time production processes. It should be noted that transport will play an important role in the variability of the propanone nitrate. Its chemical lifetime is calculated to be around 10 hours during the daytime and considerably longer at night. The mixing term dominates the modelled lifetime so the resulting mixing ratios are highly dependent on the assumptions regarding this term. However, the model can still provide insight into the dominant chemical processes.

The main source of propanone nitrate is via oxidation of isoprene, with routes via both OH and NO_3 addition to isoprene. Its primary source in the MCM simulation is via the OH oxidation of NC4CHO (i.e. the δ-ICN) and this is reflected in them sharing many similarities in their modelled time series (Fig. S4). As discussed in Sect. 5.3, the production of NC4CHO and its loss via OH oxidation occur mostly during the daytime, so this source of propanone nitrate is predominantly during the daytime. On nights when OH is present even at low concentrations it can be a sizeable source due to the relatively large amounts of NC4CHO at night. Propanone nitrate is also formed from oxidation of NC4CHO by O_3. This is a relatively small source except on nights when O_3 was present (Fig. S2).

Deleted: the concentration

Deleted: 6

Deleted: 18

Deleted: 19

Deleted: , which may be due to uncertainties in the measurement calibration (Sect. 3.2)… Looking at the diel patterns (Fig. 19) there Looking at the diel patterns (Fig. 19) there are some similarities in that both the measured and modelled values show a bi-modal pattern with maxima at night and during the daytime. The modelled night-time maximum is much greater than its daytime maximum due to the event in the early hours of the 16th June 2017 during which the modelled mixing ratios of propanone nitrate exceeded 1.5 ppb (Sect. 6.6). Removing this event from the modelled means gives a night-time maximum similar to the daytime one, which is consistent with the observed pattern. However,

Deleted: Looking at the diel patterns (Fig. 19) there are some that both the measured and modelled values show a bi-modal pattern with maxima at night and during the daytime. The modelled night-time maximum is much greater than its daytime maximum due to the event in the early hours of the 16th June 2017 during which the modelled mixing ratios of propanone nitrate exceeded 1.5 ppb (Sect. 6.6). Removing this event from the modelled means gives a night-time maximum similar to the daytime one, which is consistent with the observed pattern. However,

Deleted: whilst the modelled 15 minute means approach zero at around 08:00.

Deleted: and 20:00 local time, the average observed hourly values remain reasonably high throughout the day (>30 ppt). Fig. 19 illustrates that the observed propanone nitrate mixing ratios are at times as low as a few ppt, but that higher values occurred at most times of the day, leading to a weak diel pattern. This may be due to a lack of observations, along with daily variability, but looking at the results on individual days shows that the observations often remain high whilst the modelled values drop to much lower values and generally there is little correlation between the observed and modelled values.¶

Deleted: Both the model and observed values indicate production of propanone nitrate during day and night. …

Deleted: .

Deleted: 18

Deleted: 6

Deleted: not depleted

Deleted: 4

Deleted: (4-OH, 1-ONO_2)-IHN is also a source of propanone nitrate.¶

The modelled ratio propanone nitrate to δ-ICN is mostly much less than one. Conversely the measured propanone nitrate is typically a lot greater than the total δ-ICN observed. This might, in part be due to the model being unable to simulate the mixing correctly, but, as discussed in Sect. 5.3, the model simulates considerably larger amounts of NC4CHO than observed and getting the wrong balance between the various production and loss terms of NC4CHO (i.e. the δ-ICN) will likely impact the modelled propanone nitrate.

Propanone nitrate can also be produced following the NO_3 addition to propene. Overall, the model results suggest this to be a relatively small source, but at night it is often calculated to be the dominant source, which may explain some of the night-time peaks in propanone nitrate.

5.5 δ-IHN

The MCM simulates daytime peak mixing ratios for the δ-IHN (i.e. (1-OH, 4-ONO_2)-IHN and (4-OH, 1-ONO_2)-IHN), consistent with production from OH addition to isoprene, of around 1 ppt (Figs. 9 and S5). As mentioned above, we were unable to detect these IN in Beijing despite having been able to in the laboratory. The two δ-IHN are simulated to have very similar mixing ratios during the daytime, but on several nights, enhancements of (4-OH, 1-ONO_2)-IHN are simulated and these are coincident with enhanced modelled mixing ratios of the δ-ICN. As well as being formed by OH oxidation of isoprene, (4-OH, 1-ONO_2)-IHN is also formed in the MCM when the NISOPO2 radicals produced by NO_3 oxidation of isoprene react with other organic peroxy radicals. As discussed above in Sect. 5.3, NISOPO2 are mostly present during the daytime, but on some nights NISOPO2 mixing ratios were simulated to be high leading to elevated mixing ratios of both (4-OH, 1-ONO_2)-IHN and δ-ICN. Only a few of the simulated night-time peaks occurred at times when we were making measurements, but despite the modelled mixing ratios of around 15-30 ppt being well above our detection limit we did not to detect (4-OH, 1-ONO_2)-IHN. Also, despite successfully measuring the δ-ICN, we did not detect strong enhancements in their mixing ratios.

6 Conclusions

Examining the ratio of the two β-IHN in a box model demonstrates its sensitivity to NO, which affects the thermodynamic equilibrium of the β-ISOPOO and the competition between the reactions of the β-ISOPOO with NO and with RO_2. In both cases, lower NO mixing ratios favour (1-OH, 2-ONO_2)-IHN over (4-OH, 3-ONO_2)-IHN. Interestingly, in high NO_x conditions the modelled β-IHN ratio ((1-OH, 2-OO)-ISOPOO to (4-OH, 3-OO)-ISOPOO) of around 2 exceeds the kinetic

Deleted: (note the vertical axes scales in Fig. 18 are different by a factor of 5). Conversely the measured

Deleted: (Figs. 19 and 17)

Deleted: A

Deleted: 6

Deleted: This acts predominantly at night-time, but

Deleted: it

Deleted: in this campaign

Deleted: Whilst the main source of propanone nitrate is during the daytime, the dominant sink in the model is the ventilation which also maximises during the daytime, leading to a diel profile with similar magnitude daytime and night-time maxima (Fig. 19). As discussed above the evening ventilation might be overestimated, which could contribute to the discrepancy between the modelled and observed propanone nitrate. ¶
¶
6

Deleted: -3

Deleted: 20

Deleted: However, a

Deleted: This is illustrated both in the time series plot (Fig. 20) and diel plot (Fig. 21). Note that an event in which the modelled mixing ratios of (4-OH, 1-ONO_2)-IHN reached 0.5 ppb in the early hours of the 16th June 2017 (Sect. 6.6) skewed the night-time 15 minute mean values. Removing this event from the modelled means gives a night-time maximum similar to the daytime one. As

Deleted: 6

Deleted: at that time this source of (4-OH, 1-ONO_2)-IHN is small compared to that from OH addition to isoprene. However, on certain

Deleted: certain

Deleted: the

Deleted: would have expected

Deleted: at the mixing ratios simulated (around 15-30 ppt). This adds further weight to the idea that the NO_3 production of the IN (δ-ICN and δ-IHN) may be overestimated in the model.…

Deleted: 6.6 Modelled event on 16th June 2017¶ …

Deleted: Observed mixing ratios of the IN appear to be strongly …

Moved (insertion) [4]

Moved up [4]: The two β-IHN are well correlated with an R^2

Formatted: Not Superscript/ Subscript

Deleted: ,

Deleted: with

Deleted: ing

Deleted: in both cases

Deleted: of

Deleted:

ratio. At NO mixing ratios below 2 ppb the competition between the reactions of the β-ISOPOO with NO and with RO_2 become important and this results in modelled β-IHN ratios greater than 2, approaching 4 for NO mixing ratios of a few 10s of ppt.

The observed mean β-IHN ratio is 3.4, higher than modelled. The relationship of the observed β-IHN ratio with NO is much weaker than modelled, partly due to far fewer data points, but it confirms the theoretical understanding in so far as there tend to be larger ratios at sub 2 ppb amounts of NO.

The diel variation in NO mixing ratios means that the NO_X environment observed in Beijing typically switched from a high NO_X environment in the morning to a low NO_X environment in the afternoon resulting in a diel pattern of the modelled β-IHN ratio. However, this is not reflected in the observations, largely due to lack of measurements and the day-to-day variability seen on the few days of available data. More observations of speciated β-IHN and a more accurate calibration of (1-OH, 2-ONO_2)-IHN are needed to better constrain these relationships and the underlying chemistry.

Of the δ-ICN, the two *trans* isomers are observed to have the highest mixing ratios, with E-(1-ONO_2, 4-CO)-ICN being the most abundant. However, the mean C1:C4 isomer ratio is 1.4, which is considerably lower than would be expected based solely on the addition of NO_3 to isoprene occurring in the C1 and C4 positions in a 6:1 ratio. This raises the question as to whether it is appropriate to represent the δ-ICN by a single C1 nitrated isomer, as done in the MCM. We observed the *trans*-ICN isomers to dominate over the *cis*-ICN isomers with a mean ratio of 7 far greater than the *trans*:*cis* ratio of 1 presumed by W2018 for the reaction of NO_3 addition to isoprene. This suggests that thermodynamic redistribution of the nitrated peroxy radicals formed from the reaction of the NO_3-isoprene adducts with O_2 may also be important.

The observed δ-ICN exhibit nocturnal peaks with maximum values in the early night and minimum values during the daytime are consistent with formation from NO_3 addition to isoprene in the evening and a lifetime of the order of a few hours or less. Mixing ratios of 1-2 ppt persist through the daytime, which for the afternoon can be accounted for by the presence of 1-2 ppt of NO_3. The model produces far more δ-ICN than observed, particularly at night but it also simulates an increase in the daytime δ-ICN that greatly exceeds that seen in the observations. Reaction of NO with NISOPO2, which comes from NO_3 addition to isoprene, is modelled to be by the far the dominant source of δ-ICN. Interestingly, though this source occurs predominantly during the daytime, due to the presence in Beijing of appreciable daytime amounts of NO_3 along with isoprene.

Observed propanone nitrate shows no clear diel cycle. The pattern can change from day to day, sometimes peaking during the daytime and sometimes at night. The model suggests that the main source of propanone nitrate is the daytime OH oxidation of δ-ICN. However, the model simulates considerably larger amounts of δ-ICN than observed and getting the right

Deleted: even

Deleted: a

Deleted: as high as 100 ppb. This ratio, however, varies little for NO mixing ratios greater than 2 ppb and it is only below 1

Deleted: 1

Deleted: when

Deleted: is

Deleted: ratio increases substantially

Deleted: with decreasing NO

Deleted: The MCM model underestimates the measured RO_2 mixing ratios so this will lead to an underestimation of the competition from the RO_2 for reaction with the β-ISOPOO. Consequently, this may cause modelled ratios of (1-OH, 2-ONO_2)-IHN to (4-OH, 3-ONO_2)-IHN to be underestimated, particularly at mixing ratios of NO below ~2 ppb. The relationship of the observed

Deleted: agrees

Deleted: with the model simulation

Deleted: (up to ~6)

Deleted: 1

Deleted: .

Deleted: ¶
¶
(1-OH, 2-ONO_2)-IHN also reacts more slowly with OH than does (4-OH, 3-ONO_2)-IHN and since this is the dominant chemical loss process for the β-IHN, the effect is to increase the ratio of (1-OH, 2-ONO_2)-IHN to (4-OH, 3-ONO_2)-IHN. The simple model results demonstrate that the sensitivity of the β-IHN ratio to uncertainties in the ratio of these OH rate coefficients is of the same order as the difference between the modelled and observed β-IHN ratios.¶

Deleted: ¶

Deleted: , and will be depend on how similar their fates are

Deleted: MCM

Deleted: in the MCM but, i

Deleted: it is

Deleted: and modelled

balance between the various production and loss terms of δ-ICN is important for modelling the propanone nitrate. Whilst the model results suggest the NO_3 addition to propene to be a relatively small source of propanone nitrate, at night it is often calculated to be the dominant source, which may explain some of the night-time peaks in propanone nitrate.

The main source of the δ-IHN is modelled to come from OH addition to isoprene, but on certain nights the source from NO_3 addition to isoprene led to modelled mixing ratios of around 15-30 ppt of (4-OH, 1-ONO_2)-IHN coincident with enhanced modelled mixing ratios of the δ-ICN. We were unable to detect δ-IHN despite the modelled mixing ratios being considerably greater than our detection limit, nor did we detect strong enhancements in the mixing ratios of the δ-ICN, so again raises questions concerning our understanding of the NO_3 initiated isoprene degradation chemistry.

This study demonstrates the need for further measurements of speciated IN measurements to test our understanding of the isoprene degradation chemistry. Our interpretation is limited by the uncertainties in our measurements and relatively small data set, but highlights areas of the isoprene chemistry that warrant further study, in particular the impact of NO on the formation of the β-IHN, and the NO_3 initiated isoprene degradation chemistry.

Code Availability. The MCM code is available from the authors on request.

Data Availability. The observational data and diel cycles from the MCM in the figures are in the Supplementary Information. The 15 minute data from the MCM is available from the authors on request.

Supplement.

Author contributions. CER led the data interpretation and writing of the manuscript. GPM made the measurements of the IN with the assistance of YL. LKW did the MCM modelling. CER, WJB, SG, DEH, CNH, RLJ, JDL, XW and CY were involved in the project planning and leading the measurement groups. WJA, LRC, JRH, SK, LJK, BO, ES, FS and RW-M provided measurement data. All commented on the manuscript.

Competing interests. The authors declare that they have no conflict of interest.

Acknowledgements. We are grateful for funding provided by the UK Natural Environment Research Council (NERC), UK Medical Research Council and the Natural Science Foundation of China (NSFC) under the framework of the Newton Innovation Fund (NERC grants NE/N006909/1, NE/N006895/1, NE/N006976/1 and NE/N00700X/1; NSFC grant 41571130031). ES and RW-M are grateful to the NERC SPHERES Doctoral Training Programme for funding PhD studentships. CER acknowledges Andrew Rickard (NCAS, University of York) for providing information on the MCM.

Deleted: The modelled propanone nitrate is considerably less than observed. This might be due to large uncertainties in the measurement calibration, but it could also be linked to issues with the simulation of its precursor, δ-ICN, with the modelled ratios of δ-ICN to propanone nitrate being very different to the observed.¶

Deleted: coincident with high mixing ratios of δ-ICN

Deleted: on these nights than those we would expect to observe

Deleted: . This warrants further investigation.

Deleted: value

Deleted: ¶
¶

Deleted: , simple model data

References

Bates, K. H., and Jacob, D. J., A new model mechanism for atmospheric oxidation of isoprene: global effects on oxidants, nitrogen oxides, organic products, and secondary organic aerosol, Atmos. Chem. Phys., 19, 9613–9640, https://doi.org/10.5194/acp-19-9613-2019, 2019.

Beaver, M. R., St Clair, J. M., Paulot, F., Spencer, K. M., Crounse, J. D., LaFranchi, B. W., Min, K. E., Pusede, S. E., Wooldridge, P. J., Schade, G. W., Park, C., Cohen, R. C., and Wennberg, P. O.: Importance of biogenic precursors to the budget of organic nitrates: observations of multifunctional organic nitrates by CIMS and TD-LIF during BEARPEX 2009, Atmos. Chem. Phys., 12, 5773-5785, doi: 10.5194/acp-12-5773-2012, 2012.

Bew, S. P., Hiatt-Gipson, G. D., Mills, G. P., and Reeves, C. E.: Efficient syntheses of climate impacting isoprene nitrates and (1R,5S)-(-)-myrtenol nitrate, Beilstein J. Org. Chem., 12, 1081–1095, doi:10.3762/bjoc.12.103, 2016.

Bohn, B., Heard, D. E., Mihalopoulos, N., Plass-Dülmer, C., Schmitt, R., and Whalley, L. K.: Characterisation and improvement of $j(O^1D)$ filter radiometers, Atmos. Meas. Tech., 9, 3455– 3466, https://doi.org/10.5194/amt-9-3455-2016, 2016.

Brown, S. S., de Gouw, J. A. Warneke, C., Ryerson, T. B., Dubé, W. P., Atlas, E., Weber, R. J., Reltier, R. E., Neuman, J. A., Roberts, J. M., Swanson, A., Flocke, F., McKeen, S. A., Brioude, J., Sommariva, R., Trainer, Fehsenfeld, F. C., and Ravishankara, A. R.: Nocturnal isoprene oxidation over the Northeast United States in summer and its impact on reactive nitrogen partitioning and secondary organic aerosol, Atmos. Chem. Phys., 9, 3027-3042, 2009.

Chen, X., Hulbert, D., and Shepson, P. B.: Measurement of the organic nitrate yield from OH reaction with isoprene, J. Geophys. Res., 103, 25,563-25,568, 1998.

Chuong, B., and Stevens, P. S.: Measurements of the Kinetics of the OH-Initiated Oxidation of Isoprene. J. Geophys. Res., 107 (D13), ACH 2-1−ACH 2-12, 2002.

Crilley, L. R., Kramer, L., Pope, F. D., Whalley, L. K., Cryer, D. R., Heard, D. E., Lee, J. D., Reed, C., and Bloss, W. J.: On the interpretation of in situ HONO observations via photochemical steady state., Faraday. Discuss., 189, 191–212, 2016.

Cryer (2016): Measurements of hydroxyl radical reactivity and formaldehyde in the Atmosphere, PhD Thesis University of Leeds.

Emmerson, K. M., and Evans, M. J.: Comparison of tropospheric gas-phase chemistry schemes for use within global models, Atmos. Chem. Phys., 9, 1831-1845, 2009.

Fiore, A. M., Horowitz, L. W., Purves, D. W., Levy II, H., Evans, M. J., Wang, Y., Li, Q., and Yantosca, R. M.: Evaluating the contribution of changes in isoprene emissions to surface ozone trends over the eastern United States, J. Geophys. Res., 110, D12303, doi: 10.1029/2004JD005485, 2005.

Formatted: Default Paragraph Font

Fisher, J. A., Jacob, D. J., Travis, K. R., Kim, P. S., Marais, E. A., Chan Miller, C., Yu, K., Zhu, L., Yantosca, R. M., Sulprizio, M. P., Mao J., Wennberg, P. O., Crounse, J. D., Teng, A. P., Nguyen, T. B., St. Clair, J. M., Cohen, R. C., Romer, P., Nault, B. A., Wooldridge, P. J., Jimenez, J. L., Campuzano-Jost, P., Day, D. A., Hu, W., Shepson, P. B., Xiong, F., Blake, D. R., Goldstein, A. H., Misztal, P. K., Hanisco, T. H., Wolfe, G. M., Ryerson, T. B., Wisthaler, A., and Mikoviny, T.: Organic Nitrate Chemistry and its Implications for Nitrogen Budgets in an Isoprene- and Monoterpene-Rich Atmosphere: Constraints from Aircraft (SEAC^{4}RS) and Ground-Based (SOAS) Observations in the Southeast US. Atmos. Chem. Phys. 16, 5969−5991, 2016.

Giacopelli, P., Ford, K., Espada, C., and Shepson, P. B.: Comparison of the measured and simulated isoprene nitrate distributions above a forest canopy, J. Geophys. Res., 110, D01304, doi:10.1029/2004JD005123, 2005.

Grossenbacher, J. W., Couch, T., Shepson, P. B., Thornberry, T., Witmer-Rich, M., Carroll, M. A., Faloona, I., Tan, D., Brune, W., Ostling, K., and Bertman, S.: Measurements of isoprene nitrates above a forest canopy, J. Geophys. Res., 106, 24429–24438, 2001.

Grossenbacher, J. W., Barlet Jr., D. J., Shepson, P. B., Carroll, M. A., Olszyna, K., and Apel, E.: A comparison of isoprene nitrate concentrations at two forest-impacted sites, J. Geophys. Res., 109, D11, D11311, doi: 10.1029/2003JD003966, 2004.

Guenther, A., Jiang, X., Heald, C. L., Sakulyanontvittaya, T., Duhl, T., Emmons, L. K., and Wang, X.: The Model of Emissions of Gases and Aerosols from Nature version 2.1 (MEGAN 2.1): An Extended and Updated Framework for Modeling Biogenic Emissions. Geosci. Model Dev., 5, 1471−1492, 2012.

Horowitz, L. W., Fiore, G. P., Milly, A. M., Cohen, R. C., Perring, A., Wooldridge, P. J., Hess, P. G., Emmons, L. K., and Lamarque, J.: Observational constraints on the chemistry of isoprene nitrates over the eastern United States, J. Geophys. Res., 112, D12S08, doi:10.1029/2006JD007747, 2007.

Jacobs, M. I., Burke, W. J., and Elrod, M. J.: Kinetics of the reactions of isoprene-derived hydroxynitrates: gas phase epoxide formation and solution phase hydrolysis, Atmos. Chem. Phys., 14, 8933-8946, doi: 10.5194/acp-14-8933-2014, 2014.

Jenkin, M. E., Young, J. C., and Rickard, A. R.: The MCM v3.3.1 degradation scheme for isoprene, Atmos. Chem. Phys., 15, 11433-11459, doi: 10.5194/acp-15-11433-2015, 2015.

Kennedy, O. J., Ouyang, B., Langridge, J. M., Daniels, M. J. S., Bauguitte, S., Freshwater, R., McLeod, M. W., Ironmonger, C., Sendall, J., Norris, O., Nightingale, R., Ball, S. M., and Jones, R. L.: An aircraft based three channel broadband cavity enhanced absorption spectrometer for simultaneous measurements of NO_3, N_2O_5 and NO_2, Atmos. Meas. Tech., 4, 9, 1759-1776, DOI: 10.5194/amt-4-1759-2011, 2011.

Kotthaus, S. and Grimmond, C. S. B.: Atmospheric boundary layer characteristics from ceilometer measurements part 1: A new method to track mixed layer height and classify clouds, Q. J. Roy. Meteorol. Soc., 144, 1525–1538, https://doi.org/10.1002/qj.3299, 2018.

Kwan, A. J., Chan, A. W. H., Ng, N. L., Kjaergaard, H. G., Seinfeld, J. H., and Wennberg, P. O.: Peroxy Radical Chemistry and OH Radical Production during the NO3-Initiated Oxidation of Isoprene, Atmos. Chem. Phys., 12, 7499−7515, 2012.

Lee, L., Teng, A. P., Wennberg, P. O., Crounse, J. D., and Cohen, R. C.: On Rates and Mechanisms of OH and O_3 Reactions with Isoprene Derived Hydroxy Nitrates, J. Phys. Chem., 118, 1622-1637, doi: 10.1021/jp4107603, 2014.

Lee, B. H., Lopez-Hilfiker, F. D., D'Ambro, E. L., Zhou, P., Boy, M., Petäjä, T., Hao, L., Virtanen, A., and Thornton, J. A.: Semi-volatile and highly oxygenated gaseous and particulate organic compounds observed above a boreal forest canopy, Atmos. Chem. Phys., 18, 11547-11562, doi: 10.5194/acp-18-11547-2018, 2018.

Li, R., Jiang, X., Wang, X., Chen, T., Du, L., Xue, L., Bi, X,. Tang, M., and Wang, W., Determination of Semivolatile Organic Nitrates in Ambient Atmosphere by Gas Chromatography/Electron Ionization–Mass Spectrometry, Atmosphere, 10, 88, doi:10.3390/atmos10020088, 2019.

Lockwood, A. L., Shepson, P. B., Fiddler, M. N., and Alaghmand, M.: Isoprene nitrates: preparation, separation, identification, yields, and atmospheric chemistry, Atmos. Chem. Phys., 10, 6169-6178, doi: 10.5194/acp-10-6169-2010, 2010.

Mao, J., Paulot, F., Jacob, D. J., Cohen, R. C., Crounse, J. D., Wennberg, P. O., Keller, C. A., Hudman, R. C., Barkley, M. P., and Horowitz, L. W.: Ozone and organic nitrates over the eastern United States: Sensitivity to isoprene chemistry, J. Geophys. Res.: Atmospheres, 118, 11,256-11,268, doi: 10.1002/jgrd.50817, 2013.

Mills, G. P., Hiatt-Gipson, G. D., Bew, S. P., and Reeves, C. E.: Measurement of isoprene nitrates by GCMS, Atmos. Meas. Tech., 9, 4533-4545, doi: 10.5194/amt-9-4533-2016, 2016.

Müller, J.-F., Peeters, J., and Stavrakou, T.: Fast photolysis of carbonyl nitrates from isoprene, Atmos. Chem. Phys., 14, 2497-2508, doi: 10.5194/acp-14-2497-2014, 2014.

Newland, M. J., Bryant, D. J., Dunmore, R. E., Bannan, T. J., Acton, W. J. F., Langford, B., Hopkins, J. R., Squires, F. A., Dixon, W., Drysdale, W. S., Ivatt, P. D., Evans, M. J., Edwards, P. M., Whalley, L. K., Heard, D. E., Slater, E. J., Woodward-Massey, R., Ye, C., Mehra, A., Worrall, S. D., Bacak, A., Coe, H., Percival, C. J., Hewitt. C. N., Lee, J. D., Cui, T., Surratt, J. D., Wang, X., Lewis, A. C., Rickard. A. R., Hamilton, J. F., Rainforest-like Atmospheric Chemistry in a Polluted Megacity, Atmos. Chem, Phys., under review, https://doi.org/10.5194/acp-2020-35, 2020.

Nguyen, T. B., Crounse, J. D., Schwantes, R. H., Teng, A. P., Bates, K. H., Zhang, X., St. Clair, J. M., Brune, W. H., Tyndall, G. S., Keutsch, F. N., Seinfeld, J. H., and Wennberg, P. O.: Overview of the Focused Isoprene eXperiment at the

Formatted: Default Paragraph Font

California Institute of Technology (FIXCIT): mechanistic chamber studies on the oxidation of biogenic compounds, Atmos. Chem. Phys., 14, 13531-13549, doi: 10.5194/acp-14-13531-2014, 2014.

Nguyen, T. B., Crounse, J. D., Teng, A. P., St Clair, J. M., Paulot, F., Wolfe, G. M., and Wennberg, P. O.: Rapid deposition of oxidized biogenic compounds to a temperate forest, P. Natl. Acad. Sci., 112, E392-E401, doi: 10.1073/pnas.1418702112, 2015.

Paulot, F., Crounse, J. D., Kjaergaard, H. G., Kroll, J. H., Seinfeld, J. H., and Wennberg, P. O.: Isoprene photooxidation: new insights into the production of acids and organic nitrates, Atmos. Chem. Phys., 9, 1479-1501, 2009.

Paulot, F., Henze, D. K., and Wennberg, P. O.: Impact of the isoprene photochemical cascade on tropical ozone, Atmos. Chem. Phys., 12, 1307-1325, doi: 10.5194/acp-12-1307-2012, 2012.

Peeters, J., Nguyen, T. L., and Vereecken, L.: HOx radical regeneration in the oxidation of isoprene, Phys. Chem. Chem. Phys., 28, 5935–5939, 2009.

Perring, A.E., Bertram, T.H., Wooldridge, P.J., Fried, A., Heikes, B.G., Dibb, J., Crounse, J.D., Wennberg, P.O., Blake, N.J., Blake, D.R., Brune, W.H., Singh, H.B., and Cohen, R.C, Airborne observations of total $RONO_2$: new constraints on the yield and lifetime of isoprene nitrates., Atmos. Chem. Phys., 9 (4), 1451-1463, 2009a.

Perring, A. E., Wisthaler, A., Graus, M., Wooldridge, P. J., Lockwood, A. L., Mielke, L. H., Shepson, P. B., Hansel, A., and Cohen, R. C., A product study of the isoprene+NO_3 reaction, Atmos. Chem. Phys., 9(14), 4945-4956, 2009b.

Rollins, A. W., Kiendler-Scharr, A., Fry, J. L., Brauers, T., Brown, S. S., Dorn, H.-P., Dubé, W. P., Fuchs, H., Mensah, A., Mentel, T. F., Rohrer, F., Tillmann, R., Wegener, R., Wooldridge, P. J., and Cohen, R. C.: Isoprene oxidation by nitrate radical: alkyl nitrate and secondary organic aerosol yields, Atmos. Chem. Phys., 9, 6685-6703, 2009.

Saunders, S. M., Jenkin, M. E., Derwent, R. G., and Pilling, M. J.: Protocol for the development of the Master Chemical Mechanism, MCM v3 (Part A): tropospheric degradation of non-aromatic volatile organic compounds, Atmos. Chem. Phys., 3, 161-180, 2003.

Schwantes, R. H., Teng, A. P., Nguyen, T. B., Coggon, M. M., Crounse, J. D., St Clair, J. M., Zhang, X., Schilling, K. A., Seinfeld, J. H. and Wennberg, P. O.: Isoprene NO_3 Oxidation Products from the RO_2 + HO_2 Pathway, J. Phys. Chem., 119, 10158-10171, doi: 10.1021/acs.jpca.5b06355, 2015.

Schwantes, R. H., Emmons, L. K., Orlando, J. J., Barth, M. C., Tyndall, G. S., Hall, S. R., Ullmann, K., St. Clair, J. M., Blake, D. R., Wisthaler, A., and Bui, T. P. V., Comprehensive isoprene and terpene gas-phase chemistry improves simulated surface ozone in the southeastern US, Atmos. Chem. Phys., 20, 3739–3776, https://doi.org/10.5194/acp-20-3739-2020, 2020.

Shi, Z., Vu, T., Kotthaus, S., Harrison, R. M., Grimmond, S., Yue, S., Zhu,T., Lee,J., Han,Y., Demuzere,M., Dunmore,R.E., Ren, L., Liu,D., Wang,Y., Wild,O., Allan,J., Acton,W.J., Barlow,J., Barratt, B., Beddows, D., Bloss, W. J., Calzolai, G.,

Formatted: Default Paragraph Font

Carruthers, D., Carslaw, D. C., Chan, Q., Chatzidiakou, L., Chen, Y., Crilley, L., Coe, H., Dai, T., Doherty, R., Duan, F., Fu, P., Ge, B., Ge, M., Guan, D., Hamilton, J. F., He, K., Heal, M., Heard, D., Hewitt, C. N., Hollaway, M., Hu, M., Ji, D., Jiang, X., Jones, R., Kalberer, M., Kelly, F. J., Kramer, L., Langford, B., Lin, C., Lewis, A. C., Li, J., Li, W., Liu, H., Liu, J., Loh, M., Lu, K., Lucarelli, F., Mann, G., McFiggans, G., Miller, M. R., Mills, G., Monk, P., Nemitz, E., O'Connor, F., Ouyang, B., Palmer, P. I., Percival, C., Popoola, O., Reeves, C., Rickard, A. R., Shao, L., Shi, G., Spracklen, D., Stevenson, D., Sun, Y., Sun, Z., Tao, S., Tong, S., Wang, Q., Wang, W., Wang, X., Wang, X., Wang, Z., Wei, L., Whalley, L., Wu, X., Wu, Z., Xie, P., Yang, F., Zhang, Q.,Zhang, Y.,Zhang,Y., and Zheng, M.: Introduction to the special issue "In-depth study of air pollution sources and processes within Beijing and its surrounding region (APHH-Beijing)", Atmos. Chem. Phys., 19, 7519–7546, https://doi.org/10.5194/acp19-7519-2019, 2019.

Smith, K. R., Edwards, P. M., Evans, M. J., Lee, J. D., Shaw, M. D., Squires, F., Wilde, S., and Lewis, A. C.: Clustering approaches to improve the performance of low cost air pollution sensors, Faraday Discuss., 200, 321–637, https://doi.org/10.1039/C7FD00020K, 2017.

Squire, O. J., Archibald, A. T., Griffiths, P. T., Jenkin, M. E., Smith, D., and Pyle, J. A: Influence of isoprene chemical mechanism on modelled changes in tropospheric ozone due to climate and land use over the 21st century, Atmos. Chem. Phys., 15, 5123-5143, doi: 10.5194/acp-15-5123-2015, 2015.

Teng, A. P., Crounse, J. D., and Wennberg, P. O.: Isoprene Peroxy Radical Dynamics, J. Am. Che. Soc., 139, 5367-5377, doi: 10.121/jacs.6b12838, 2017.

Vasquez, K. T., Allen, H. M., Crounse, J. D., Praske, E., Xu, L., Noelscher, A. C., and Wennberg, P. O.: Low-pressure gas chromatography with chemical ionization mass spectrometry for quantification of multifunctional organic compounds in the atmosphere, Atmos. Meas. Tech., 11, 6815-6832, doi: 10.5194/amt-11-6815-2018, 2018.

Von Kuhlmann, R., Lawrence, M. G., Pöschl, U., and Crutzen, P. J.: Sensitivities in global scale modeling of isoprene, Atmos. Chem. Phys., 4, 1-17, 2004.

Werner, G., Kastler, J ., Looser, R., and Ballschmiter, K., Organic nitrates of isoprene as atmospheric trace compounds, Angewandte Chemie-Int. Ed., 38(11), 1634-1637. 1999. DOI: 10.1002/(SICI)1521-3773(19990601)38:11

Wennberg, P. O., Bates, K. H., Crounse, J. D., Dodson, L. G., McVay, R. C., Mertens, L. A., Nguyen, T. B., Praske, E., Schwantes, R. H., Smarte, M. D., St Clair, J. M., Teng, A. P., Zhang, X., and Seinfeld, J. H.: Gas-Phase Reactions of Isoprene and Its Major Oxidation Products, Chem. Rev., 118, 3337-3390, doi: 10.1021/acs.chemrev.7b00439, 2018.

Wu, S., Mickley, L. J., Jacob, D. J., Logan, J. A. Yantosca, R. M., and Rind, D.: Why are there large differences between models in global budgets of tropospheric ozone?, J. Geophys. Res., 112, D5, D05302, doi: 10.1029/2006JD007801, 2007.

Xie, Y., Paulot, F., Carter, W. P. L., Nolte, C. G., Luecken, D. J., Hutzell, W. T., Wennberg, P. O., Cohen, R. C., and Pinder, R. W.: Understanding the impact of recent advances in isoprene photooxidation on simulations of regional air quality, Atmos. Chem. Phys., 13, 8439-8455, doi: doi:10.5194/acp-13-8439-2013, 2013.

Xiong, F., McAvey, K. M., Pratt, K. A., Groff, C. J., Hostetler, M. A., Lipton, M. A., Starn, T. K., Seeley, J. V., Bertman, S. B., Teng, A. P., Crounse, J. D., Nguyen, T. B., Wennberg, P. O., Misztal, P. K., Goldstein, A. H., Guenther, A. B., Koss, A. R., Olson,K. F., de Gouw, J. A., Baumann, K., Edgerton, E. S., Feiner, P. A., Zhang, L., Miller, D. O., Brune, W. H., and Shepson, P. B.: Observation of isoprene hydroxynitrates in the southeastern United States and implications for the fate of NOx, Atmos. Chem. Phys., 15, 11257-11272, doi: 10.5194/acp-15-11257-2015, 2015.

Xiong, F., Borca, C. H., Slipchenko, L. V., and Shepson, P. B.: Photochemical degradation of isoprene-derived 4,1-nitrooxy enal, Atmos. Chem. Phys., 16, 5595-5610, doi: 10.5194/acp-16-5595-2016, 2016.

Zare, A., Romer, P. S., Nguyen, T., Keutsch, F. N., Skog, K., and Cohen, R. C.: A comprehensive organic nitrate chemistry: insights into the life time of atmospheric organic nitrates, Atmos. Chem. Phys., 15, 15419-15436, doi: 10.5194/acp-18-15419-2018, 2018.

Table 1: Uncertainties in the measurements of the isoprene nitrates

Isoprene nitrate	Period 1 (metal valve, column and trap)	Period 2 (plastic valve and direct injection)	Period 3 (plastic valve, column and trap)
(4-OH, 3-ONO_2)-IHN	15% + 0.1 ppt	14% + 1 ppt	14% +0.1 ppt
(1-OH, 2-ONO_2)-IHN	-	22% + 1 ppt	-
E-(1-OH, 4-ONO_2)-ICN	27% + 0.1 ppt	-	22% +0.1 ppt
E-(4-OH, 1-ONO_2)-ICN	24% + 0.1 ppt	-	22% +0.1 ppt
Z-(1-OH, 4-ONO_2)-ICN	23% + 0.1 ppt	-	22% +0.1 ppt
Z-(4-OH, 1-ONO_2)-ICN	24% + 0.1 ppt	-	22% +0.1 ppt
Propanone nitrate	18% + 0.1 ppt	-	17% +0.1 ppt

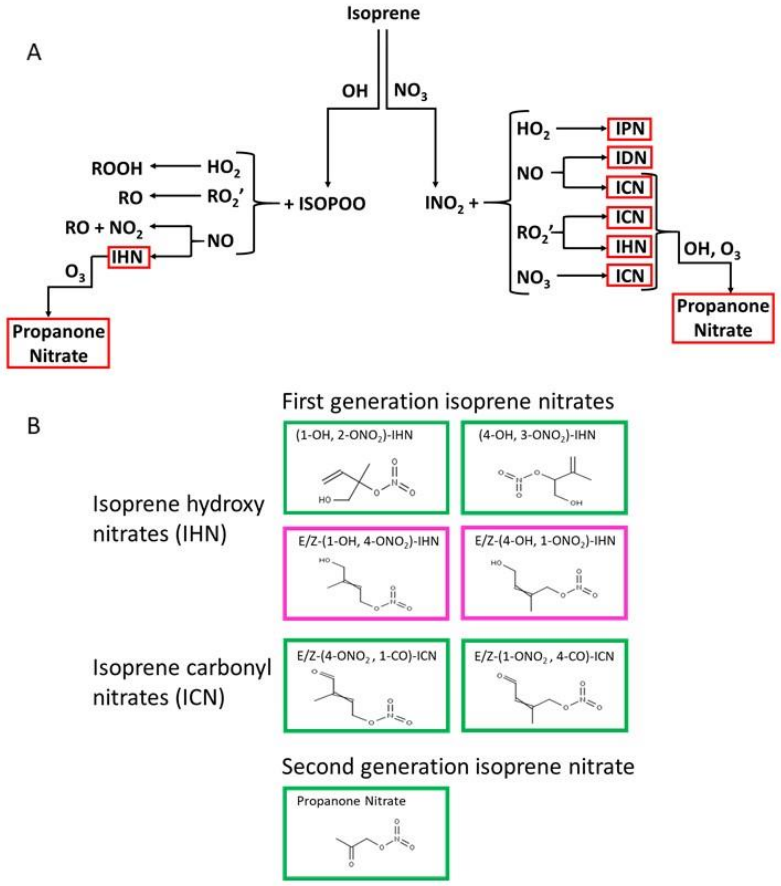

Figure 1: A) Formation of IN (red boxes) from isoprene oxidation by OH and NO_3: isoprene hydroxy nitrates (IHN): isoprene hydroperoxy nitrates (IPN); isoprene dinitrates (IDN); isoprene carbonyl nitrates (ICN); and propanone nitrate. B) The skeletal formula of the specific IN discussed in this paper. Box colours: Green - measured in Beijing; Pink - measured by the analytical system previously in the laboratory, but not discernible in Beijing.

Deleted: ¶

Page Break

¶

¶

Figure 2: Isoprene nitrates.

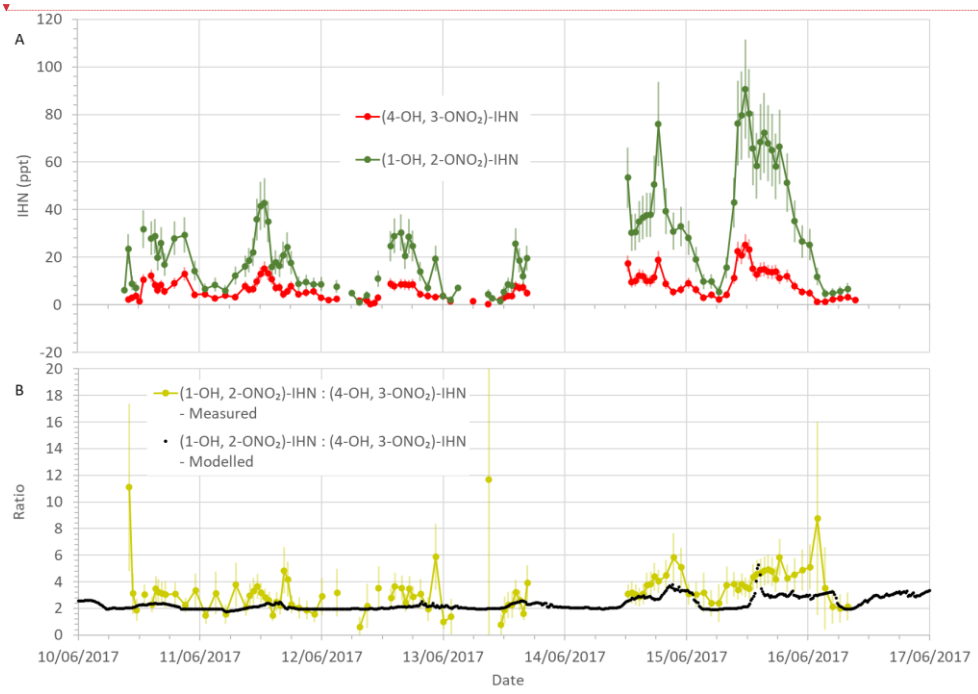

Figure 2: a) Measured β-IHN mixing ratios. b) Measured and modelled ratio (1-OH, 2-ONO_2)-IHN:(4-OH, 3-ONO_2)-IHN. Error bars are the measurement uncertainties (see Sect. 3.3 for details).

Deleted: ¶

Deleted: **Figure 3: Isoprene nitrates mixing ratios measured in Beijing.** ¶

Page Break

¶

¶

Deleted: **Figure 4: Isoprene, CO, NO, NO_2 and O_3 mixing ratios measured in Beijing for the times corresponding to the IN data shown in Fig. 3.** ¶

Page Break

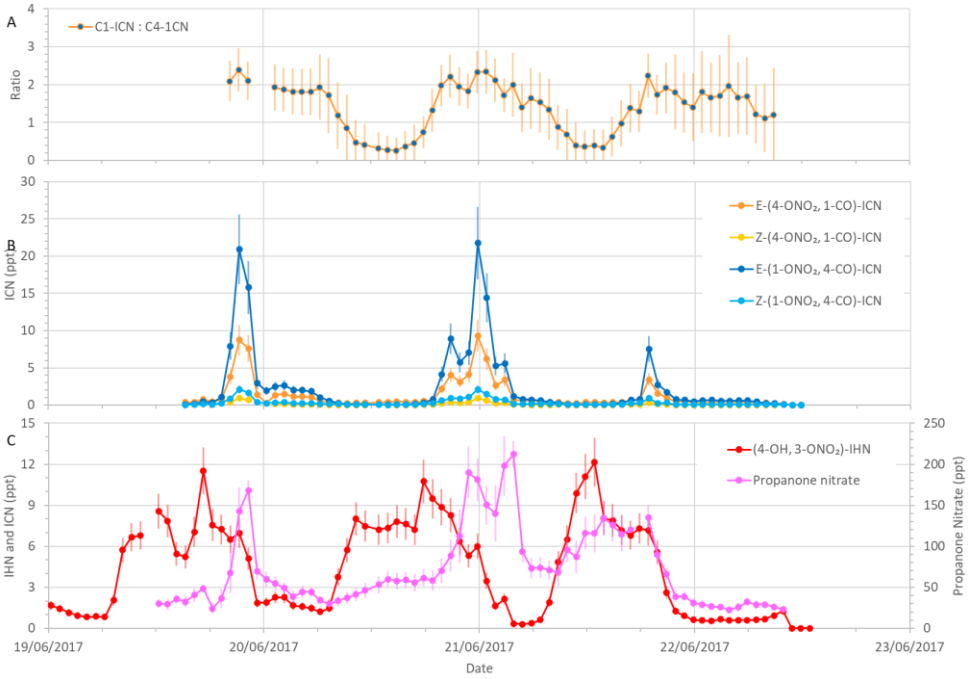

Figure 3: Measured δ-ICN mixing ratios and ratios of C1-ICN to C4-ICN, along with (4-OH, 3-ONO_2)-IHN and propanone nitrate mixing ratios during the last four days of the summer campaign. Error bars are the measurement uncertainties (see Sect. 3.3 for details).

Deleted: 6

Deleted:

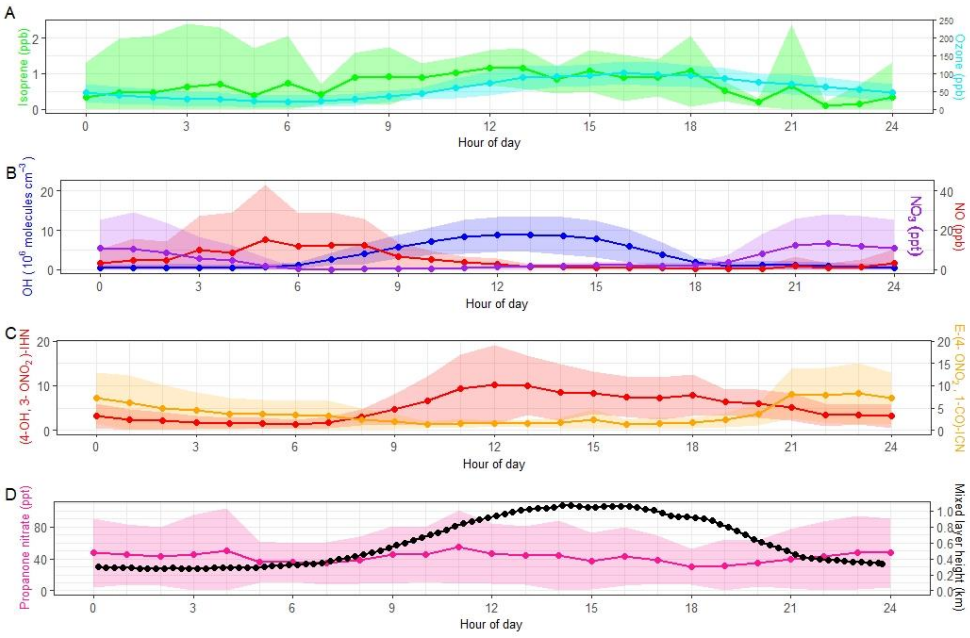

Figure 4: Diel patterns of trace gases derived from the measured mixing ratios for each hour of the day. Data points for the mixing ratios are the means and the shaded areas represent ±1 s.d. in the variability of values for each hour of the day. Also shown are the means of the mixed layer height for each 15 minute period of the day.

Deleted: 7

Deleted: medians of the

Deleted: . The observed 15 minute mean mixed layer heights used as input to the MCM model.

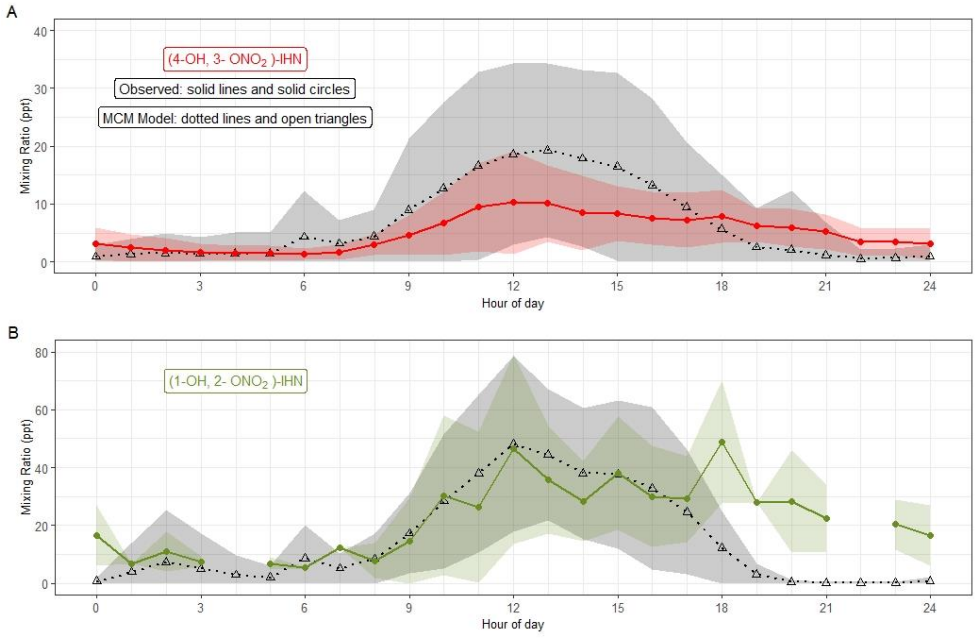

1565

Figure 5: Modelled and observed mixing ratios of (a) (4-OH, 3-ONO_2)-IHN and (b) (1-OH, 2-ONO_2)-IHN. Data points are the means and the shaded areas represent ±1 s.d. in the variability of values for each hour of the day.

Moved (insertion) [1]

Deleted: 9

Deleted: Bottom row:

Deleted: (left)

Deleted: (right)

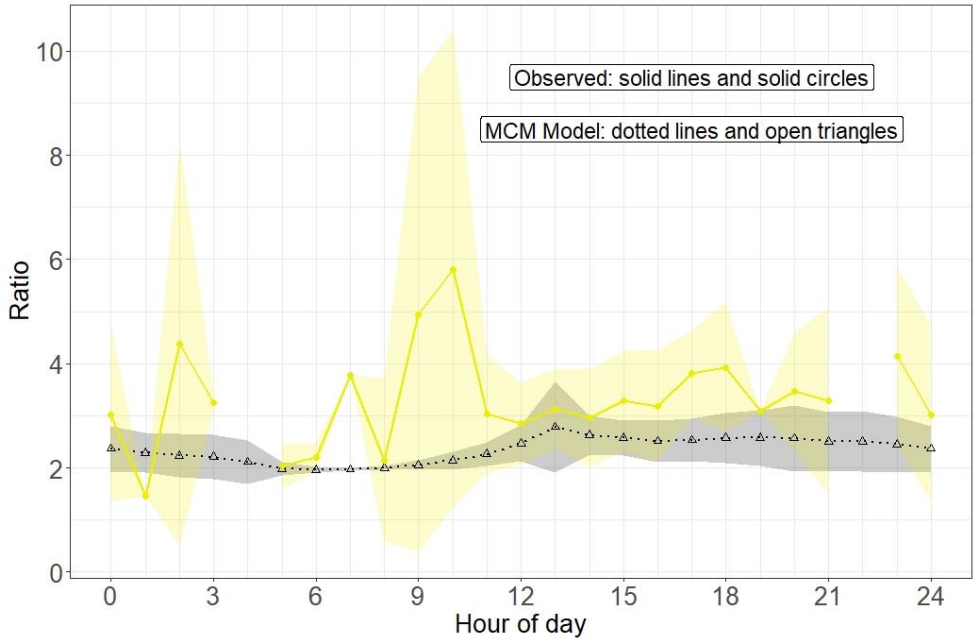

Figure 6: Modelled and observed (1-OH, 2-ONO_2)-IHN / (4-OH, 3-ONO_2)-IHN ratio. Data points are the means and the shaded areas represent ±1 s.d. in the variability of values for each hour of the day.

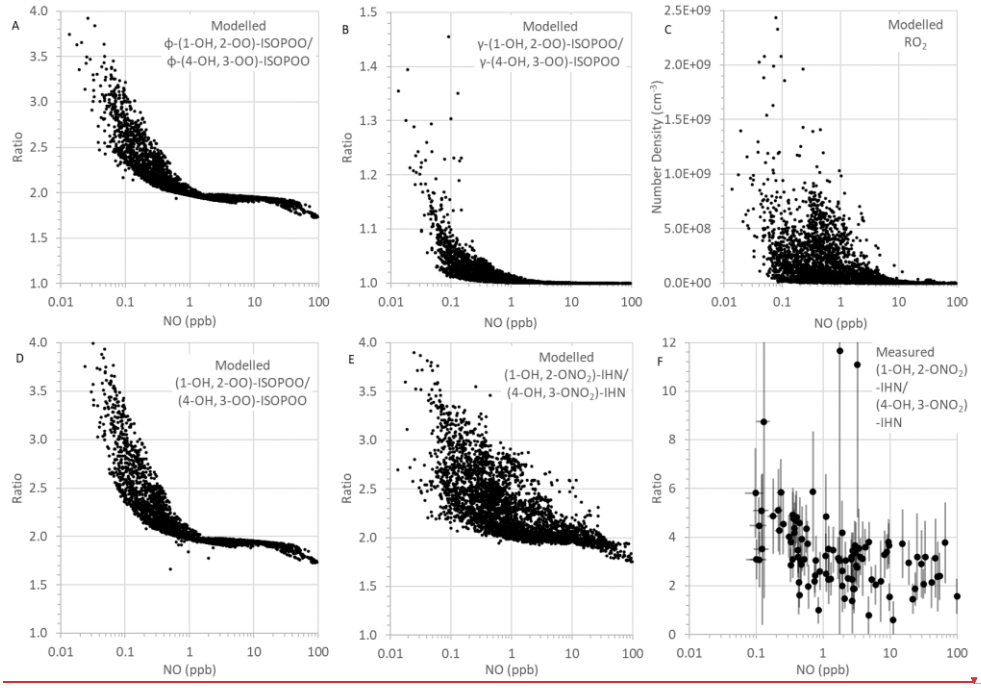

Figure 7: MCM modelled and measured parameters as a function of NO mixing ratio: (a) Modelled ratio of φ-(1-OH, 2-OO)-ISOPOO to φ- (4-OH, 3-OO)-ISOPOO; (b) Modelled ratio of γ-(1-OH, 2-OO)-ISOPOO to γ-(4-OH, 3-OO)-ISOPOO; (c) Modelled RO_2 number density; (d) Modelled ratio of (1-OH, 2-OO)-ISOPOO to (4-OH, 3-OO)-ISOPOO; (e) Modelled ratio of (1-OH, 2-ONO_2)-IHN to (4-OH, 3-ONO_2)-IHN; (f) Measured ratio of (1-OH, 2-ONO_2)-IHN to (4-OH, 3-ONO_2)-IHN (error bars are the measurement uncertainties (see Sect. 3.3 for details)).

Deleted: Top row: Calculated production rates of (4-OH, 3-ONO_2)-IHN (left) and (1-OH, 2-ONO_2)-IHN (right)….

Deleted: ¶

¶

¶

Figure 8: Measured mixing ratios of (4-OH, 3-ONO_2)-IHN, E-(4-ONO_2, 1-CO)-ICN, and propanone nitrate during the last five days of the campaign.¶

Page Break

¶

¶

Moved up [1]: Figure 9: Bottom row: Modelled and observed mixing ratios of (4-OH, 3-ONO_2)-IHN (left) and (1-OH, 2-ONO_2)-IHN (right). Top row: Calculated production rates of (4-OH, 3-ONO_2)-IHN (left) and (1-OH, 2-ONO_2)-IHN (right).¶

Deleted: Page Break

¶

¶

Figure 10: Modelled and observed (1-OH, 2-ONO_2)-IHN / (4-OH, 3-ONO_2)-IHN ratio. Coloured lines come from sensitivity runs in which the rates of production or losses of each of the β-IHN have been changed in the simple model. The MCM run is described in Sect. 6.¶

Page Break

¶

¶

¶

Figure 11: Time series of β-IHN as modelled using the MCM and measured.¶

Page Break

¶

¶

Figure 12: Diel patterns of β-IHN as modelled using the MCM and measured. Bottom row: MCM modelled and observed (4-OH, 3-ONO_2)-IHN (left) and (1-OH, 2-ONO_2)-IHN (right). The modelled values are means for each 15 minute period of the day for the whole modelled period, whereas the observed values are hourly medians. Top row: Modelled production rates of (4-OH, 3-ONO_2)-IHN (left) and (1-OH, 2-ONO_2)-IHN (right).¶

Page Break

¶

¶

Figure 13: MCM modelled parameters as a function of NO mixing ratio (top row logarithmic scale, bottom row linear scale). Left column: the ratio of (1-OH, 2-ONO_2)-IHN to (4-OH, 3-ONO_2)-IHN. Middle panel: the ratio of (1-OH, 2-OO)-ISOPOO to (4-OH, 3-OO)-ISOPOO. Right panel: the ratio of φ-(1-OH, 2-OO)-ISOPOO to φ- (4-OH, 3-OO)-ISOPOO.¶

Page Break

¶

¶

¶

Figure 14: MCM modelled parameters as a function of NO mixing ratio (top row logarithmic scale, bottom row linear scale). Left column: the ratio of γ-(1-OH, 2-OO)-ISOPOO to γ-(4-OH, 3-OO)-ISOPOO. Right panel: RO_2 number density.¶

Page Break

¶

¶

…

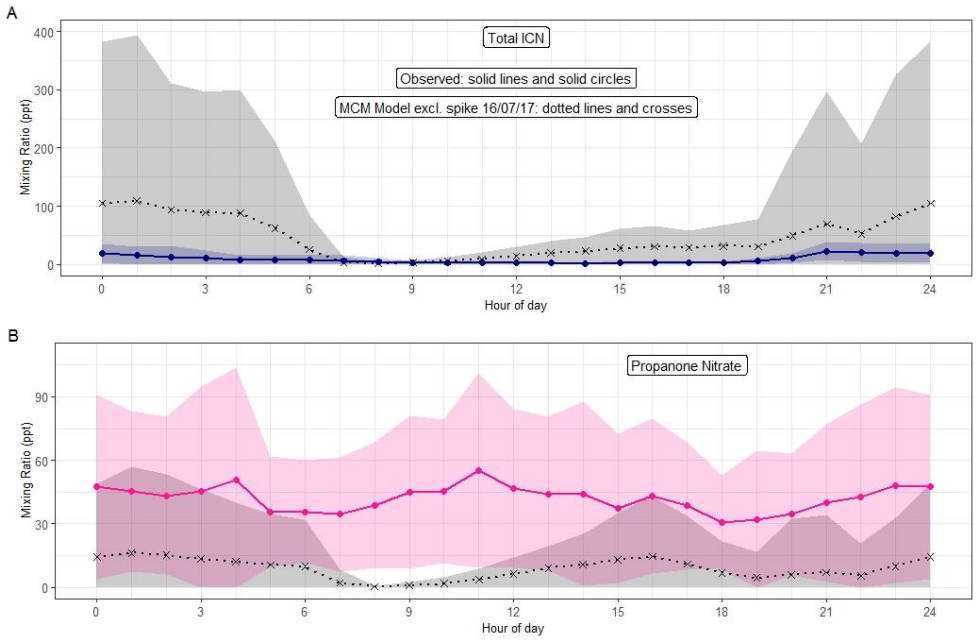

Figure 8: (a) Diel pattern of total ICN as modelled using the MCM and measured. For the MCM this is the specie NC4CHO, whilst the measurements are the sum of the four δ-ICN (E and Z-(1-ONO_2, 4-CO)-ICN and E and Z-(4-ONO_2, 1-CO)-ICN). (b) Diel pattern of propanone as modelled using the MCM and measured. Data points are the means and the shaded areas represent ±1 s.d. in the variability of values for each hour of the day.

Moved (insertion) [2]

Deleted: 7

Deleted: ¶
Figure 19:

Moved (insertion) [3]

Deleted: The dotted line with crosses is calculated with the spike in the modelled ICN in the early morning of 16th June 2017 removed. The modelled values are means for each 15 minute period of the day for the whole modelled period.(b) ¶

Deleted: The dotted line with crosses is calculated with the spike in the modelled propanone nitrate in the early morning of 16th June 2017 removed. The modelled values are means for each 15 minute period of the day for the whole modelled period.…

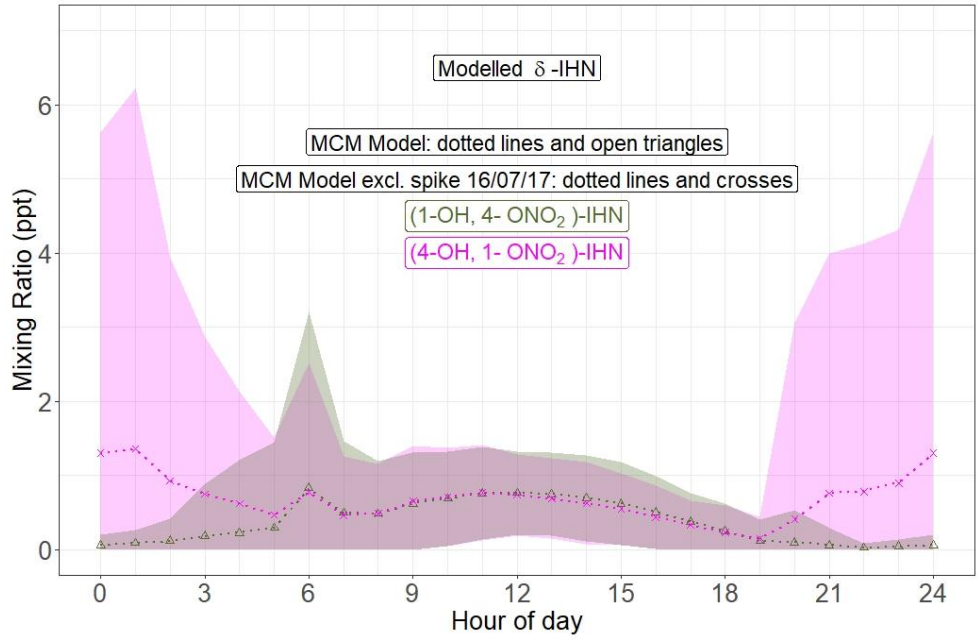

1715 **Figure 9: Diel pattern of MCM modelled δ-IHN ((1-OH, 4-ONO_2)-IHN and (4-OH, 1-ONO_2)-IHN). Data points are the means and the shaded areas represent ±1 s.d. in the variability of values for each hour of the day.**

Deleted: Page Break

Deleted: ¶

Moved up [2]: Figure 17: Diel pattern of total ICN as modelled using the MCM and measured. For the MCM this is the specie NC4CHO, whilst the measurements are the sum of the four δ-ICN (E and Z-(1-ONO_2, 4-CO)-ICN and E and Z-(4-ONO_2, 1-CO)-ICN). The dotted line with crosses is calculated with the spike in the modelled ICN in the early morning of 16th June 2017 removed. The modelled values are means for each 15 minute period of the day for the whole modelled period.¶

Deleted: Page Break

¶

¶

Figure 18: Time series of propanone nitrate as modelled using the MCM and measured, along with modelled δ-ICN (NC4CHO).¶

¶

¶

Moved up [3]: Figure 19: Diel pattern of propanone as modelled using the MCM and measured. The dotted line with crosses is calculated with the spike in the modelled propanone nitrate in the early morning of 16th June 2017 removed. The modelled values are means for each 15 minute period of the day for the whole modelled period.¶

Deleted: ¶

Page Break

¶

¶

Figure 20: Time series the MCM modelled δ-IHN ((1-OH, 4-ONO_2)-IHN and (4-OH, 1-ONO_2)-IHN) and δ-ICN (NC4CHO).¶

Page Break

¶

¶

Figure 21: Diel pattern of MCM modelled δ-IHN ((1-OH, 4-ONO_2)-IHN and (4-OH, 1-ONO_2)-IHN). The pink dotted line with crosses is calculated with the spike in the modelled (4-OH, 1-ONO_2)-IHN in the early morning of 16th June 2017 removed. The modelled values are means for each 15 minute period of the day for the whole modelled period.¶

Observations of speciated isoprene nitrates in Beijing: implications for isoprene chemistry

Claire E. Reeves[1], Graham P. Mills[1], Lisa K. Whalley[2], W. Joe F. Acton[3], William J. Bloss[4], Leigh R. Crilley[4,5], Sue Grimmond[6], Dwayne E. Heard[7], C. N. Hewitt[3], James R. Hopkins[8], Simone Kotthaus[6,9], Louisa J. Kramer[4], Roderic L. Jones[10], James D. Lee[8], Yanhui Liu[1], Bin Ouyang[10], Eloise Slater[7], Freya Squires[11], Xinming Wang[12], Robert Woodward-Massey[13], and Chunxiang Ye[13]

[1]Centre for Ocean and Atmospheric Sciences, School of Environmental Sciences, University of East Anglia, UK
[2]National Centre for Atmospheric Science, School of Chemistry, University of Leeds, UK
[3]Lancaster Environment Centre, Lancaster University, Lancaster, UK
[4]School of Geography, Earth and Environmental Sciences, the University of Birmingham, Birmingham, B15 2TT, UK
[5]now at Department of Chemistry, York University, Toronto, Canada.
[6]Department of Meteorology, University of Reading, Reading, UK
[7]School of Chemistry, University of Leeds, UK
[8]National Centre for Atmospheric Science, Wolfson Atmospheric Chemistry Laboratories, Department of Chemistry, University of York, UK
[9]Institut Pierre Simon Laplace, Ecole Polytechnique, France
[10]Department of Chemistry, University of Cambridge, UK
[11]Wolfson Atmospheric Chemistry Laboratories, Department of Chemistry, University of York, UK
[12]Guangzhou Institute of Geochemistry, Chinese Academy of Sciences, Guangzhou, China
[13]Beijing Innovation Center for Engineering Science and Advanced Technology, State Key Joint Laboratory for Environmental Simulation and Pollution Control, Center for Environment and Health, College of Environmental Sciences and Engineering, Peking University, Beijing, 100871, China

Correspondence to: Claire E. Reeves (c.reeves@uea.ac.uk)

Supplementary Information

S1. Isoprene Nitrate Chemistry

A detailed description of the gas-phase chemistry of isoprene and its major oxidation products is given in the recent review by Wennberg et al. (2018) (hereafter referred to as W2018). In this section a summary of the chemistry relating to IN (largely based on W2018) is provided with a focus on those IN that we are able to measure in the field.

S1.1. Formation of First Generation IN via Oxidation of Isoprene by OH

The OH reaction dominates accounting for around 85 % of the reactive fate of isoprene largely due to concurrent daytime presence of isoprene and OH. On addition of OH to isoprene 6 OH-adducts are formed. Addition at C2 and C3 constitute only very minor channels (<2%). The 4 main adducts are formed through C1 and C4 addition (approximately in a 63:37 ratio (Teng et al., 2017)), each with a pair of *cis* (Z) and *trans* (E) isomers (approximately 50:50 *cis*:*trans* for 1-OH adducts and 70:30 *cis*:*trans* for 4-OH adducts) (W2018). On reaction with O_2 these adducts form peroxy radicals (ISOPOO). These reactions are reversible and have differing rates which along with rapid 1,6 H atom shift isomerisation of the Z-δ-ISOPOO leading to hydroperoxyaldeyhyde (HPALD), this leads to interconversion of the peroxy radicals within a sub group (i.e. having a common OH position) and an equilibrated thermal peroxy radical distribution that has a greater β:δ ratio to the kinetic one (Teng et al., 2017; Peeters et al. 2009; Peeters et al. 2014). Note, that this change from the kinetic to thermodynamic equilibrium will be more important when the peroxy radical

bimolecular lifetimes exceed around 0.01 – 0.1 s, which is not the case when NO is greater than 10 ppb. Uncertainty in the peroxy distribution remains, but β peroxy radicals (i.e. β-(1-OH, 2-OO)-ISOPOO and β-(4-OH, 3-OO)-ISOPOO) dominate over the δ peroxy radicals (i.e. E/Z δ-(1-OH, 4-OO)-ISOPOO and E/Z δ-(4-OH, 1-OO)-ISOPOO).

These peroxy radicals react with nitric oxide (NO) forming primarily alkoxy radicals and nitrogen dioxide (NO_2), but with a channel leading to the production of isoprene hydroxy nitrates (IHN). The rates of these reaction do not seem very sensitive to small changes in the structure of the peroxy radical (W2018). However, there is considerably uncertainty over the branching ratio for the formation of the IHN. This is important since the primary reaction leads to O_3 formation, via NO_2 photolysis, and to radical propagation, whilst the formation of IHN acts as a chain-terminating step, with the IHN being a reservoir for NO_X and radicals.

Estimates of the branching ratio for the formation of IHN from these reactions vary from 0.04 to 0.15 (Tuazon at al., 1990; Chen et al., 1998; Chuong et al., 2002; Sprengnether et al., 2002; Patchen et al., 2007; Paulot et al., 2009; Lockwood et al., 2010; Xiong et al., 2015; Teng et al., 2017), with the most recent estimate being 0.13 (Teng et al., 2017). Moreover, the branching ratio is poorly constrained for individual peroxy radicals, with Paulot et al (2009) estimating that they may vary from 0.067 to 0.24 for different isomers whilst Teng et al., (2017) estimate that they differ by only about 10% (i.e. 0.12 to 0.14). It is thought that some of these discrepancies can be explained by the differing experimental techniques used to derive these branching ratios, but there are also uncertainties associated with the temperature and pressure dependencies of these branching ratios (Piletic et al., 2017; W2018).

These reactions of the peroxy radicals with NO are in competition with reactions with the hydro peroxy radical (HO_2) (Jenkin et al., 1998) , other organic peroxy radicals (RO_2) (Jenkin and Hayman, 1995) and H-shift isomerization (Peeters and Nguyen, 2012; Crounse et al., 2011; Teng et al., 2017), all of which have their own uncertainties, which will consequently affect the yield of IHN.

S1.2. Formation of First Generation IN via Oxidation of Isoprene by NO_3

Addition of NO_3 to the isoprene double bond followed by addition of O_2 produces nitroxy peroxy radicals (INO_2). The NO_3 addition at C1 dominates over C4 by 6:1 and the subsequent addition of O_2 leads to β-INO_2 and δ-INO_2 in approximately a 50:50 ratio, with the β-(1-ONO_2, 2-OO)-INO_2 and δ-(1-ONO_2, 4-OO)-INO_2 dominating (W2018). The E and Z isomers are presumed to be formed in equal amounts and their subsequent chemistry largely the same. The details of this understanding are based largely on one study (Schwantes et al., 2015) and there remains considerable uncertainty (W2018).

These INO_2 can go on to form different types of isoprene derived nitrates through various reaction pathways: 1) isoprene hydroperoxy nitrates (IPN) following reaction of INO_2 with HO_2; 2) isoprene carbonyl nitrates (ICN) from the δ-nitroxy alkoxy radicals formed from the major channel of the δ-INO_2 reaction with NO; 3) ICN from reaction of δ-INO_2 with NO_3; 4) isoprene dinitrates (IDN) in a minor channel following reaction of INO_2 with NO; and 5) IHN and ICN following reactions of INO_2 with RO_2 (including self-reactions of INO_2) (W2018).

In pathway 5, Schwantes et al (2015) reckon that 80% of IHN formed are δ-IHN and 20% are β-IHN. Note that because the NO_3 addition to isoprene occurs at the C1 and C4 positions, the β-IHN formed are β-(2-OH, 1-ONO_2)-IHN and β-(3-OH, 4-ONO_2)-IHN and not the more common β-IHN formed from the OH oxidation of isoprene (i.e. β-(1-OH, 2-ONO_2)-IHN and β-(4-OH, 3-ONO_2)-IHN). The ICN formed from the δ-INO_2 peroxy radicals (in 3 and 5 above) are the E/Z-δ-(1-ONO_2, 4-CO)-ICN and E/Z-δ-(4-ONO_2, 1-CO)-ICN and as the NO_3 addition to isoprene predominantly occurs in the C1 position the main ICN formed are the E/Z-δ-(1-ONO_2, 4-CO)-ICN.

S1.3. Fate of IN and Formation of Second Generation IN

S1.3.1 Reaction with OH

For the dominant β-IHN (i.e. β-(1-OH, 2-ONO_2)-IHN and β-(4-OH, 3-ONO_2)-IHN) reaction with OH occurs via addition to one of the two carbons in the remaining double bond, giving lifetimes of around 6-10 hours for OH mixing ratios of 0.04 ppt at 298K and 993 hPa (based on the rates from Teng et al. (2017), Lee et al. (2014), Jacobs et al. (2014) and W2018). The resulting adduct predominantly reacts with O_2 to form a peroxy radical, but a fraction can undergo unimolecular rearrangement to form an isoprene expoxydiol (IEPOX) releasing NO_2 (Jacobs et al., 2014; St Clair et al., 2016; W2018). The peroxy radicals formed can react with NO or with HO_2, potentially releasing NO_2. In theory (Kurtén et al., 2017) both of these reactions have a branch leading to the formation HO_2 and formaldehyde along with second-generation nitrates: methacrolein nitrate ((2-ONO_2, 3-OH)-MACR) in the case of the β-(1-OH, 2-ONO_2)-IHN, and methyl vinyl ketone nitrate ((3-ONO_2, 4-OH)-MVK)) in the case of the β-(4-OH, 3-ONO_2)-IHN. With respect to β-(1-OH, 2-ONO_2)-IHN, however, W2018 states that there is evidence of only low yields of MACR nitrate. There is also evidence of a small yield of dinitrates (Lee et al., 2014).

The mechanisms for the OH oxidation of the β-(2-OH, 1-ONO_2)-IHN and β-(3-OH, 4-ONO_2)-IHN are less well constrained but are thought to yield peroxy radicals which can react with NO and HO_2 to form a range of products including smaller chained carbonyls and nitrates (i.e. MACR nitrate and propanone nitrate from β-(2-OH, 1-ONO_2)-IHN, and MVK nitrate and ethanal nitrate from β-(3-OH, 4-ONO_2)-IHN), but not direct release of NO_2 (W2018).

For δ-IHN the reaction rates with OH are 2-3 times faster than for the β-IHN, having lifetimes of around 3-4 hours for OH mixing ratios of 0.04 ppt at 298K and 993 hPa (based on the rates from Teng et al. (2017), Lee et al. (2014) and W2018). OH adds to the C2 and C3 positions of the δ-IHN followed primarily by O_2 addition to form peroxy radicals, but a minor pathway is decomposition to form IEPOX and NO_2. Similar to the β-IHN, the peroxy radicals react with NO and HO_2 leading to smaller chained carbonyls and nitrates (i.e. MACR nitrate and propanone nitrate from δ-(4-OH, 1-ONO_2)-IHN, and MVK nitrate and ethanal nitrate from δ-(1-OH, 4-ONO_2)-IHN), but not direct release of NO_2.

As for reactions of ICN with OH, Xiong et al., (2016) only measured the rate for (4-ONO2, 1-CO)-ICN so W2018 recommends that the rate for the major isomer, (1-ONO_2, 4-CO)-ICN, is scaled based on the rates of reactions of the respective IHN isomer counterparts with OH. The OH loss rates for δ-ICN are slower than for the δ-IHN, instead being similar to those of the β-IHN. Following OH addition, NO_2 release can occur but the dominant products are peroxy radicals following O_2 addition (W2018). Reaction of the peroxy radicals with NO lead to MVK nitrate, ethanal nitrate

(Xiong et al., 2016) and propanone nitrate (MCM (http://mcm.york.ac.uk)). H abstraction is of similar importance to OH addition for reactions of OH with δ-ICN oxidation.

S1.3.2 Reaction with O_3

Reaction rates of five IHN with O_3 have been reported: (2-OH, 1-ONO_2)-IHN (Lockwood et al., 2010); (1-OH, 2-ONO_2)-IHN (Lockwood et al., 2010; Teng et al., 2017); E-δ-(1-OH, 4-ONO_2)-IHN (Lockwood et al., 2010; Lee et al., 2014); Z-δ-(1-OH, 4-ONO_2)-IHN (Lee et al., 2014); and (4-OH, 3-ONO_2)-IHN (Lee et al., 2014). However, the rates of Lockwood et al. (2010) are 2-3 orders of magnitude faster than those of Lee et al. (2014) and Teng et al. (2017). Due to the observed presence of IHN at night (Beaver et al., 2012), W2018 recommend the lower rates of Lee et al. (2014) and Teng et al. (2017) (i.e. β-IHN lifetimes of around 500-1000 hours and δ-IHN lifetimes of around 10 hours for O_3 mixing ratios of 40 ppb at 298K and 993 hPa). The rate constant for the reaction of O_3 with one of the ICN has been measure: (1-CO, 4-ONO_2)-ICN (Xiong et al., 2016), giving a lifetime of around 65 hours for O_3 mixing ratios of 40 ppb at 298K and 993 hPa (W2018). Rates for all other IHN, IPN and ICN are extrapolated from these rates with the loss rate for the δ-IN by O_3 oxidation approximately 2 orders of magnitude faster than those of the β-IN (W2018).

Reactions of O_3 with both δ-(4-OH, 1-ONO_2)-IHN and (1-ONO_2, 4-CO)-ICN can lead to propanone nitrate (MCM (http://mcm.york.ac.uk)), so it can be formed from IN both during the day and during the night.

S1.3.3 Reaction with NO_3

For the reactions of IN with NO_3, there has only been one published study which measured the rate of reaction of NO_3 with bulk IHN (Rollins et al., 2009) and one unpublished study that assessed the reaction of NO_3 with (4-OH, 3-ONO_2)-IHN (W2018). Rates for all IN can be constrained by extrapolations from these two studies, with the loss rate for the δ-IN by NO_3 oxidation assumed to be 4 times faster than those of the β-IN (W2018).

Reactions of NO_3 with (1-ONO_2, 4-CO)-ICN can also lead to propanone nitrate (MCM, (http://mcm.york.ac.uk)).

S1.3.4 Photolysis

Very few studies provide information on the photolysis of IN. Xiong et al. (2016) measured the absorption cross-section for (1-CO, 4-ONO_2)-ICN and estimated its ambient photolysis frequency to be 3.1 x 10^{-4} s^{-1} for a solar zenith angle of 45° and 4.6 x 10^{-4} s^{-1} for a solar zenith angle of 0°, with photolysis being a dominant daytime sink. Müller et al. (2014) make recommendations for the photolysis rates of second-generation IN such as propane nitrates, ethanal nitrate, MACR nitrates and MVK nitrates, based on published values for nitroxy-ketones. They estimate the photolysis rates of key carbonyl nitrates from isoprene to be typically between 3 and 20 times higher than their sink due to reaction with OH in relevant atmospheric conditions. Moreover, since the reaction is expected to release NO_2, photolysis is especially effective in recycling NO_X. Xiong et al. (2015) found that when they enhanced the photolysis rates of the IHN in their model to about 30-50% of their total loss, they had better agreement with observed mixing ratios.

S1.3.5 Hydrolysis

Very little is known about this, but hydrolysis lifetimes of 18 h and 2.5 min have been reported for (4-OH, 3-ONO_2)-IHN and (1-OH, 4-ONO_2)-IHN (Jacobs et al., 2014) and a further unpublished study suggests that (1-OH, 2-ONO_2)-IHN has a lifetime of less than 1 second in water (W2018).

S1.3.5 Deposition

Nguyen et al. (2015) measured the deposition velocity of temperate forest and found a string diurnal pattern, with a daytime (10:00-15:00 h) mean of 1.5 ± 0.6 cm s^{-1} and low values during the night-time. They also reported similar daytime means for the second generation IN, MACR and MVK nitrates (1.5 ± 0.5 cm s^{-1}) and propanone nitrate (1.7 ± 0.6 cm s^{-1}).

S2. Supporting data – instrumentation and uncertainties

A large suite of meteorological and chemical measurements was made during the campaigns (Shi et al., 2019). Here we describe briefly those used in this paper. Isoprene was measured using a dual channel GC with a flame ionisation detector (DC-GC-FID) (Hopkins et al. (2011), with an uncertainty of around 5% depending on the mixing ratio calculated following procedures set out in the ACTRIS Measurement Guidelines (Reimann et al, 2018). Measurements of OH, HO_2 and RO_2 were obtained using the fluorescence assay by gas expansion (FAGE) technique equipped with a scavenger inlet for OH, with the OH chem method used to obtain the background OH signal (Whalley et al., 2010; Whalley et al., 2018; Woodward-Massey et al., 2019). The median limit of detection (LOD) during the campaign was 6.1×10^5 molecule cm^{-3} for OH, 2.8×10^6 molecule cm^{-3} for HO_2 and 7.2×10^6 molecule cm^{-3} for CH_3O_2 at a typical laser power of 11 mW for a 5 minute data acquisition cycle (SNR=2). The accuracy of the measurements was ~ 26 % (2 σ) and is derived from the error in the calibration.

A Thermo Environmental Instruments (TEI) 49i UV absorption analyser was used to measure O_3 (uncertainty 4.04%, precision 0.28 ppb). NO was measured using a TEI 42i (uncertainty 4.58%, precision 0.03 ppb), NO_2 by a Teledyne cavity attenuated phase shift (CAPS) instrument (uncertainty 5.73%, precision 0.04 ppb) and CO by a sensor box (uncertainty 9.14%, precision 2.14 ppb) (Smith et al., 2017). The precisions quoted above are 2 σ precisions calculated from the standard deviation of the zero calibration and then divided by square root of the number of measurements during a 15-minute averaging time. The O_3 uncertainty is derived from the uncertainty of its reaction with NO in the sample line. The uncertainties in the NO measurements are calculated as the sum of the uncertainty in calibration cylinder, the standard deviation of the calibration and the uncertainty due to reaction of O_3 with NO in the sample line. Both the NO and NO_2 calibration cylinders are traceable to the National Physics Laboratory NO scale. The CO uncertainty is the sum of the uncertainty in calibration cylinder and the standard deviation of the calibration.

NO_3 and glyoxal were measured using broadband cavity enhanced absorption spectroscopy (Kennedy et al., 2011). The measurement accuracy of NO_3 is around 1 ppt at 5 seconds sampling rate, which can be reduced by averaging, such that during the early afternoon the hourly mean uncertainties are greatest at around 0.5 ppt, i.e. 20% of the mean mixing ratio. HONO was measured by a long path absorption photometer (LOPAP) (Crilley et al., 2016). A proton transfer reaction-time of flight-mass spectrometer (PTR-ToF-MS) was used to measure multi-functional aromatics and monoterpenes, whilst HCHO was measured by LIF (Cryer, 2016). SO_2 was measured by a TEI 43i instrument. The

mixed layer height was determined from the attenuated backscatter measured with a Vaisala CL31 ceilometer (Kotthaus and Grimmond (2018), and photolysis rates from spectral radiometer measurements (Bohn et al., 2016).

S3. References

Beaver, M. R., St Clair, J. M., Paulot, F., Spencer, K. M., Crounse, J. D., LaFranchi, B. W., Min, K. E., Pusede, S. E., Wooldridge, P. J., Schade, G. W., Park, C., Cohen, R. C., and Wennberg, P. O.: Importance of biogenic precursors to the budget of organic nitrates: observations of multifunctional organic nitrates by CIMS and TD-LIF during BEARPEX 2009, Atmos. Chem. Phys., 12, 5773-5785, doi: 10.5194/acp-12-5773-2012, 2012.

Chen, X., Hulbert, D., and Shepson, P. B.: Measurement of the organic nitrate yield from OH reaction with isoprene, J. Geophys. Res., 103, 25,563-25,568, 1998.

Chuong, B., and Stevens, P. S.: Measurements of the Kinetics of the OH-Initiated Oxidation of Isoprene. J. Geophys. Res., 107 (D13), ACH 2-1−ACH 2-12, 2002.

Crounse, J. D., Paulot, F., Kjaergaard, H. G., and Wennberg, P. O.: Peroxy radical isomerization in the oxidation of isoprene, Phys. Chem. Chem. Phys., 13, 13607-13613, doi: 10.1039/c1cp21330j, 2011.

Hopkins, J. R., Jones, C. E., and Lewis, A. C.: A dual channel gas chromatograph for atmospheric analysis of volatile organic compounds including oxygenated and monoterpene compounds, J. Environ. Monitor., 13, 2268–2276, 2011.

Jacobs, M. I., Burke, W. J., and Elrod, M. J.: Kinetics of the reactions of isoprene-derived hydroxynitrates: gas phase epoxide formation and solution phase hydrolysis, Atmos. Chem. Phys., 14, 8933-8946, doi: 10.5194/acp-14-8933-2014, 2014.

Jenkin, M. E, and Hayman, G. D.: Kinetics of Reactions of Primary, Secondary and Tertiary β-Hydroxy Peroxyl Radicals: Application to Isoprene Degradation, J. Chem. Soc., 13, 1911-1922, 1995.

Jenkin, M. E., Boyd, A. A., and Lesclaux, R.: Peroxy Radical Kinetics Resulting from the OH-Initiated Oxidation of 1,3-Butadiene, 2,3-Dimethyl-1,3-Butadiene and Isoprene, J. Atmos. Chem., 29, 267-298, 1998.

Kurtén, T., Møller, K. H., Nguyen, T. B., Schwantes, R. H., Misztal, P. K., Su, L., Wennberg, P. O., Fry, J. L., and Kjaergaard, H. G., Alkoxy Radical Bond Scissions Explain the Anomalously Low Secondary Organic Aerosol and Organonitrate Yields From α-Pinene + NO_3, J. Phys. Chem. Lett., 8, 2826−2834, 2017.

Lee, L., Teng, A. P., Wennberg, P. O., Crounse, J. D., and Cohen, R. C.: On Rates and Mechanisms of OH and O_3 Reactions with Isoprene Derived Hydroxy Nitrates, J. Phys. Chem., 118, 1622-1637, doi: 10.1021/jp4107603, 2014.

Lockwood, A. L., Shepson, P. B., Fiddler, M. N., and Alaghmand, M.: Isoprene nitrates: preparation, separation, identification, yields, and atmospheric chemistry, Atmos. Chem. Phys., 10, 6169-6178, doi: 10.5194/acp-10-6169-2010, 2010.

Mills, G. P., Hiatt-Gipson, G. D., Bew, S. P., and Reeves, C. E.: Measurement of isoprene nitrates by GCMS, Atmos. Meas. Tech., 9, 4533-4545, doi: 10.5194/amt-9-4533-2016, 2016.

Müller, J.-F., Peeters, J., and Stavrakou, T.: Fast photolysis of carbonyl nitrates from isoprene, Atmos. Chem. Phys., 14, 2497-2508, doi: 10.5194/acp-14-2497-2014, 2014.

Nguyen, T. B., Crounse, J. D., Teng, A. P., St Clair, J. M., Paulot, F., Wolfe, G. M., and Wennberg, P. O.: Rapid deposition of oxidized biogenic compounds to a temperate forest, P. Natl. Acad. Sci., 112, E392-E401, doi: 10.1073/pnas.1418702112, 2015.

Patchen, A. K., Pennino, M. J., Kiep, C. A., and Elrod, M. J.: Direct Kinetics Study of the Product-Forming Channels of the Reaction of Isoprene-Derived Hydroxyperoxy Radicals with NO, Int. J. Chem. Kinet., 39, 353-361, doi: 10.1002/kin.20248, 2007.

Paulot, F., Crounse, J. D., Kjaergaard, H. G., Kroll, J. H., Seinfeld, J. H., and Wennberg, P. O.: Isoprene photooxidation: new insights into the production of acids and organic nitrates, Atmos. Chem. Phys., 9, 1479-1501, 2009.

Peeters, J. and Nguyen, T. L: Unusually fast 1,6-H shifts of enolic hydrogens in peroxy radicals: formation of the first-generation C_2 and C_3 carbonyls in the oxidation of isoprene, J. Phys. Chem. A, 116, 6134–6141, 2012.

Peeters, J., Nguyen, T. L., and Vereecken, L.: HOx radical regeneration in the oxidation of isoprene, Phys. Chem. Chem. Phys., 28, 5935–5939, 2009.

Peeters, J., Müller, J. F., Stavrakou, T., and Nguyen, V. S.: Hydroxyl Radical Recycling in Isoprene Oxidation Driven by Hydrogen Bonding and Hydrogen Tunneling: The Upgraded LIM1 Mechanism, J. Phys. Chem., 118, 8625-8643, doi: 10.1021/jp5033146, 2014.

Piletic, I. R., Edney, E. O., and Bartolotti, L. J.: Barrierless Reactions with Loose Transition States Govern the Yields and Lifetimes of Organic Nitrates Derived from Isoprene, J. Phys. Chem., 121, 8306-8321, doi: 10.1021/acs.jpca.7b08229, 2017.

Reimann, S., Wegener, R., Claude, A., and Sauvage, S.: ACTRIS-2 WP3 - Deliverable 3.17. Updated Measurement Guideline for NOx, and VOCs, https://www.actris.eu/Portals/46/Documentation/actris2/Deliverables/public/WP3_D3.17_M42.pdf?ver=2018-11-12-143115-077, 2018.

Rollins, A. W., Kiendler-Scharr, A., Fry, J. L., Brauers, T., Brown, S. S., Dorn, H.-P., Dubé, W. P., Fuchs, H., Mensah, A., Mentel, T. F., Rohrer, F., Tillmann, R., Wegener, R., Wooldridge, P. J., and Cohen, R. C.: Isoprene oxidation by nitrate radical: alkyl nitrate and secondary organic aerosol yields, Atmos. Chem. Phys., 9, 6685-6703, 2009.

Schwantes, R. H., Teng, A. P., Nguyen, T. B., Coggon, M. M., Crounse, J. D., St Clair, J. M., Zhang, X., Schilling, K. A., Seinfeld, J. H., and Wennberg, P. O.: Isoprene NO_3 Oxidation Products from the $RO_2 + HO_2$ Pathway, J. Phys. Chem., 119, 10158-10171, doi: 10.1021/acs.jpca.5b06355, 2015.

Sprengnether, M., Demerjian, K. L., Donahue, N. M., and Anderson, J. G.: Product analysis of the OH oxidation of isoprene and 1,3-butadiene in the presence of NO, J. Geophys. Res., 107, D15, 4268, doi: 10.1029/2001JD000716, 2002.

St Clair, J. M., Rivera-Rios, J. C., Crounse, J. D., Knap, H. C., Bates, K. H., Teng, A. P., Jørgensen, S., Kjaergaard, H. G., Keutsch, F. N., and Wennberg, P. O., Kinetics and Products of the Reaction of the First- Generation Isoprene Hydroxy Hydroperoxide (ISOPOOH) with OH, J. Phys. Chem., 120, 1441−1451, 2016.

Tuazon, E. C., Atkinson, R. A, Product Study of the Gas-Phase Reaction of Methacrolein with the OH Radical in the Presence of NOx, Int. J. Chem. Kinet., 22, 591−602, 1990.

Teng, A. P., Crounse, J. D., and Wennberg, P. O.: Isoprene Peroxy Radical Dynamics, J. Am. Che. Soc., 139, 5367-5377, doi: 10.121/jacs.6b12838, 2017.

Wennberg, P. O., Bates, K. H., Crounse, J. D., Dodson, L. G., McVay, R. C., Mertens, L. A., Nguyen, T. B., Praske, E., Schwantes, R. H., Smarte, M. D., St Clair, J. M., Teng, A. P., Zhang, X., and Seinfeld, J. H.: Gas-Phase Reactions of Isoprene and Its Major Oxidation Products, Chem. Rev., 118, 3337-3390, doi: 10.1021/acs.chemrev.7b00439, 2018.

Whalley, L. K., Furneaux, K. L., Goddard, A., Lee, J. D., Mahajan, A., Oetjen, H., Read, K. A., Kaaden, N., Carpenter, L. J., Lewis, A. C., Plane, J. M. C., Saltzman, E. S., Wiedensohler, A., and Heard, D. E.: The chemistry of OH and HO_2 radicals in the boundary layer over the tropical Atlantic Ocean, Atmos. Chem. Phys., 10, 1555–1576, https://doi.org/10.5194/acp10-1555-2010, 2010.

Whalley, L. K., Stone, D., Dunmore, R., Hamilton, J., Hopkins, J. R., Lee, J. D., Lewis, A. C., Williams, P., Kleffmann, J., Laufs, S., Woodward-Massey, R., and Heard, D. E.: Understanding in situ ozone production in the summertime through radical observations and modelling studies during the Clean air for London project (ClearfLo), Atmos. Chem. Phys., 18, 2547–2571, https://doi.org/10.5194/acp-18-2547-2018, 2018.

Woodward-Massey, R., Whalley, L. K., Slater, E. J., Allen, J., Ingham, T., Cyer, D. R., Stimpson, L. M., Ye, C., Seakins, P. W., and Heard, D. E.: Implementation of a chemical background method for atmospheric OH measurements by laser-induced fluorescence: characterisation and observations from the UK and China, Atmos. Meas. Tech., 13, 3119–3146, https://doi.org/10.5194/amt-13-3119-2020, 2020

Xiong, F., McAvey, K. M., Pratt, K. A., Groff, C. J., Hostetler, M. A., Lipton, M. A., Starn, T. K., Seeley, J. V., Bertman, S. B., Teng, A. P., Crounse, J. D., Nguyen, T. B., Wennberg, P. O., Misztal, P. K., Goldstein, A. H., Guenther, A. B., Koss, A. R., Olson,K. F., de Gouw, J. A., Baumann, K., Edgerton, E. S., Feiner, P. A., Zhang, L., Miller, D. O., Brune, W. H., and Shepson, P. B.: Observation of isoprene hydroxynitrates in the southeastern United States and implications for the fate of NOx, Atmos. Chem. Phys., 15, 11257-11272, doi: 10.5194/acp-15-11257-2015, 2015.

Xiong, F., Borca, C. H., Slipchenko, L. V., and Shepson, P. B.: Photochemical degradation of isoprene-derived 4,1-nitrooxy enal, Atmos. Chem. Phys., 16, 5595-5610, doi: 10.5194/acp-16-5595-2016, 2016.

S4. Figures

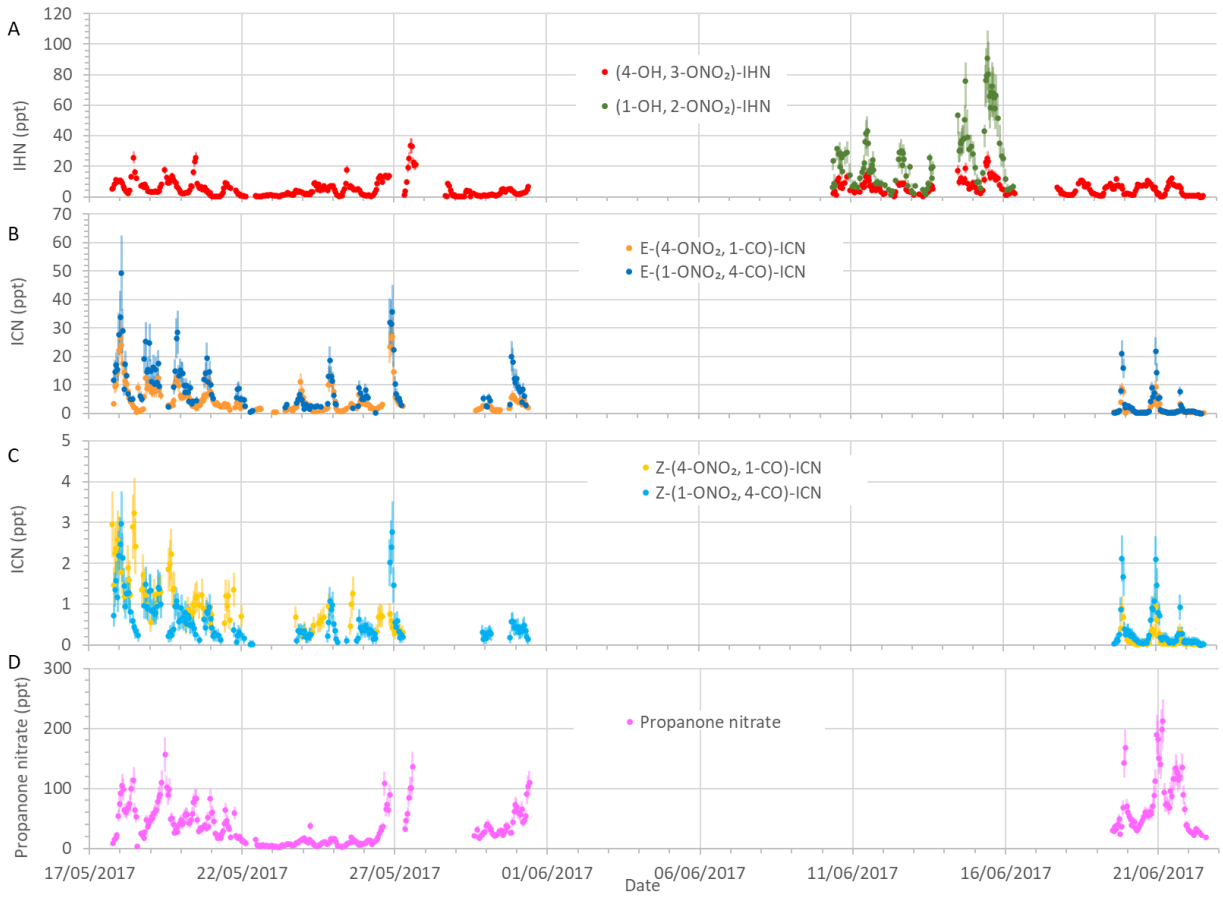

Figure S1: Isoprene nitrates mixing ratios measured in Beijing. Error bars are the measurement uncertainties (see Sect. 3.2 for details).

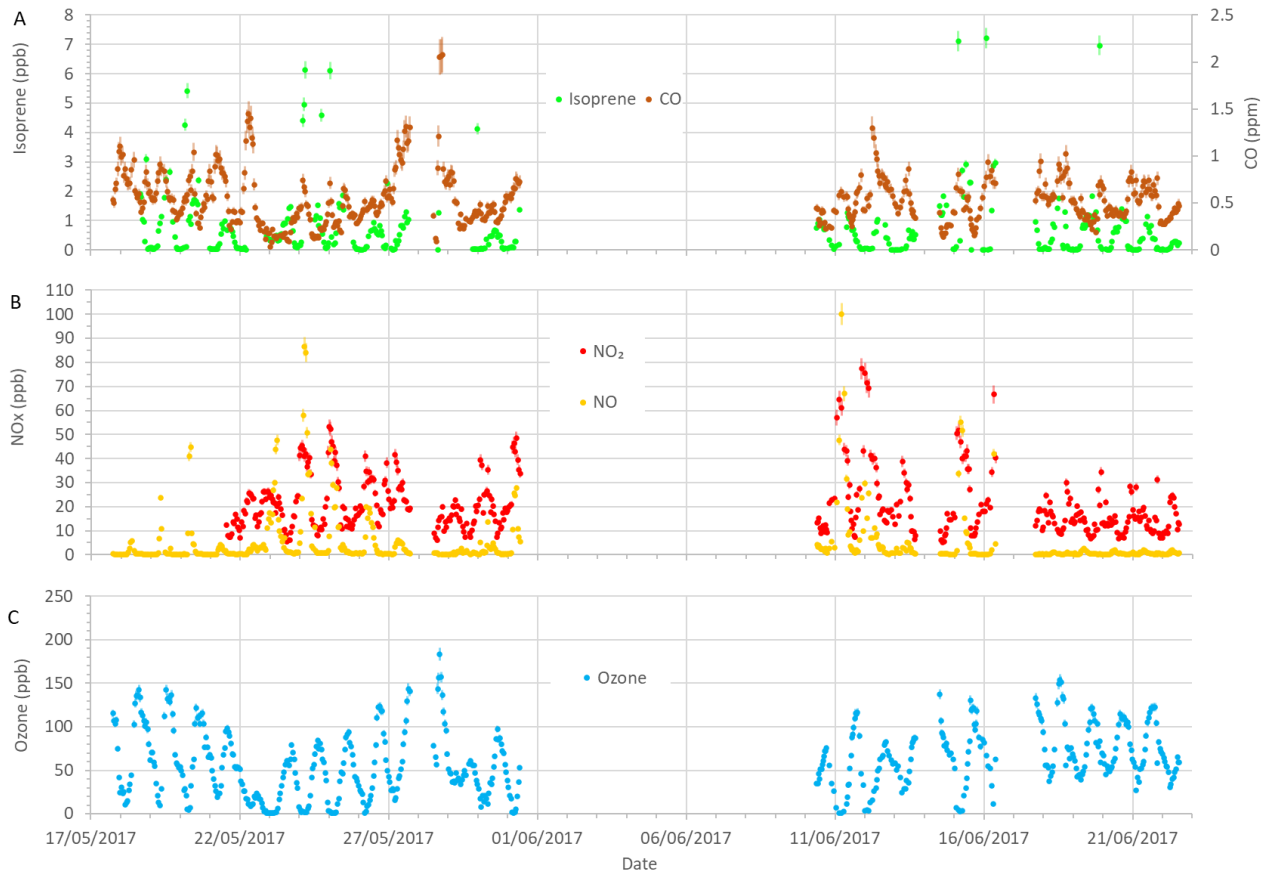

Figure S2: Isoprene, CO, NO, NO_2 and O_3 mixing ratios measured in Beijing for the times corresponding to the IN data shown in Fig. S1. Error bars are the measurement uncertainties (see Sect. S2 for details).

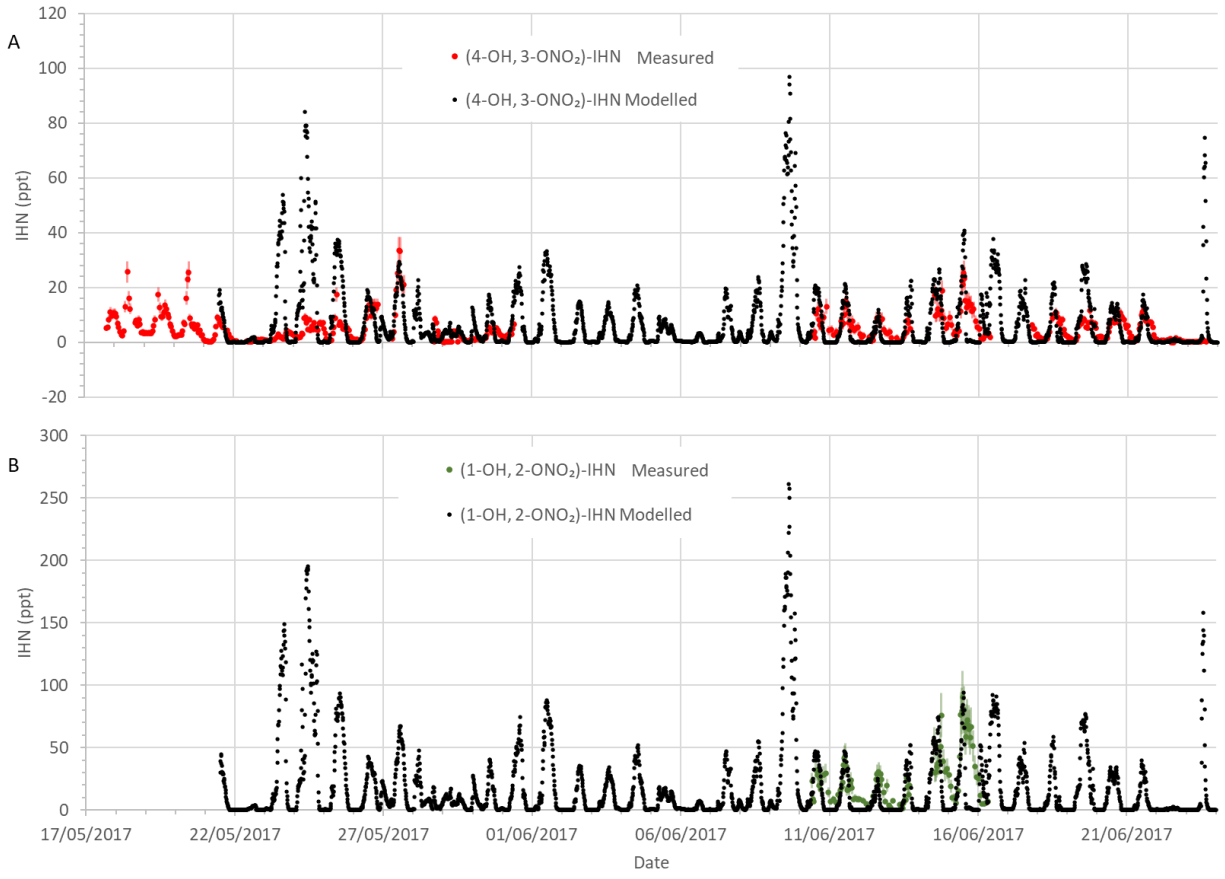

Figure S3: Time series of β-IHN as modelled using the MCM and measured. Error bars are the measurement uncertainties (see Sect. 3.3 for details).

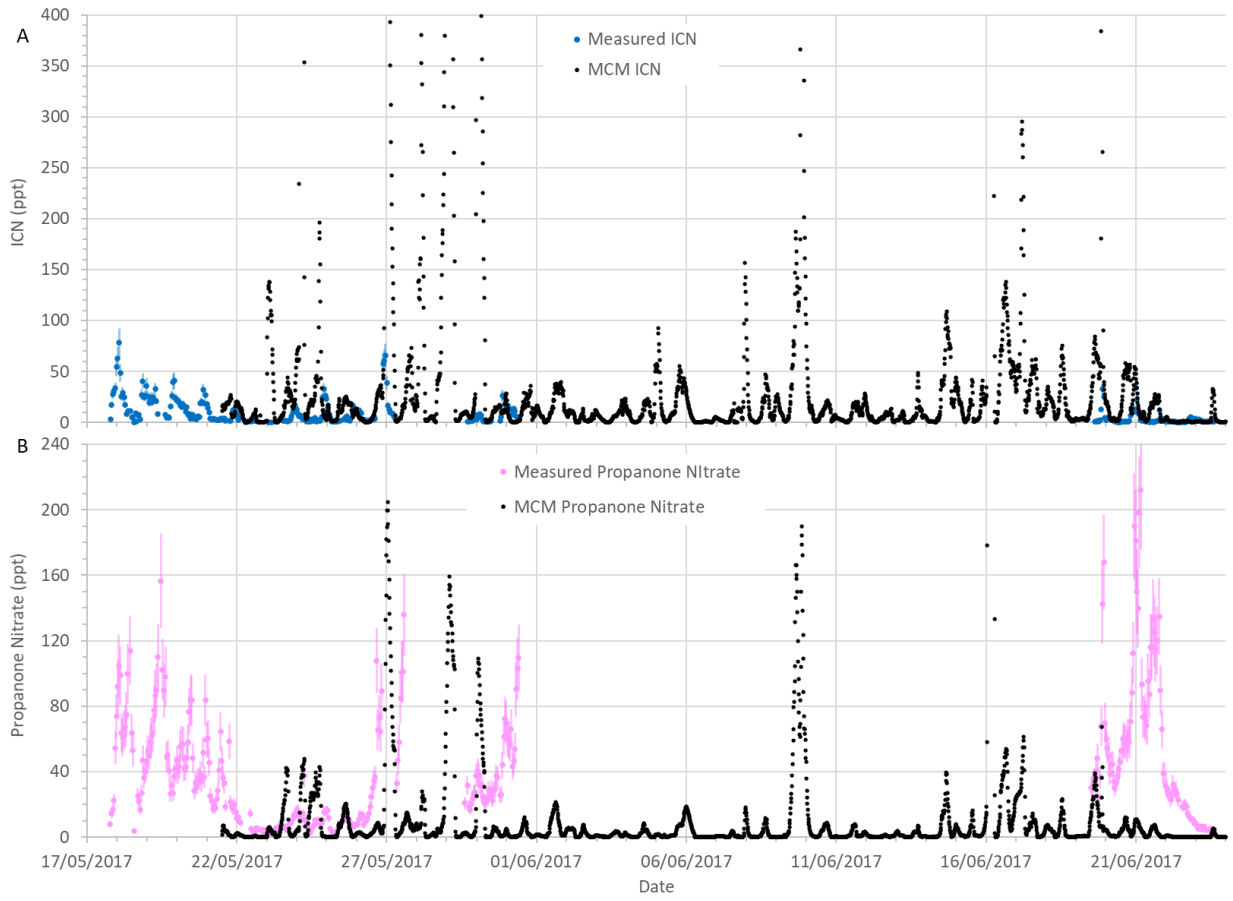

Figure S4: (a) Time series of total δ-ICN as modelled using the MCM and measured. For the MCM this is the species NC4CHO, whilst the measurements are the sum of the four δ-ICN (E and Z-(1-ONO_2, 4-CO)-ICN and E and Z-(4-ONO_2, 1-CO)-ICN). (b) Time series of propanone nitrate as modelled using the MCM and measured. Error bars are the measurement uncertainties (see Sect. 3.3 for details).

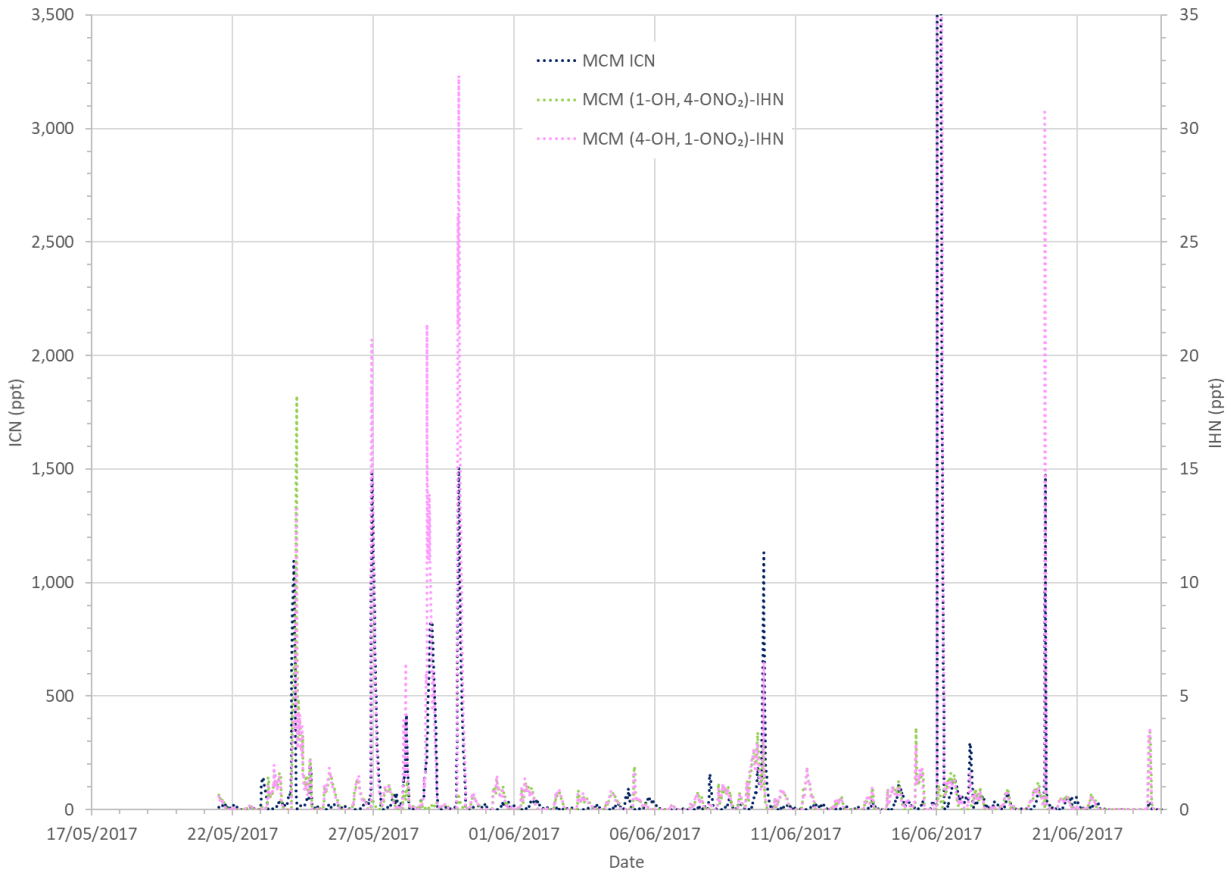

Figure S5: Time series the MCM modelled δ-IHN ((1-OH, 4-ONO_2)-IHN and (4-OH, 1-ONO_2)-IHN) and δ-ICN (NC4CHO).

S5. Tables

Table S1: Data used for plotting Figs. 2, 3, S1, S3 and S4.

Date Time (DD/MM/YYYY hh:mm)	(4-OH, 3-ONO_2)-IHN (ppt)	(1-OH, 2-ONO_2)-IHN (ppt)	E-(4-ONO_2, 1-CO)-ICN (ppt)	Z-(1-ONO_2, 4-CO)-ICN (ppt)	E-(1-ONO_2, 4-CO)-ICN (ppt)	Z-(4-ONO_2, 1-CO)-ICN (ppt)	Propanone nitrate (ppt)
17/05/2017 17:40	5.19						
17/05/2017 18:40	5.56					2.95	8.03
17/05/2017 19:40	8.33		3.27	0.73	11.65	1.46	14.42
17/05/2017 20:40	11.01		9.37	1.36	14.69	2.24	16.69
17/05/2017 21:40	9.66		9.95	1.58	16.91	2.36	22.21
17/05/2017 22:40	10.06		14.27	1.17	15.50	2.57	54.42
17/05/2017 23:40	10.67		22.08	2.18	27.72	2.45	73.78
18/05/2017 00:40	10.53		26.68	2.46	33.86		92.10
18/05/2017 01:40	9.30		23.97	2.98	49.39	1.78	104.52
18/05/2017 02:40	6.94		17.57	2.14	28.93		98.76
18/05/2017 03:40	5.35		14.24	1.45	8.45	1.18	63.62
18/05/2017 04:40	3.70		11.38	0.95	17.16		60.87
18/05/2017 05:40	2.72		10.20	1.27	13.19		65.45
18/05/2017 06:40	2.38		7.68	1.26	6.76	1.89	67.56
18/05/2017 07:40	3.99		5.50	1.28		1.60	74.75
18/05/2017 08:40	13.04		4.17	0.81	4.83	1.23	99.95
18/05/2017 10:44	25.69		2.92	0.59	5.02	2.90	114.00
18/05/2017 11:44	16.09		1.99	0.44		3.23	63.81
18/05/2017 12:44	12.20		1.85	0.35		2.41	52.86
18/05/2017 13:44			0.45				3.66
18/05/2017 14:44			8.85	0.24			
18/05/2017 15:44			0.78				
18/05/2017 16:44	7.16		0.86		6.08		25.31
18/05/2017 17:44	7.95		1.23		4.98	1.36	21.94
18/05/2017 18:44	6.09		1.49			1.71	17.02
18/05/2017 19:44	8.35		5.71	0.96	19.17	1.44	26.92
18/05/2017 20:44	6.44		12.44	1.48	25.31	1.23	47.10
18/05/2017 21:44	3.52		8.71	0.95	14.44	0.99	36.44
18/05/2017 22:44	3.67		9.88	0.88	15.46		40.04
18/05/2017 23:44	3.20		10.19	1.32	24.77		46.70
19/05/2017 00:44	3.35		8.85	1.33	14.87	0.56	52.27
19/05/2017 01:44	3.47		7.35	0.83	11.11		49.96
19/05/2017 02:44	3.28		7.90	0.88	16.14		58.45
19/05/2017 03:44	3.50		7.65	0.77	10.19	1.23	61.74
19/05/2017 04:44	3.35		7.63	0.80	15.51	0.88	63.81
19/05/2017 05:44	3.12		9.24	0.95	10.92	0.98	77.75
19/05/2017 06:44	3.96		12.39	1.41	17.49	1.28	86.20
19/05/2017 07:44	6.12		8.73	1.38	9.52	1.32	89.54

19/05/2017 08:44	8.32		6.33	1.00		1.31	109.90
19/05/2017 11:23	17.43						156.64
19/05/2017 12:37	12.60						102.27
19/05/2017 13:47	9.34						89.48
19/05/2017 14:54	9.37		2.79	0.22	2.42	1.85	98.05
19/05/2017 15:54	10.97		2.24	0.31		1.99	48.87
19/05/2017 16:54	13.61		3.11	0.24		2.23	50.39
19/05/2017 17:54	12.02		2.80	0.36		1.35	40.58
19/05/2017 18:54	10.19		4.54	0.40	9.13	1.38	26.59
19/05/2017 19:55	9.11		10.40	0.94	14.93		31.61
19/05/2017 20:55	6.65		12.49	1.07	26.23		26.95
19/05/2017 21:55	5.74		11.75	0.95	28.35		37.24
19/05/2017 22:55	4.03		9.81	0.58	13.28		41.60
19/05/2017 23:55	2.77		6.18	0.62	15.03		47.19
20/05/2017 00:55	2.16		5.60	0.92	14.30		39.88
20/05/2017 01:55	2.27		5.61	0.66	14.15		43.02
20/05/2017 02:55	2.34		6.11	0.58	9.71		55.37
20/05/2017 03:55	2.58		6.90	0.81	7.39		57.33
20/05/2017 04:55	2.79		7.43	0.52	9.66	0.48	56.61
20/05/2017 05:55	2.83		6.90	0.72	7.25	0.86	41.98
20/05/2017 06:55	4.12		5.48	0.68	4.15		42.67
20/05/2017 07:55	7.12		4.79	0.47	9.03	0.73	48.21
20/05/2017 08:55	6.66		2.85	0.49	3.38	0.79	58.02
20/05/2017 09:55	16.12		2.66	0.51	4.15	0.81	76.71
20/05/2017 10:55	23.07		2.77	0.42		0.98	83.70
20/05/2017 11:54	25.60		2.32	0.25		1.14	83.42
20/05/2017 12:54	8.91		1.76		4.54	1.18	48.23
20/05/2017 13:54	6.70		3.86				28.17
20/05/2017 14:54	5.88		3.52	0.12		0.98	33.63
20/05/2017 15:54	6.48		2.88				31.61
20/05/2017 16:54	4.83		4.64			1.23	35.20
20/05/2017 17:54	5.07		4.39			0.91	35.71
20/05/2017 18:54	6.22		6.28	0.62	11.98		38.99
20/05/2017 19:54	3.53		5.92	0.43	14.00		34.29
20/05/2017 20:54	4.47		11.00	0.81	19.46	0.87	51.66
20/05/2017 21:54	2.46		6.87	0.77	11.01		36.64
20/05/2017 22:54	2.75		11.34	0.93	14.58		83.63
20/05/2017 23:54	0.93		7.33	0.65	9.90	0.49	59.36
21/05/2017 00:54	0.49		6.39	0.42	6.57	0.74	60.23
21/05/2017 01:54	0.45		4.41	0.23	5.17		45.76
21/05/2017 02:54	0.36		3.68	0.29			25.12
21/05/2017 03:54	0.26		3.09	0.23			22.29
21/05/2017 04:54	0.25		3.53				17.48
21/05/2017 05:54	0.32		2.70	0.24			19.34
21/05/2017 06:54	0.47		2.76				17.66

21/05/2017 07:54	1.05		2.17	0.13			23.35
21/05/2017 08:54	2.78		2.44				28.53
21/05/2017 09:54	5.62		2.23				41.00
21/05/2017 10:59	8.98		3.34			0.54	64.62
21/05/2017 11:59	8.57		2.24			1.21	46.71
21/05/2017 12:59	7.15		3.04			0.96	36.48
21/05/2017 13:59	6.24		2.34			1.20	33.05
21/05/2017 14:59	5.60		1.35			0.62	18.84
21/05/2017 15:56							
21/05/2017 16:56							
21/05/2017 18:05				0.37		1.35	58.72
21/05/2017 19:05	4.30		1.92				21.31
21/05/2017 20:05	3.06		3.50	0.08	5.61		18.12
21/05/2017 21:05	1.55		3.52	0.24	8.45		16.79
21/05/2017 22:05	1.66		3.92	0.32	8.71		19.83
21/05/2017 23:05	0.87		1.81	0.26	4.96		15.44
22/05/2017 00:05	0.51		2.43		4.91	0.70	11.82
22/05/2017 01:05	0.55		2.50				12.15
22/05/2017 02:05	0.39		2.21	0.16	4.58		9.80
22/05/2017 03:05	0.27		2.20		2.51		8.73
22/05/2017 04:05							
22/05/2017 05:05							
22/05/2017 06:05							
22/05/2017 07:05				0.02	0.39		
22/05/2017 08:05				0.02	0.59		
22/05/2017 09:05				0.02	0.87		
22/05/2017 10:05							
22/05/2017 10:46	0.57						14.70
22/05/2017 11:46	0.13		1.14				5.27
22/05/2017 12:46	0.14		1.46				3.67
22/05/2017 13:46	0.28		1.58				4.16
22/05/2017 14:46	0.30		1.78				3.81
22/05/2017 15:44	0.47		1.55				5.43
22/05/2017 16:44	0.66						4.85
22/05/2017 17:44	0.76						4.63
22/05/2017 18:44	0.79						4.29
22/05/2017 19:44	1.00						4.54
22/05/2017 20:45	0.78						3.94
22/05/2017 21:45	1.03						2.87
22/05/2017 22:45	1.09						4.10
22/05/2017 23:45	1.02						4.58
23/05/2017 00:45	0.81						2.61
23/05/2017 01:45	0.70		0.30				3.45
23/05/2017 02:45	0.69						3.58
23/05/2017 03:45	0.54		0.48				2.18

23/05/2017 04:45	0.47						2.67
23/05/2017 05:45	0.46						2.38
23/05/2017 06:45	0.82						4.31
23/05/2017 07:45	1.08						5.72
23/05/2017 08:45	1.11						5.10
23/05/2017 10:05							
23/05/2017 10:51	1.88		0.92		1.90		7.47
23/05/2017 11:51	2.90		1.12		2.97		7.13
23/05/2017 12:51	2.48		1.46				6.58
23/05/2017 13:51	1.96		1.53				6.75
23/05/2017 14:51	1.94		1.53				5.83
23/05/2017 15:51	1.26		1.34				4.29
23/05/2017 16:51	1.24		0.99				5.44
23/05/2017 17:51	3.36		1.95				7.45
23/05/2017 18:51	4.40		2.11			0.68	9.15
23/05/2017 19:51	3.14		2.58	0.11	3.60		9.06
23/05/2017 20:51	3.94		4.14	0.35	5.03		11.19
23/05/2017 21:51	3.48		6.24	0.32	6.62		13.39
23/05/2017 22:51	3.04		11.15	0.34	5.25		13.74
23/05/2017 23:51	2.97		7.80	0.31	4.72	0.27	16.35
24/05/2017 00:51	2.38		5.49	0.30	3.15		16.76
24/05/2017 01:51	1.96		4.01	0.35	1.54	0.39	12.82
24/05/2017 02:51	2.07		3.58	0.19	2.99		13.33
24/05/2017 03:51	1.70		2.97	0.19	2.46		10.30
24/05/2017 04:51	1.89		2.61	0.20			14.49
24/05/2017 05:51	1.79		2.70	0.26	1.48	0.24	37.48
24/05/2017 06:51	3.20		2.00	0.26	2.47		10.95
24/05/2017 07:51	3.05		0.84			0.32	8.69
24/05/2017 08:51	8.87		0.68			0.47	5.96
24/05/2017 09:51	9.05		0.71		2.17		4.80
24/05/2017 10:51	7.07		1.15				3.06
24/05/2017 11:51	4.69		0.59		2.62		4.58
24/05/2017 12:51	8.20		0.97			0.53	6.19
24/05/2017 13:51	4.24		1.15			0.56	7.30
24/05/2017 14:51	5.83		1.51		2.20	0.63	10.19
24/05/2017 15:51	4.59		0.89				9.15
24/05/2017 16:51	7.00		1.42			0.69	10.49
24/05/2017 17:51	5.22		1.54				9.26
24/05/2017 18:51	4.71		1.36				6.60
24/05/2017 19:51	4.23		1.93	0.22	3.27		8.54
24/05/2017 20:51	6.93		10.03	0.55	13.09	0.95	10.39
24/05/2017 21:51	7.24		12.96	1.07	18.55		15.56
24/05/2017 22:51	6.61		12.08	0.87	13.04		15.76
24/05/2017 23:51	7.02		10.63	0.98	11.34		15.70
25/05/2017 00:51	4.84		7.61	0.52	6.18		16.12

25/05/2017 01:51	3.16		4.06	0.35	3.45		11.46
25/05/2017 02:51	1.35		1.86	0.14	3.10		5.23
25/05/2017 03:51	0.66		1.03	0.08			
25/05/2017 04:51	0.48		0.74				3.10
25/05/2017 05:51	0.59		0.62				2.88
25/05/2017 06:51	0.85		0.61				2.42
25/05/2017 07:51	3.25		0.84				3.18
25/05/2017 08:51	5.42		0.86				4.81
25/05/2017 09:51	8.88		1.24				5.91
25/05/2017 10:51	17.47		1.69	0.11			8.92
25/05/2017 11:51							
25/05/2017 12:51	6.40						9.96
25/05/2017 13:50	7.28		2.56			0.47	18.20
25/05/2017 14:50	6.21		3.29			1.00	11.45
25/05/2017 15:50	4.85		2.84		1.85	1.27	14.62
25/05/2017 16:50	4.82		2.52				11.83
25/05/2017 17:50	4.57		2.14				10.69
25/05/2017 18:50	4.62		1.64	0.11			8.72
25/05/2017 19:50	5.29		2.16	0.17	2.52		6.34
25/05/2017 20:50	4.25		6.52	0.63	9.06		7.89
25/05/2017 21:50	2.02		4.23	0.43	7.18		6.40
25/05/2017 22:50	1.60		3.44	0.35	4.96		7.23
25/05/2017 23:50	1.40		3.55	0.42	5.41		7.89
26/05/2017 00:50	1.16		3.68	0.36	5.06		7.93
26/05/2017 01:50	0.97		3.10	0.48	8.16		10.90
26/05/2017 02:50	0.96		3.16	0.37	6.15		13.96
26/05/2017 03:50	1.04		3.20	0.39	5.49		12.13
26/05/2017 04:50	0.88		2.77	0.29			13.66
26/05/2017 05:50	0.49		1.64	0.37			7.32
26/05/2017 06:50	0.63		1.97	0.34			9.43
26/05/2017 07:50	1.29		1.37	0.15			10.37
26/05/2017 08:50	2.57		1.47	0.28			11.72
26/05/2017 09:50	4.58		1.45	0.17	0.16		14.65
26/05/2017 10:50	8.92		1.58			0.33	18.72
26/05/2017 11:50	11.99		2.06			0.68	24.63
26/05/2017 12:50	13.52		2.27			0.71	30.08
26/05/2017 13:50	13.20		2.20			0.74	34.49
26/05/2017 14:50	9.57		3.17			0.71	36.69
26/05/2017 16:02	13.39						107.95
26/05/2017 17:02	13.64						65.58
26/05/2017 18:02	13.68						73.04
26/05/2017 19:02	12.46						64.44
26/05/2017 20:02	13.72						89.41
26/05/2017 21:02			23.27	2.02	31.85	0.75	
26/05/2017 22:02			26.33	2.39	31.35	0.60	

26/05/2017 23:02			27.10	2.77	35.71	0.44	
27/05/2017 00:02			14.62	1.47	22.24	0.40	
27/05/2017 01:02			5.72	0.56	10.28	0.30	
27/05/2017 02:02			5.72	0.45	6.91		
27/05/2017 03:02			4.12	0.59	5.18		
27/05/2017 04:02			3.23	0.33	5.32	0.31	
27/05/2017 05:02			3.67	0.19	4.24	0.35	
27/05/2017 06:02			2.93	0.25	2.81		
27/05/2017 07:02			2.60	0.20		0.32	
27/05/2017 08:02	1.26						32.98
27/05/2017 09:02	3.92						46.78
27/05/2017 10:02	9.85						58.31
27/05/2017 11:02	19.07						84.93
27/05/2017 12:02	25.31						100.82
27/05/2017 13:02	33.39						101.07
27/05/2017 14:02	33.28						135.89
27/05/2017 15:02	22.41						
27/05/2017 16:02	20.76						
27/05/2017 17:02	21.14						
28/05/2017 12:28							
28/05/2017 13:49							
28/05/2017 14:45							
28/05/2017 15:40							
28/05/2017 16:22	0.81						
28/05/2017 17:22	0.29						
28/05/2017 18:22	8.50						
28/05/2017 19:22	7.02						
28/05/2017 20:22	4.15						
28/05/2017 21:22	2.34						
28/05/2017 22:22	0.62						
28/05/2017 23:22	1.00						
29/05/2017 00:22	0.14						
29/05/2017 01:22	0.05						
29/05/2017 02:22	0.10						
29/05/2017 03:22	0.10						
29/05/2017 04:22	0.19						
29/05/2017 05:22	0.14						
29/05/2017 06:22	0.19						
29/05/2017 07:22	0.29						
29/05/2017 08:22	3.44						
29/05/2017 09:22	4.06						
29/05/2017 10:22	3.94						
29/05/2017 11:22	3.71						
29/05/2017 12:22	0.12						
29/05/2017 13:25							

29/05/2017 14:37	2.06						20.75
29/05/2017 16:50	1.12		0.85				31.72
29/05/2017 17:50	0.95		1.20				18.88
29/05/2017 18:50	0.78		1.42				16.74
29/05/2017 19:50	0.55		1.51				20.51
29/05/2017 20:50	0.50		1.77				24.01
29/05/2017 21:50	0.54		2.46	0.31			26.49
29/05/2017 22:50	1.12		2.53	0.15	5.20		27.35
29/05/2017 23:50	0.89		2.57	0.27			37.85
30/05/2017 00:50	0.93		2.55	0.17	2.48		40.57
30/05/2017 01:50	0.74		2.94	0.27	2.27		38.13
30/05/2017 02:50	1.34		2.61	0.31	5.41		31.61
30/05/2017 03:50	1.38		1.94	0.32	4.38		31.99
30/05/2017 04:50	1.51		2.18	0.27			24.51
30/05/2017 05:50	1.02		1.16				22.52
30/05/2017 06:50	1.04		1.28				20.52
30/05/2017 07:50	0.86		0.80				22.18
30/05/2017 08:50	0.93		1.18				23.73
30/05/2017 09:50	1.18		1.10				28.90
30/05/2017 10:50	1.63		0.55				26.62
30/05/2017 11:50	2.77		1.33				29.33
30/05/2017 12:50	4.90						22.59
30/05/2017 13:47	5.37						28.25
30/05/2017 14:47	4.24						29.23
30/05/2017 15:47	3.42						37.52
30/05/2017 16:47	4.98						36.37
30/05/2017 17:47							
30/05/2017 18:47	5.20		1.66				25.58
30/05/2017 19:47	5.06		1.90	0.19	3.20		26.18
30/05/2017 20:47	4.27		5.50	0.57	20.03		43.95
30/05/2017 21:47	3.61		6.31	0.58	17.98		61.32
30/05/2017 22:47	2.81		5.59	0.44	12.29		72.36
30/05/2017 23:47	2.29		4.71	0.42	10.83		69.82
31/05/2017 00:47	1.75		4.30	0.44	12.13		60.93
31/05/2017 01:47	1.60		3.88	0.45	9.35		59.20
31/05/2017 02:47	1.52		4.04	0.31	8.51		56.68
31/05/2017 03:47	2.41		4.62	0.34	7.70		66.02
31/05/2017 04:47	2.04		3.07	0.35	3.90		43.40
31/05/2017 05:47	2.87		4.88	0.43	8.43		46.30
31/05/2017 06:47	2.75		4.81	0.48	5.93		53.77
31/05/2017 07:47	3.02		3.02	0.35	2.86		90.40
31/05/2017 08:47	4.80		2.19	0.21			102.99
31/05/2017 09:47	6.71		1.98	0.15			109.41
10/06/2017 09:16		6.02					
10/06/2017 10:01	2.12	23.54					

10/06/2017 10:46	2.85	8.87					
10/06/2017 11:31	3.81	7.11					
10/06/2017 12:16	1.46						
10/06/2017 13:01	10.43	31.80					
10/06/2017 13:46							
10/06/2017 14:31	12.18	27.98					
10/06/2017 15:16	8.28	28.81					
10/06/2017 15:48	6.18	19.74					
10/06/2017 16:28	8.25	25.83					
10/06/2017 17:09	5.54	16.83					
10/06/2017 19:08	9.04	27.95					
10/06/2017 21:08	13.04	29.30					
10/06/2017 23:07	4.25	14.25					
11/06/2017 01:07	4.54	6.61					
11/06/2017 03:07	2.69	8.43					
11/06/2017 05:06	3.83	5.99					
11/06/2017 07:06	3.25	12.26					
11/06/2017 09:05	7.74	16.11					
11/06/2017 09:50	6.33	18.70					
11/06/2017 10:35	6.73	22.11					
11/06/2017 11:20	9.81	35.83					
11/06/2017 12:05	13.00	41.50					
11/06/2017 12:50	15.14	42.80					
11/06/2017 13:35	13.30	34.87					
11/06/2017 14:20	10.88	16.02					
11/06/2017 15:05	7.20	17.90					
11/06/2017 15:50	7.42	16.27					
11/06/2017 16:35	4.31	20.89					
11/06/2017 17:20	5.76	24.13					
11/06/2017 18:05	7.74	17.72					
11/06/2017 19:35	4.38	8.92					
11/06/2017 21:04	5.09	9.51					
11/06/2017 22:34	5.54	8.51					
12/06/2017 00:04	3.00	8.70					
12/06/2017 01:33	1.92						
12/06/2017 03:03	2.41	7.68					
12/06/2017 04:32							
12/06/2017 06:02		4.86					
12/06/2017 07:31	1.75	1.03					
12/06/2017 09:01	1.75	3.83					
12/06/2017 09:46	0.39						
12/06/2017 10:31	0.79						
12/06/2017 11:16	3.08	10.90					
12/06/2017 12:04							
12/06/2017 13:42	8.90	24.61					

12/06/2017 14:27	7.91	28.92					
12/06/2017 15:48	8.62	30.32					
12/06/2017 16:33	8.48	20.47					
12/06/2017 17:19	8.26	28.70					
12/06/2017 18:04	8.60	24.70					
12/06/2017 19:34	4.51	13.89					
12/06/2017 21:03	3.61	7.12					
12/06/2017 22:33	3.31	19.44					
13/06/2017 00:03	3.76	3.75					
13/06/2017 01:32	1.50	2.06					
13/06/2017 03:02		7.19					
13/06/2017 04:31							
13/06/2017 06:01	1.53						
13/06/2017 07:30							
13/06/2017 09:00	0.39	4.54					
13/06/2017 09:45		2.74					
13/06/2017 11:23	1.98	1.55					
13/06/2017 12:06	2.91	5.43					
13/06/2017 12:51	3.78	8.52					
13/06/2017 13:36	3.59	8.13					
13/06/2017 14:21	7.92	25.62					
13/06/2017 15:06	7.18	18.67					
13/06/2017 15:51	7.41	12.02					
13/06/2017 16:36	4.99	19.61					
14/06/2017 12:29	17.25	53.40					
14/06/2017 13:13	9.51	30.26					
14/06/2017 13:58	10.06	30.48					
14/06/2017 14:43	12.24	34.89					
14/06/2017 15:28	11.91	36.67					
14/06/2017 16:13	10.11	37.66					
14/06/2017 16:58	9.93	37.82					
14/06/2017 17:43	11.53	50.48					
14/06/2017 18:28	18.87	75.97					
14/06/2017 19:58	8.77	39.25					
14/06/2017 21:28	5.31	30.86					
14/06/2017 22:57	6.46	32.90					
15/06/2017 00:27	9.13	28.21					
15/06/2017 01:56	6.28	19.03					
15/06/2017 03:26	3.06	9.75					
15/06/2017 04:56	4.10	9.81					
15/06/2017 06:25	2.31	5.52					
15/06/2017 07:55	4.17	15.60					
15/06/2017 09:24	11.28	42.95					
15/06/2017 10:09	22.41	76.29					
15/06/2017 10:54	20.89	79.56					

15/06/2017 11:39	25.20	90.63					
15/06/2017 12:23	23.25	80.38					
15/06/2017 13:08	15.12	65.78					
15/06/2017 13:53	12.75	58.43					
15/06/2017 14:38	14.63	68.35					
15/06/2017 15:23	14.99	72.21					
15/06/2017 16:08	13.85	68.04					
15/06/2017 16:53	13.63	64.99					
15/06/2017 17:38	13.93	58.14					
15/06/2017 18:23	11.38	66.37					
15/06/2017 19:53	12.03	51.40					
15/06/2017 21:22	7.75	35.12					
15/06/2017 22:52	5.46	26.58					
16/06/2017 00:22	4.95	25.23					
16/06/2017 01:51	1.35	11.84					
16/06/2017 03:21	1.34	4.71					
16/06/2017 04:50	2.29	4.90					
16/06/2017 06:20	2.79	5.58					
16/06/2017 07:49	3.16	6.74					
16/06/2017 09:19	2.00						
17/06/2017 17:42							
17/06/2017 18:46	6.31						
17/06/2017 19:46	4.91						
17/06/2017 20:46	4.97						
17/06/2017 21:46	2.37						
17/06/2017 22:46	2.95						
17/06/2017 23:46	1.99						
18/06/2017 00:46	1.97						
18/06/2017 01:46	1.39						
18/06/2017 02:46	1.29						
18/06/2017 03:46	1.19						
18/06/2017 04:46	1.09						
18/06/2017 05:46	1.35						
18/06/2017 06:46	1.28						
18/06/2017 07:46	2.36						
18/06/2017 08:46	3.80						
18/06/2017 11:16	8.67						
18/06/2017 12:16							
18/06/2017 13:16	10.53						
18/06/2017 14:16	10.82						
18/06/2017 15:16	9.09						
18/06/2017 16:16	6.91						
18/06/2017 17:16	6.55						
18/06/2017 18:16	8.27						
18/06/2017 19:16	8.33						

18/06/2017 20:16	4.76						
18/06/2017 21:16	3.09						
18/06/2017 22:16	2.29						
18/06/2017 23:16	2.21						
19/06/2017 00:16	1.69						
19/06/2017 01:16	1.45						
19/06/2017 02:16	1.14						
19/06/2017 03:16	0.95						
19/06/2017 04:16	0.83						
19/06/2017 05:16	0.88						
19/06/2017 06:16	0.83						
19/06/2017 07:16	2.08						
19/06/2017 08:16	5.72						
19/06/2017 09:16	6.67						
19/06/2017 10:16	6.79						
19/06/2017 11:16							
19/06/2017 12:16	8.57						30.45
19/06/2017 13:16	7.85						29.24
19/06/2017 14:16	5.46						35.68
19/06/2017 15:16	5.22		0.35	0.03	0.11		32.48
19/06/2017 16:16	7.06		0.41	0.06	0.16		40.45
19/06/2017 17:16	11.53		0.75	0.16	0.44		48.54
19/06/2017 18:17	7.54		0.47	0.10	0.31		24.14
19/06/2017 19:16	7.24		0.76	0.26	1.06		36.53
19/06/2017 20:16	6.51		3.81	0.88	7.93	0.41	67.83
19/06/2017 21:16	6.98		8.74	2.11	20.91	0.90	142.65
19/06/2017 22:17	5.10		7.61	1.66	15.80	0.69	168.21
19/06/2017 23:16	1.86		1.43	0.39	2.98		69.92
20/06/2017 00:17	1.89		0.24	0.26	1.92		59.92
20/06/2017 01:17	2.26		1.34	0.34	2.50	0.14	54.60
20/06/2017 02:16	2.26		1.50	0.36	2.67	0.12	49.25
20/06/2017 03:17	1.67		1.15	0.26	2.03	0.10	38.48
20/06/2017 04:17	1.60		1.15	0.22	2.01	0.09	44.52
20/06/2017 05:17	1.47		1.08	0.27	1.85	0.08	44.50
20/06/2017 06:16	1.21		0.57	0.20	1.01	0.06	34.15
20/06/2017 07:17	1.47		0.38	0.16	0.56	0.03	30.09
20/06/2017 08:17	3.76		0.31	0.13	0.26	0.02	33.54
20/06/2017 09:17	5.72		0.23	0.11	0.11	0.03	37.38
20/06/2017 10:17	8.01		0.28	0.07	0.07	0.02	41.37
20/06/2017 11:17	7.48		0.30	0.05	0.08	0.03	46.07
20/06/2017 12:49	7.22		0.36	0.06	0.07	0.04	53.18
20/06/2017 13:49	7.34		0.40	0.04	0.09	0.06	59.79
20/06/2017 14:49	7.81		0.45	0.05	0.08	0.04	57.81
20/06/2017 15:49	7.62		0.41	0.06	0.11	0.04	58.83
20/06/2017 16:49	7.23		0.37	0.06	0.13	0.02	55.59

20/06/2017 17:49	10.75		0.57	0.15	0.31	0.05	61.42
20/06/2017 18:49	9.48		0.70	0.24	0.75	0.05	58.17
20/06/2017 19:49	8.86		2.18	0.62	4.15	0.23	70.45
20/06/2017 20:49	8.27		4.04	0.91	8.90	0.40	88.35
20/06/2017 21:49	6.36		3.12	0.88	5.75	0.29	112.38
20/06/2017 22:49	5.31		4.09	1.08	7.02	0.36	189.71
20/06/2017 23:49	6.01		9.28	2.10	21.74	0.95	181.21
21/06/2017 00:49	3.48		6.18	1.46	14.41	0.60	150.17
21/06/2017 01:49	1.64		2.63	0.80	5.26	0.22	139.67
21/06/2017 02:49	2.14		3.40	0.73	5.62	0.29	198.08
21/06/2017 03:49	0.36		0.64	0.18	1.20	0.05	212.10
21/06/2017 04:49	0.30		0.63	0.13	0.81	0.04	93.21
21/06/2017 05:49	0.37		0.52	0.17	0.72	0.03	73.44
21/06/2017 06:49	0.62		0.48	0.18	0.61	0.04	74.17
21/06/2017 07:49	1.91		0.39	0.16	0.41	0.04	71.11
21/06/2017 08:49	4.85		0.39	0.14	0.24	0.04	68.14
21/06/2017 09:49	6.51		0.27	0.10	0.11	0.04	95.44
21/06/2017 10:49	9.89		0.26	0.06	0.05	0.03	87.41
21/06/2017 11:49	11.09		0.37	0.08	0.06	0.03	116.18
21/06/2017 12:52	12.14		0.40	0.09	0.08	0.02	115.90
21/06/2017 13:52	8.07		0.31	0.05	0.06	0.03	134.33
21/06/2017 14:52	7.87		0.38	0.10	0.16	0.03	125.57
21/06/2017 15:52	7.19		0.41	0.11	0.34	0.05	114.89
21/06/2017 16:52	6.81		0.58	0.21	0.68	0.06	119.98
21/06/2017 17:52	7.31		0.74	0.28	0.76	0.06	
21/06/2017 18:52	7.16		3.43	0.93	7.52	0.35	134.83
21/06/2017 19:52	5.57		1.58	0.27	2.73	0.15	89.72
21/06/2017 20:52	2.62		0.97	0.29	1.74	0.09	65.92
21/06/2017 21:52	1.25		0.42	0.08	0.74	0.04	39.02
21/06/2017 22:52	0.91		0.48	0.11	0.68	0.04	38.97
21/06/2017 23:52	0.61		0.36	0.05	0.50	0.03	30.98
22/06/2017 00:52	0.57		0.36	0.08	0.63	0.03	29.04
22/06/2017 01:52	0.53		0.41	0.09	0.66	0.04	27.03
22/06/2017 02:52	0.65		0.34	0.06	0.57	0.03	25.85
22/06/2017 03:52	0.59		0.28	0.06	0.56	0.03	22.61
22/06/2017 04:52	0.61		0.40	0.10	0.62	0.04	25.67
22/06/2017 05:52	0.61		0.37	0.08	0.59	0.03	32.20
22/06/2017 06:52	0.62		0.39	0.08	0.43	0.03	28.87
22/06/2017 07:52	0.68		0.28	0.07	0.27	0.03	29.04
22/06/2017 08:52	0.95		0.20	0.06	0.20	0.02	26.33
22/06/2017 09:52	1.28		0.17	0.05	0.12		22.94
22/06/2017 10:50	0.00		0.00	0.00	0.00		
22/06/2017 11:50	0.00		0.00	0.00	0.00		
22/06/2017 12:50	0.00						
22/06/2017 13:27	0.77		0.06	0.02			18.83

22/06/2017 14:27	1.49		0.08	0.03	0.03		19.58
22/06/2017 15:27	1.06		0.01	0.00	0.00		19.50
22/06/2017 16:44	0.85		0.41	0.03	0.70		18.67
22/06/2017 17:44	1.16		0.85	0.02	0.75		14.54
22/06/2017 18:44	0.43		1.07	0.02	2.91		12.85
22/06/2017 19:44	0.41		1.25	0.01	4.31		11.32
22/06/2017 20:44	0.31		0.95	0.01	3.36		10.85
22/06/2017 21:44	0.25		1.05	0.01	2.16		10.86
22/06/2017 22:44	0.13		0.95	0.02	1.08		8.57
22/06/2017 23:44	0.14		0.91	0.02	3.05		9.06
23/06/2017 00:44	0.12		1.10	0.02	0.51		6.87
23/06/2017 01:44	0.11		1.17	0.01	0.11		5.19
23/06/2017 02:44	0.11		0.95	0.03	2.35		5.10
23/06/2017 03:44	0.10		1.08	0.03	0.26		6.81
23/06/2017 04:44	0.08		0.86	0.01	0.64		4.61
23/06/2017 05:44	0.08		0.59	0.02	0.52		4.68
23/06/2017 06:44	0.08		0.82	0.01	0.37		6.56
23/06/2017 07:44	0.07		0.51	0.01	0.38		4.91
23/06/2017 08:44	0.09		0.28	0.03	0.54		4.10
23/06/2017 09:44	0.14		0.60	0.01	0.41		
23/06/2017 10:44	0.14		0.53	0.02	0.28		4.27
23/06/2017 11:44	0.42		0.96	0.01	0.36		5.43
23/06/2017 12:44	0.33		0.80	0.02	0.42		4.42
23/06/2017 13:44	0.43		0.83	0.02	0.10		5.03
23/06/2017 14:57	0.27		0.47	0.04	0.17		4.70

Table S2: Data plotted in Figs. 7 and S2.

Date Time (DD/MM/YYYY hh:mm)	Isoprene (ppb)	O_3 (ppb)	CO (ppm)	NO (ppb)	NO_2 (ppb)
17/05/2017 17:40		115	0.532	0.38	
17/05/2017 18:40		107	0.497	0.17	
17/05/2017 19:40		103	0.649	0.09	
17/05/2017 20:40		108	0.708	0.10	
17/05/2017 21:40		75	0.862	0.10	
17/05/2017 22:40		42	1.048	0.21	
17/05/2017 23:40		25	1.101	0.16	
18/05/2017 00:40		30	0.989	0.13	
18/05/2017 01:40		24	1.015	0.14	
18/05/2017 02:40		26	0.786	0.12	
18/05/2017 03:40		10	0.862	0.13	
18/05/2017 04:40		13	0.758	0.14	
18/05/2017 05:40		15	0.701	1.07	
18/05/2017 06:40		27	0.711	2.69	
18/05/2017 07:40		34	0.709	5.18	
18/05/2017 08:40		44	0.851	5.85	
18/05/2017 10:44		103	0.959	1.76	
18/05/2017 11:44		127	0.631	0.53	
18/05/2017 12:44		136	0.599	0.30	
18/05/2017 13:44		137	0.557	0.32	
18/05/2017 14:44		142	0.597	0.31	
18/05/2017 15:44	1.92	134	0.512	0.35	
18/05/2017 16:44	1.81	117	0.402	0.32	
18/05/2017 17:44	1.05	113	0.442	0.18	
18/05/2017 18:44	0.95	107	0.511	0.16	
18/05/2017 19:44	0.30	101	0.723	0.12	
18/05/2017 20:44	3.10	106	0.827	0.11	
18/05/2017 21:44	0.04	97	0.701	0.11	
18/05/2017 22:44	0.06	80	0.605	0.12	
18/05/2017 23:44	0.07	62	0.624	0.17	
19/05/2017 00:44	0.09	70	0.561	0.10	
19/05/2017 01:44	0.03	71	0.529	0.09	
19/05/2017 02:44	0.04	59	0.549	0.09	
19/05/2017 03:44	0.06	55	0.536	0.10	
19/05/2017 04:44	0.09	35	0.604	0.17	
19/05/2017 05:44	0.14	21	0.732	0.80	
19/05/2017 06:44	0.66	13	0.824	6.60	
19/05/2017 07:44	0.92	9	0.911	23.81	
19/05/2017 08:44	1.14	29	0.864	10.79	
19/05/2017 11:23	1.79	112	0.842	1.06	
19/05/2017 12:37	2.39	143	0.736	0.51	

19/05/2017 13:47		132	0.621	0.33	
19/05/2017 14:54		133	0.559	0.35	
19/05/2017 15:54	2.67	129	0.534	2.65	
19/05/2017 16:54	1.72	137	0.551	0.26	
19/05/2017 17:54	0.95	114	0.416	0.18	
19/05/2017 18:54		95	0.533	0.16	
19/05/2017 19:55	0.43	68	0.401	0.17	
19/05/2017 20:55	0.07	58	0.325	0.18	
19/05/2017 21:55	0.04	57	0.338	0.14	
19/05/2017 22:55	0.04	53	0.375	0.13	
19/05/2017 23:55		54	0.404	0.10	
20/05/2017 00:55	0.03	49	0.390	0.12	
20/05/2017 01:55	0.05	45	0.446	0.10	
20/05/2017 02:55	0.07	27	0.515	0.37	
20/05/2017 03:55	4.26	29	0.559	0.13	
20/05/2017 04:55	0.10	21	0.521	0.12	
20/05/2017 05:55	5.42	5	0.592	8.89	
20/05/2017 06:55	1.00	4	0.746	40.92	
20/05/2017 07:55	1.14	7	0.784	44.72	
20/05/2017 08:55	0.89	32	0.638	8.86	
20/05/2017 09:55	1.58	54	0.837	4.51	
20/05/2017 10:55	1.72	62	1.041	4.09	
20/05/2017 11:54	1.69	104	0.601	1.47	
20/05/2017 12:54	1.64	122	0.388	0.51	
20/05/2017 13:54	1.56	110	0.286	0.48	
20/05/2017 14:54	2.38	111	0.281	0.43	
20/05/2017 15:54		103	0.237	0.46	
20/05/2017 16:54		114	0.350	0.28	
20/05/2017 17:54		116	0.423	0.26	
20/05/2017 18:54		104	0.493	0.21	
20/05/2017 19:54		77	0.452	0.26	
20/05/2017 20:54		88	0.577	0.27	
20/05/2017 21:54		77	0.538	0.18	
20/05/2017 22:54		65	0.738	0.13	
20/05/2017 23:54	0.05	68	0.838	0.20	
21/05/2017 00:54	0.04	64	0.726	0.14	
21/05/2017 01:54	0.03	50	0.566	0.14	
21/05/2017 02:54	0.02	40	0.550	0.16	
21/05/2017 03:54	0.02	32	0.888	0.17	
21/05/2017 04:54	0.03	26	1.019	0.24	
21/05/2017 05:54	0.04	19	1.010	2.04	
21/05/2017 06:54	0.13	23	0.951	3.04	
21/05/2017 07:54	0.21	24	0.971	4.06	
21/05/2017 08:54	0.56	32	0.874	3.45	
21/05/2017 09:54	0.88	53	0.822	2.17	

21/05/2017 10:59	0.74	68	0.817	1.81	
21/05/2017 11:59	0.98	75	0.781	1.73	
21/05/2017 12:59		95	0.730	0.89	12.23
21/05/2017 13:59	0.68	99	0.576	0.56	7.99
21/05/2017 14:59		94	0.415	0.50	7.50
21/05/2017 15:56	0.83	90	0.260	0.44	7.33
21/05/2017 16:56	0.73	81	0.220	0.45	8.73
21/05/2017 18:05	0.63	69	0.299	0.41	13.72
21/05/2017 19:05	0.47	68	0.415	0.41	13.16
21/05/2017 20:05	0.27	54	0.403	0.10	16.74
21/05/2017 21:05	0.10	52	0.294	0.16	14.89
21/05/2017 22:05	0.05	54	0.308	0.27	11.59
21/05/2017 23:05	0.05	53	0.306	0.44	10.11
22/05/2017 00:05	0.05	51	0.293		7.00
22/05/2017 01:05	0.03	38	0.416	0.30	13.72
22/05/2017 02:05	0.04	34	0.401	0.10	11.71
22/05/2017 03:05	0.03	26	0.651	0.24	18.27
22/05/2017 04:05	0.08	26	0.819	0.10	17.07
22/05/2017 05:05	0.01	17	1.164	0.24	22.47
22/05/2017 06:05		16	1.370	0.94	21.96
22/05/2017 07:05		12	1.449	2.38	25.71
22/05/2017 08:05		10	1.304	1.24	25.41
22/05/2017 09:05		9	1.404	2.14	24.74
22/05/2017 10:05		10	1.196	3.84	23.25
22/05/2017 10:46		12	1.131	4.17	23.37
22/05/2017 11:46		20	0.697	3.03	15.31
22/05/2017 12:46		18	0.454	3.36	16.48
22/05/2017 13:46		24	0.335	1.57	11.66
22/05/2017 14:46		21	0.315	2.57	13.63
22/05/2017 15:44		18	0.262	2.99	16.79
22/05/2017 16:44		17	0.212	3.14	17.56
22/05/2017 17:44		12	0.284	2.91	22.10
22/05/2017 18:44		7	0.284	4.18	26.26
22/05/2017 19:44		2	0.196	2.61	26.15
22/05/2017 20:45		3	0.113	2.01	23.15
22/05/2017 21:45	0.48	1	0.230	10.99	26.08
22/05/2017 22:45		1	0.175	14.74	26.31
22/05/2017 23:45	0.36	1	0.180	17.50	24.08
23/05/2017 00:45	0.32	1	0.037	13.25	24.58
23/05/2017 01:45	0.32	1	0.080	16.82	23.19
23/05/2017 02:45	0.35	1	0.221	26.91	21.74
23/05/2017 03:45		1	0.150	29.86	21.52
23/05/2017 04:45	0.42	2	0.148	43.76	17.36
23/05/2017 05:45	0.49	2	0.122	47.62	20.13
23/05/2017 06:45	0.32	6		14.71	24.14

23/05/2017 07:45	0.35	17		9.84	21.55
23/05/2017 08:45	0.52	24	0.156	7.71	19.08
23/05/2017 10:05	0.54	32		5.45	16.62
23/05/2017 10:51	0.84	42	0.137	2.85	10.33
23/05/2017 11:51	0.92	48	0.173	7.01	10.53
23/05/2017 12:51	0.91	56	0.175	1.74	8.24
23/05/2017 13:51		61	0.114	1.30	5.50
23/05/2017 14:51	1.06	61	0.095	0.98	6.03
23/05/2017 15:51	1.42	56	0.094	1.06	6.09
23/05/2017 16:51	1.47	63	0.185	1.02	9.31
23/05/2017 17:51	1.03	79	0.291	0.66	11.80
23/05/2017 18:51	0.64	71	0.343	0.48	16.19
23/05/2017 19:51	0.24	62	0.306	0.30	15.85
23/05/2017 20:51	0.10	47	0.346	1.06	22.24
23/05/2017 21:51	0.08	36	0.389	0.73	24.32
23/05/2017 22:51	0.09	30	0.350	1.04	24.27
23/05/2017 23:51	0.17	8	0.444	4.81	41.27
24/05/2017 00:51	0.16	4	0.433	9.39	44.41
24/05/2017 01:51	0.27	2	0.464	23.52	45.31
24/05/2017 02:51	4.41	2	0.742	58.06	43.94
24/05/2017 03:51	4.96	2	0.667	86.67	40.98
24/05/2017 04:51	6.13	1	0.621	84.02	41.81
24/05/2017 05:51		1	0.486	50.71	36.48
24/05/2017 06:51		6	0.467	33.58	38.58
24/05/2017 07:51		9	0.379	33.94	40.23
24/05/2017 08:51		21	0.320	17.04	33.59
24/05/2017 09:51		42	0.171	3.43	14.71
24/05/2017 10:51		52	0.136	2.74	12.52
24/05/2017 11:51		57	0.121	11.44	11.84
24/05/2017 12:51	1.04	69	0.144	1.81	11.65
24/05/2017 13:51	1.16	78	0.127	0.87	8.16
24/05/2017 14:51	1.52	84	0.149	0.78	7.99
24/05/2017 15:51	0.83	75	0.134	0.83	10.60
24/05/2017 16:51	1.09	81	0.226	0.77	11.33
24/05/2017 17:51	4.59	74	0.211	0.67	10.61
24/05/2017 18:51	0.54	63	0.232	0.63	14.92
24/05/2017 19:51	0.27	60	0.222	0.66	12.78
24/05/2017 20:51	0.08	47	0.266	0.84	20.00
24/05/2017 21:51	0.06	38	0.302	0.61	23.43
24/05/2017 22:51	0.12	13	0.379	1.71	42.69
24/05/2017 23:51	0.24	3	0.497	7.78	53.25
25/05/2017 00:51	6.11	2	0.713	43.72	52.43
25/05/2017 01:51	0.44	1	0.515	38.02	46.93
25/05/2017 02:51		1	0.372	29.11	45.07
25/05/2017 03:51	0.17	1	0.242	19.62	39.01

25/05/2017 04:51	0.23	1	0.276	19.84	42.48
25/05/2017 05:51	0.57	2	0.303	27.72	37.06
25/05/2017 06:51	0.92	12	0.263	11.32	30.45
25/05/2017 07:51	1.58	17	0.306	11.87	27.68
25/05/2017 08:51	1.44	38	0.207	2.98	12.52
25/05/2017 09:51	1.50	48	0.189	1.97	10.71
25/05/2017 10:51	1.86	47	0.464	4.23	20.06
25/05/2017 11:51	1.36	59	0.654	3.04	19.41
25/05/2017 12:51		74	0.635	1.67	15.12
25/05/2017 13:50		88	0.562	1.01	11.81
25/05/2017 14:50		91	0.547	1.31	14.46
25/05/2017 15:50		94	0.459	0.86	11.43
25/05/2017 16:50		82	0.352	0.84	13.11
25/05/2017 17:50		77	0.377	0.49	10.76
25/05/2017 18:50		68	0.391	0.32	12.34
25/05/2017 19:50	0.26	57	0.345	0.50	14.44
25/05/2017 20:50	0.11	42	0.374	0.62	19.39
25/05/2017 21:50	0.04	40	0.281	0.59	16.08
25/05/2017 22:50	0.03	37	0.281	0.48	16.56
25/05/2017 23:50	0.02	32	0.310	0.88	17.51
26/05/2017 00:50	0.00	27	0.334	0.81	20.12
26/05/2017 01:50	0.00	26	0.367	0.43	18.46
26/05/2017 02:50	0.00	22	0.397	0.54	19.13
26/05/2017 03:50		13	0.429	0.94	28.43
26/05/2017 04:50	0.04	1	0.513	7.48	41.12
26/05/2017 05:50	0.11	2	0.427	19.84	34.74
26/05/2017 06:50	0.10	9	0.427	15.31	30.38
26/05/2017 07:50	0.47	10	0.455	19.18	34.49
26/05/2017 08:50		16	0.460	17.50	31.06
26/05/2017 09:50	0.65	21	0.489	13.19	31.97
26/05/2017 10:50	0.66	30	0.530	11.29	31.60
26/05/2017 11:50	0.92	44	0.528	6.92	31.21
26/05/2017 12:50	0.73	59	0.466	3.79	25.62
26/05/2017 13:50	0.66	79	0.393	2.06	20.41
26/05/2017 14:50	0.57	111	0.372	0.86	13.13
26/05/2017 16:02	0.51	122	0.404	0.43	11.68
26/05/2017 17:02	0.82	123	0.464	0.62	18.56
26/05/2017 18:02	0.65	119	0.498	0.33	17.51
26/05/2017 19:02	0.49	118	0.476	0.25	16.93
26/05/2017 20:02	0.11	92	0.596	0.51	29.48
26/05/2017 21:02	0.06	83	0.629	0.37	30.79
26/05/2017 22:02	0.17	62	0.731	0.49	38.30
26/05/2017 23:02	2.28	50	0.558	0.28	26.55
27/05/2017 00:02		43	0.575	0.54	23.01
27/05/2017 01:02		36	0.644	0.41	19.28

27/05/2017 02:02	0.06	27	0.547	0.16	21.47
27/05/2017 03:02	0.02	29	0.510	0.12	19.75
27/05/2017 04:02	0.00	27	0.653	0.57	22.47
27/05/2017 05:02	0.03	15	0.853	3.41	41.68
27/05/2017 06:02	0.32	19	0.878	4.81	38.50
27/05/2017 07:02	0.17	28	1.168	6.24	35.04
27/05/2017 08:02	0.32	41	1.084	4.74	27.35
27/05/2017 09:02	0.52	44	1.013	5.56	28.28
27/05/2017 10:02	0.84	51	0.955	4.74	27.28
27/05/2017 11:02	0.82	60	0.926	4.63	30.07
27/05/2017 12:02	0.76	80	1.069	2.43	22.76
27/05/2017 13:02	1.14	94	1.266	1.88	22.59
27/05/2017 14:02	1.29	107	1.312	1.38	22.07
27/05/2017 15:02	0.93	130	1.137	0.89	18.87
27/05/2017 16:02	1.03	144	1.160	0.59	18.61
27/05/2017 17:02		141	1.304	0.42	19.42
28/05/2017 12:28		78	0.367	0.73	8.86
28/05/2017 13:49		65	0.121	0.70	6.88
28/05/2017 14:45		57	0.094	0.69	6.20
28/05/2017 15:40	0.00	144	0.873	0.27	11.58
28/05/2017 16:22	1.27	156	1.211	0.25	14.36
28/05/2017 17:22		184	2.055		15.65
28/05/2017 18:22		157	2.057	0.11	15.98
28/05/2017 19:22		137	2.077	0.12	20.00
28/05/2017 20:22		117	0.860	0.13	9.97
28/05/2017 21:22		104	0.727	0.12	13.50
28/05/2017 22:22		95	0.705	0.15	11.30
28/05/2017 23:22		69	0.753	0.10	14.25
29/05/2017 00:22		51	0.784	0.10	15.13
29/05/2017 01:22		47	0.696	0.11	14.32
29/05/2017 02:22		46	0.831	0.55	16.52
29/05/2017 03:22		37	0.820	0.08	20.25
29/05/2017 04:22		38	0.734	0.95	20.04
29/05/2017 05:22		36	0.519	0.16	22.60
29/05/2017 06:22		47	0.507	0.34	16.88
29/05/2017 07:22		39	0.499	1.30	20.26
29/05/2017 08:22		41	0.281	1.52	15.07
29/05/2017 09:22		39	0.225	1.46	13.94
29/05/2017 10:22		34	0.377	2.48	18.94
29/05/2017 11:22		39	0.262	0.90	11.72
29/05/2017 12:22		44	0.223	0.93	9.62
29/05/2017 13:25		49	0.257	1.03	7.45
29/05/2017 14:37		44	0.335	1.75	12.87
29/05/2017 16:50		58	0.307	0.41	9.02
29/05/2017 17:50		61	0.303	0.22	7.46

29/05/2017 18:50		58	0.324	0.37	10.32
29/05/2017 19:50	0.03	55	0.344	1.07	13.10
29/05/2017 20:50	0.03	56	0.378	0.69	13.81
29/05/2017 21:50	0.04	47	0.408	0.85	20.25
29/05/2017 22:50	0.04	38	0.367	0.44	18.00
29/05/2017 23:50	4.13	34	0.407	0.18	20.42
30/05/2017 00:50	0.03	29	0.410	0.14	23.12
30/05/2017 01:50	0.04	17	0.484	5.29	39.37
30/05/2017 02:50	0.05	8	0.389	1.01	37.30
30/05/2017 03:50	0.04	21	0.323	1.24	17.45
30/05/2017 04:50	0.05	14	0.334	0.66	25.02
30/05/2017 05:50	0.05	21	0.313	1.09	25.28
30/05/2017 06:50	0.37	17	0.358	3.98	26.62
30/05/2017 07:50		11	0.469	13.61	35.26
30/05/2017 08:50	0.19	23	0.393	3.09	24.71
30/05/2017 09:50	0.46	36	0.394	2.24	17.80
30/05/2017 10:50	0.47	34	0.427	3.36	23.04
30/05/2017 11:50	0.48	41	0.474	4.86	20.13
30/05/2017 12:50	0.62	54	0.483	3.34	16.91
30/05/2017 13:47	0.68	66	0.406	2.27	14.06
30/05/2017 14:47	0.65	86	0.301	0.95	7.37
30/05/2017 15:47	0.44	98	0.295	0.83	8.87
30/05/2017 16:47	0.53	86	0.326	0.79	13.26
30/05/2017 17:47	0.49	87	0.331	0.41	10.88
30/05/2017 18:47	0.30	80	0.362	0.21	11.56
30/05/2017 19:47	0.09	73	0.425	0.38	17.54
30/05/2017 20:47	0.04	70	0.440	0.22	14.64
30/05/2017 21:47	0.06	57	0.511	0.32	19.15
30/05/2017 22:47		48	0.574	0.23	17.58
30/05/2017 23:47		39	0.554	0.29	18.45
31/05/2017 00:47	0.07	30	0.563	0.49	19.97
31/05/2017 01:47	0.09	21	0.574	0.41	20.67
31/05/2017 02:47	0.08	17	0.550	0.73	20.93
31/05/2017 03:47	0.10	1	0.596	10.62	44.81
31/05/2017 04:47	0.09	1	0.665	25.60	46.45
31/05/2017 05:47	0.28	2	0.656	24.66	42.85
31/05/2017 06:47	0.29	5	0.761	27.65	48.40
31/05/2017 07:47		20	0.741	10.78	39.56
31/05/2017 08:47		36	0.712	7.24	35.36
31/05/2017 09:47	1.37	53	0.727	5.48	33.83
10/06/2017 09:16	0.76	34	0.446	4.27	13.40
10/06/2017 10:01	0.91	35	0.437	3.25	13.71
10/06/2017 10:46	0.91	46	0.323	3.91	15.16
10/06/2017 11:31	1.03	40	0.259	2.83	11.21
10/06/2017 12:16		52	0.289	2.18	8.97

10/06/2017 13:01		51	0.392	2.16	10.10
10/06/2017 13:46		57	0.424	2.38	11.39
10/06/2017 14:31	0.81	61	0.402	2.34	12.08
10/06/2017 15:16	0.70	67	0.285	1.41	9.53
10/06/2017 15:48	0.70	72	0.294	2.68	12.39
10/06/2017 16:28		72	0.224	1.67	10.56
10/06/2017 17:09		76	0.227	0.78	9.22
10/06/2017 19:08	0.33	56	0.253	2.65	21.39
10/06/2017 21:08	0.15	35	0.232	5.31	22.86
10/06/2017 23:07	0.03	26	0.421	3.08	23.30
11/06/2017 01:07	0.13	7	0.403	21.86	56.96
11/06/2017 03:07	0.19	1	0.580	47.73	64.59
11/06/2017 05:06		1	0.620	99.96	61.24
11/06/2017 07:06		3	0.565	66.99	43.97
11/06/2017 09:05	0.78	11	0.570	31.70	43.20
11/06/2017 09:50	1.27	19	0.569	19.09	39.15
11/06/2017 10:35	1.14	33	0.439	8.29	24.00
11/06/2017 11:20	1.06	34	0.377	9.60	29.13
11/06/2017 12:05	1.06	52	0.349	3.60	18.02
11/06/2017 12:50	0.97	67	0.294	3.09	14.16
11/06/2017 13:35	0.68	88	0.250	1.93	10.68
11/06/2017 14:20	0.70	91	0.326	2.11	12.61
11/06/2017 15:05	0.70	99	0.362	1.11	8.10
11/06/2017 15:50	0.51	110	0.401	0.75	7.35
11/06/2017 16:35	0.34	116	0.499	1.10	15.41
11/06/2017 17:20	0.28	115	0.604	1.93	24.98
11/06/2017 18:05	0.28	117	0.618	1.31	18.64
11/06/2017 19:35	0.10	90	0.658	6.12	27.40
11/06/2017 21:04	0.04	46	0.796	23.84	77.41
11/06/2017 22:34	0.04	33	0.426	9.81	43.07
12/06/2017 00:04	0.06	4	0.424	29.68	75.62
12/06/2017 01:33	0.05	5	0.552	15.19	71.39
12/06/2017 03:03	0.04	4	0.466	25.46	69.21
12/06/2017 04:32	0.02	13	0.586	7.17	41.40
12/06/2017 06:02	0.05	15	1.299	7.04	39.75
12/06/2017 07:31	0.58	26	1.190	11.15	40.20
12/06/2017 09:01	0.62	30	1.032	7.29	36.29
12/06/2017 09:46	0.96	39	0.967	8.65	29.57
12/06/2017 10:31	1.04	50	0.840	4.25	23.84
12/06/2017 11:16		53	0.793	3.42	24.31
12/06/2017 12:04		63	0.712	2.31	16.83
12/06/2017 13:42		65	0.794	3.22	18.43
12/06/2017 14:27		67	0.782	2.97	18.83
12/06/2017 15:48		80	0.768	1.21	14.21
12/06/2017 16:33	0.87	82	0.691	0.76	13.78

12/06/2017 17:19	0.41	82	0.667	0.42	13.36
12/06/2017 18:04	0.39	72	0.727	0.47	18.39
12/06/2017 19:34	0.21	67	0.640	0.11	17.71
12/06/2017 21:03	0.00	62	0.644	0.60	18.65
12/06/2017 22:33	0.00	58	0.574	0.70	15.86
13/06/2017 00:03	0.00	58	0.492	0.85	12.58
13/06/2017 01:32	0.00	50	0.457	2.72	21.00
13/06/2017 03:02	0.01	55	0.387	0.63	15.99
13/06/2017 04:31	0.00	41	0.448	0.85	22.00
13/06/2017 06:01	0.04	24	0.522	2.92	38.80
13/06/2017 07:30		29	0.621	2.66	33.95
13/06/2017 09:00	0.06	28	0.739	1.78	30.00
13/06/2017 09:45	0.14	38	0.629	5.08	27.05
13/06/2017 11:23	0.68	35	0.864	4.81	29.18
13/06/2017 12:06	0.40	49	0.596	2.92	23.40
13/06/2017 12:51	0.40	63	0.502	2.71	15.78
13/06/2017 13:36	0.53	77	0.432	1.21	9.84
13/06/2017 14:21	0.62	82	0.391	1.09	9.85
13/06/2017 15:06	0.38	84	0.415	0.89	9.43
13/06/2017 15:51	0.38	87	0.360	0.44	6.56
13/06/2017 16:36	0.53	87	0.340	0.48	7.87
14/06/2017 12:29	1.51	137	0.395	0.52	9.87
14/06/2017 13:13	1.20	107	0.234	0.42	6.17
14/06/2017 13:58	1.20	93	0.179	0.46	5.97
14/06/2017 14:43	1.28	92	0.154	0.33	5.08
14/06/2017 15:28	1.84	88	0.139	0.35	5.50
14/06/2017 16:13		78	0.167	0.58	7.83
14/06/2017 16:58		77	0.182	0.33	8.59
14/06/2017 17:43	1.52	81	0.245	0.38	11.14
14/06/2017 18:28		73	0.271	0.31	17.15
14/06/2017 19:58		68	0.268	0.11	14.67
14/06/2017 21:28		70	0.260	0.10	14.62
14/06/2017 22:57	0.02	63	0.402	0.12	17.17
15/06/2017 00:27	0.03	52	0.400	0.10	15.41
15/06/2017 01:56	0.10	7	0.659	1.76	50.51
15/06/2017 03:26	7.11	4	0.803	33.70	51.79
15/06/2017 04:56	0.32	3	0.627	55.14	46.81
15/06/2017 06:25	2.70	3	0.620	51.52	39.93
15/06/2017 07:55	1.80	21	0.429	15.34	40.96
15/06/2017 09:24	2.92	29	0.450	9.50	40.83
15/06/2017 10:09		41	0.557	9.00	43.33
15/06/2017 10:54		57	0.529	4.86	35.53
15/06/2017 11:39		71	0.566	4.25	35.72
15/06/2017 12:23	2.29	83	0.422	2.79	27.27
15/06/2017 13:08	2.29	130	0.334	0.56	11.01

15/06/2017 13:53	0.00	119	0.268	0.45	7.86
15/06/2017 14:38		121	0.218	0.39	8.13
15/06/2017 15:23		122	0.195	0.40	8.06
15/06/2017 16:08		102	0.151	0.35	8.06
15/06/2017 16:53		96	0.179	0.36	9.01
15/06/2017 17:38		104	0.232	0.37	11.04
15/06/2017 18:23		118	0.320	0.23	13.77
15/06/2017 19:53		88	0.350	0.22	16.87
15/06/2017 21:22		77	0.446	0.25	20.89
15/06/2017 22:52	0.00	86	0.560	0.18	18.07
16/06/2017 00:22	0.02	82	0.679	0.21	18.04
16/06/2017 01:51	7.21	67	0.771	0.13	21.24
16/06/2017 03:21	0.00	55	0.931	0.12	22.90
16/06/2017 04:50	0.02	52	0.779	0.43	19.69
16/06/2017 06:20	1.35	32	0.843	1.95	34.41
16/06/2017 07:49	2.88	11	0.716	42.07	66.62
16/06/2017 09:19	2.96	62	0.711	4.61	40.29
17/06/2017 17:42	0.95	133	0.526	0.15	12.05
17/06/2017 18:46	0.66	126	0.607	0.12	14.30
17/06/2017 19:46	0.22	117	0.626	0.25	17.94
17/06/2017 20:46	0.04	114	0.837	0.34	18.94
17/06/2017 21:46		110	0.944	0.11	18.32
17/06/2017 22:46	0.03	107	0.574	0.38	10.13
17/06/2017 23:46	0.02	94	0.570	0.25	11.52
18/06/2017 00:46	0.07	74	0.572	0.11	18.21
18/06/2017 01:46	0.09	55	0.705	0.29	24.75
18/06/2017 02:46	0.03	56	0.558	0.13	16.66
18/06/2017 03:46	0.03	53	0.486	0.11	13.20
18/06/2017 04:46	0.03	37	0.523	0.16	21.90
18/06/2017 05:46	0.27	43	0.550	0.31	18.15
18/06/2017 06:46	0.38	48	0.544	0.69	16.44
18/06/2017 07:46	0.88	55	0.588	1.18	15.84
18/06/2017 08:46	0.79	74	0.563	0.96	13.12
18/06/2017 11:16	1.41	128	0.730	0.47	10.43
18/06/2017 12:16	1.76	149	0.912	0.33	9.37
18/06/2017 13:16		154	0.864	0.31	8.87
18/06/2017 14:16		151	0.765	0.26	8.68
18/06/2017 15:16	0.16	135	0.559	0.11	10.63
18/06/2017 16:16	0.06	132	0.787	0.22	11.26
18/06/2017 17:16	1.30	104	0.833	0.53	14.38
18/06/2017 18:16	0.81	56	1.020	0.31	30.11
18/06/2017 19:16	0.14	77	0.869	1.00	26.26
18/06/2017 20:16	0.03	74	0.707	0.28	21.20
18/06/2017 21:16	0.03	64	0.708	0.44	23.42
18/06/2017 22:16	0.02	76	0.526	0.46	13.70

18/06/2017 23:16	0.03	68	0.507	0.44	14.78
19/06/2017 00:16	0.02	65	0.530	0.18	12.96
19/06/2017 01:16	0.00	61	0.497	0.79	13.66
19/06/2017 02:16	0.03	52	0.437	0.24	16.51
19/06/2017 03:16	0.02	43	0.430	0.18	20.20
19/06/2017 04:16	0.03	45	0.390	0.15	17.09
19/06/2017 05:16	0.14	45	0.353	0.54	14.37
19/06/2017 06:16		40	0.551	1.25	17.71
19/06/2017 07:16	0.74	45	0.423	1.88	14.58
19/06/2017 08:16	0.86	49	0.400	2.57	15.28
19/06/2017 09:16	0.76	54	0.325	2.13	13.48
19/06/2017 10:16	1.13	68	0.325	1.61	10.04
19/06/2017 11:16	0.87	81	0.369	1.19	10.43
19/06/2017 12:16	1.19	97	0.358	0.74	8.16
19/06/2017 13:16	1.17	105	0.302	0.47	7.51
19/06/2017 14:16		121	0.270	0.31	6.76
19/06/2017 15:16	1.83	122	0.222	0.35	7.24
19/06/2017 16:16	1.04	115	0.297	0.38	7.96
19/06/2017 17:16		107	0.374	0.36	12.77
19/06/2017 18:17	1.30	82	0.184	0.47	10.08
19/06/2017 19:16	0.67	104	0.331	0.21	10.52
19/06/2017 20:16	0.31	77	0.684	0.21	27.00
19/06/2017 21:16	6.96	83	0.590	0.28	20.65
19/06/2017 22:17	0.10	59	0.726	0.18	34.49
19/06/2017 23:16	0.02	69	0.683	0.15	13.06
20/06/2017 00:17		67	0.650	0.22	13.37
20/06/2017 01:17		57	0.526	0.22	11.97
20/06/2017 02:16	0.02	45	0.421	0.17	21.87
20/06/2017 03:17	0.00	55	0.360	0.10	13.06
20/06/2017 04:17	0.00	51	0.444	0.27	12.00
20/06/2017 05:17	0.00	48	0.462	0.21	15.34
20/06/2017 06:16	0.08	52	0.383	0.38	12.51
20/06/2017 07:17	0.28	54	0.428	1.38	14.27
20/06/2017 08:17	0.60	60	0.367	1.61	13.44
20/06/2017 09:17	0.63	64	0.417	2.12	16.07
20/06/2017 10:17	0.75	75	0.432	1.51	13.53
20/06/2017 11:17	0.63	88	0.396	0.89	9.38
20/06/2017 12:49	0.78	103	0.362	0.56	6.57
20/06/2017 13:49	1.22	115	0.393	0.61	8.24
20/06/2017 14:49	1.40	109	0.381	0.43	7.46
20/06/2017 15:49	1.07	110	0.368	0.41	8.25
20/06/2017 16:49		111	0.350	0.33	7.01
20/06/2017 17:49	0.99	108	0.385	0.27	9.41
20/06/2017 18:49	0.99	103	0.410	0.19	11.27
20/06/2017 19:49	0.13	105	0.539	0.26	13.54

20/06/2017 20:49	0.04	100	0.730	0.11	15.77
20/06/2017 21:49	0.08	80	0.765	0.35	28.32
20/06/2017 22:49	0.03	73	0.830	0.31	26.08
20/06/2017 23:49	0.02	62	0.738	1.01	18.67
21/06/2017 00:49	0.00	59	0.599	0.35	16.07
21/06/2017 01:49	0.00	54	0.608	0.10	14.94
21/06/2017 02:49	0.00	27	0.741	0.31	28.11
21/06/2017 03:49	0.00	42	0.526	0.12	15.63
21/06/2017 04:49	0.03	37	0.499	0.15	17.92
21/06/2017 05:49	0.30	51	0.515	0.92	14.02
21/06/2017 06:49	0.37	53	0.579	0.69	15.62
21/06/2017 07:49	0.39	56	0.677	1.49	18.65
21/06/2017 08:49		60	0.737	2.07	19.46
21/06/2017 09:49		74	0.723	1.64	16.26
21/06/2017 10:49	0.88	90	0.610	1.14	12.05
21/06/2017 11:49	1.14	105	0.645	0.65	10.88
21/06/2017 12:52	0.76	111	0.738	0.65	14.18
21/06/2017 13:52	0.59	116	0.645	0.47	10.35
21/06/2017 14:52	0.84	122	0.577	0.31	9.55
21/06/2017 15:52	0.39	122	0.574	0.30	9.02
21/06/2017 16:52	0.40	123	0.691	0.21	9.72
21/06/2017 17:52	0.36	122	0.631	0.21	15.44
21/06/2017 18:52	0.04	104	0.581	0.66	14.13
21/06/2017 19:52	0.09	59	0.763	0.15	31.26
21/06/2017 20:52	0.03	82	0.460	0.76	9.05
21/06/2017 21:52	0.02	75	0.280	0.52	6.96
21/06/2017 22:52	0.00	72	0.303	0.26	8.58
21/06/2017 23:52	0.03	69	0.275	0.33	6.93
22/06/2017 00:52	0.00	64	0.279	0.12	9.09
22/06/2017 01:52		60	0.275	0.22	8.98
22/06/2017 02:52	0.00	54	0.296	0.12	9.99
22/06/2017 03:52	0.02	54	0.313	0.17	8.88
22/06/2017 04:52	0.02	47	0.318	0.72	11.68
22/06/2017 05:52	0.05	31	0.349	0.50	21.88
22/06/2017 06:52	0.11	34	0.342	1.60	23.94
22/06/2017 07:52	0.24	40	0.391	2.10	24.58
22/06/2017 08:52	0.26	42	0.404	0.93	23.82
22/06/2017 09:52	0.28	48	0.442	0.95	19.78
22/06/2017 10:50	0.29	52	0.401	0.74	17.01
22/06/2017 11:50	0.17	65	0.431	0.52	10.61
22/06/2017 12:50	0.23	59	0.496	0.38	13.39
22/06/2017 13:27	0.23	59	0.466	0.60	12.54
22/06/2017 14:27	0.41	60	0.530	0.47	12.70
22/06/2017 15:27	0.21	57	0.543	0.38	12.80
22/06/2017 16:44	0.41	40	0.714	0.31	20.77

22/06/2017 17:44		39	0.965	0.32	26.32
22/06/2017 18:44		48	0.892	0.15	20.33
22/06/2017 19:44	0.11	44	0.965	0.12	19.31
22/06/2017 20:44	0.10	43	1.108	0.14	18.74
22/06/2017 21:44	0.07	40	1.191	0.14	16.56
22/06/2017 22:44	0.04	53	0.716	0.13	11.19
22/06/2017 23:44	0.03	54	0.589	0.11	9.43
23/06/2017 00:44	0.02	48	0.566	0.12	10.17
23/06/2017 01:44	0.03	56	0.512	0.12	5.16
23/06/2017 02:44	0.03	56	0.422	0.13	4.31
23/06/2017 03:44	0.01	58	0.343	0.10	4.07
23/06/2017 04:44	0.00	57	0.338	0.10	3.82
23/06/2017 05:44	0.02	55	0.307	0.10	5.71
23/06/2017 06:44	0.04	47	0.383	0.13	11.26
23/06/2017 07:44	0.05	41	0.446	0.19	16.59
23/06/2017 08:44	0.17	43	0.403	0.98	13.25
23/06/2017 09:44	0.25	43	0.373	1.06	11.30
23/06/2017 10:44		47	0.384	0.62	7.06
23/06/2017 11:44	0.28	43	0.476	1.08	11.51
23/06/2017 12:44	7.50	43	0.583	1.19	11.53
23/06/2017 13:44	7.29	37	0.649	0.96	15.50
23/06/2017 14:57	0.23	34	0.494	0.74	12.36

Table S3: Chemical data plotted in Fig. 4.

Hour of Day (h)	Isoprene (ppb)	O_3 (ppb)	OH (cm^{-3})	NO (ppb)	NO_3 (ppt)	(4-OH, 3-ONO_2)-IHN (ppt)	E-(1-ONO_2, 4-CO)-ICN (ppt)	Propanone nitrate (ppt)
0	0.33	47	4.72E+05	3.1	10.7	3.2	7.3	47
1	0.47	40	3.82E+05	4.9	10.5	2.4	6.2	45
2	0.47	34	3.58E+05	4.8	8.3	2.1	4.8	43
3	0.62	28	3.65E+05	9.8	5.8	1.7	4.4	45
4	0.70	28	3.92E+05	8.4	4.8	1.5	3.7	51
5	0.39	22	5.93E+05	15.3	1.9	1.5	3.6	36
6	0.72	21	1.16E+06	11.7	0.3	1.4	3.4	36
7	0.42	23	2.65E+06	12.3	0.2	1.7	3.3	35
8	0.88	27	4.05E+06	12.5	0.2	3.0	2.4	39
9	0.93	36	5.82E+06	6.7	0.3	4.7	1.9	45
10	0.88	44	7.24E+06	5.0	0.5	6.7	1.2	45
11	1.03	59	8.34E+06	3.7	0.8	9.4	1.5	55
12	1.17	73	8.90E+06	2.9	1.2	10.2	1.5	47
13	1.15	89	8.91E+06	1.5	1.7	10.1	1.5	44
14	0.83	91	8.55E+06	1.2	2.0	8.5	1.6	44
15	1.07	95	7.78E+06	0.8	2.2	8.3	2.4	37
16	0.89	102	6.04E+06	0.9	2.3	7.5	1.4	43
17	0.88	98	3.92E+06	0.7	2.1	7.2	1.6	39
18	1.07	94	1.83E+06	0.5	2.2	7.9	1.7	31
19	0.52	87	1.04E+06	0.7	3.6	6.3	2.3	32
20	0.19	76	1.14E+06	0.7	8.2	5.9	3.6	35
21	0.65	69	1.09E+06	1.7	12.2	5.2	8.1	40
22	0.09	63	8.81E+05	1.0	13.1	3.5	7.9	43
23	0.16	54	5.94E+05	1.5	12.1	3.5	8.2	48
24	0.33	47	4.72E+05	3.1	10.7	3.2	7.3	47

Table S4: Mixing layer height data plotted in Fig. 4.

Hour of Day (h)	Mixed Layer Height (m*10)
0.125	30.7
0.375	28.7
0.625	28.6
0.875	29.0
1.125	29.0
1.375	28.2
1.625	27.9
1.875	28.0
2.125	28.3
2.375	28.3
2.625	28.3
2.875	28.3
3.125	28.1
3.375	28.3
3.625	28.8
3.875	28.7
4.125	28.6
4.375	28.9
4.625	29.1
4.875	29.0
5.125	29.8
5.375	30.9
5.625	31.4
5.875	31.9
6.125	32.7
6.373	33.3
6.625	33.9
6.875	35.0
7.125	37.1
7.375	39.3
7.625	40.6
7.875	42.9
8.125	45.7
8.375	48.1
8.625	50.8
8.875	53.8
9.125	56.8
9.375	59.4
9.625	62.9
9.875	66.9
10.125	69.9
10.375	73.1

10.625	76.6
10.875	80.5
11.125	84.7
11.375	87.5
11.625	89.5
11.877	91.8
12.125	94.1
12.375	96.2
12.625	98.4
12.875	100.8
13.125	102.5
13.375	103.4
13.625	103.9
13.875	105.2
14.125	107.0
14.375	106.8
14.625	105.4
14.875	104.5
15.125	104.9
15.375	105.3
15.625	105.3
15.875	105.9
16.125	106.3
16.375	104.6
16.625	102.6
16.875	100.6
17.125	97.1
17.375	94.1
17.625	93.0
17.875	92.8
18.125	91.6
18.375	90.1
18.625	87.7
18.875	83.9
19.125	79.4
19.375	75.3
19.625	70.2
19.875	64.8
20.125	61.2
20.375	57.7
20.625	54.3
20.875	49.9
21.125	45.0
21.375	42.1
21.625	40.4

21.875	39.1
22.125	38.7
22.375	38.0
22.625	36.7
22.875	36.0
23.125	35.8
23.375	35.3
23.625	34.3
23.750	33.7

Table S5: Data plotted in Fig. 5.

Hour of Day (h)	Modelled (4-OH, 3-ONO_2)-IHN (ppt)	Modelled (1-OH, 2-ONO_2)-IHN (ppt)	Observed mean (4-OH, 3-ONO_2)-IHN (ppt)	Observed mean (1-OH, 2 -ONO_2)-IHN (ppt)
0	0.9	0.7	3.2	16.5
1	1.3	3.9	2.4	6.6
2	1.5	7.4	2.1	11.0
3	1.4	5.0	1.7	7.6
4	1.4	2.9	1.5	
5	1.5	2.0	1.5	6.9
6	4.3	8.7	1.4	5.3
7	3.2	5.2	1.7	12.3
8	4.3	8.5	3.0	7.8
9	9.0	17.2	4.7	14.7
10	12.7	28.3	6.7	30.3
11	16.6	38.0	9.4	26.5
12	18.6	48.2	10.2	46.4
13	19.2	44.4	10.1	35.8
14	17.9	38.0	8.5	28.4
15	16.4	37.7	8.3	38.2
16	13.2	32.7	7.5	30.0
17	9.4	24.7	7.2	29.2
18	5.6	12.3	7.9	48.9
19	2.5	3.1	6.3	28.0
20	2.1	0.4	5.9	28.4
21	1.2	0.2	5.2	22.4
22	0.5	0.2	3.5	
23	0.7	0.2	3.5	20.3
24	0.9	0.7	3.2	16.5

Table S6: Observed and Modelled data plotted in Fig. 6.

	(1-OH, 2-ONO_2)-IHN / (4-OH, 3-ONO_2)-IHN ratio	
Hour of Day (h)	**Observed**	**Modelled**
0	3.02	2.36
1	1.45	2.29
2	4.38	2.23
3	3.25	2.21
4		2.11
5	2.03	1.98
6	2.19	1.96
7	3.77	1.97
8	2.15	2.00
9	4.94	2.05
10	5.82	2.14
11	3.03	2.26
12	2.85	2.47
13	3.13	2.78
14	2.95	2.63
15	3.29	2.57
16	3.18	2.51
17	3.81	2.53
18	3.93	2.57
19	3.09	2.57
20	3.47	2.57
21	3.29	2.51
22		2.51
23	4.14	2.45
24	3.02	2.36

Table S7: Observed data plotted in Figs. 8 and 9.

Hour of Day (h)	Observed ICN Total (ppt)	Observed Propanone Nitrate (ppt)	Modelled ICN Total (ppt)	Modelled Propanone Nitrate (ppt)	Modelled (1-OH, 4-ONO_2)-IHN (ppt)	Modelled (4-OH, 1-ONO_2)-IHN (ppt)
0	18.9	47	105.1	14.2	0.06	1.30
1	15.1	45	108.6	16.2	0.08	1.36
2	13.1	43	93.5	15.2	0.11	0.93
3	11.3	45	88.8	13.3	0.18	0.75
4	7.7	51	87.6	12.0	0.22	0.62
5	7.7	36	62.2	10.5	0.29	0.46
6	7.1	36	25.2	9.9	0.83	0.77
7	6.1	35	3.3	2.1	0.49	0.46
8	4.4	39	1.5	0.3	0.48	0.48
9	2.9	45	3.1	0.8	0.61	0.65
10	2.0	45	5.2	1.7	0.68	0.71
11	2.5	55	9.3	3.6	0.76	0.76
12	2.5	47	14.3	6.2	0.76	0.73
13	2.4	44	19.6	9.1	0.74	0.69
14	1.7	44	22.5	10.7	0.69	0.62
15	2.9	37	27.4	12.9	0.62	0.55
16	2.0	43	30.3	14.5	0.50	0.44
17	2.7	39	28.7	11.0	0.37	0.33
18	2.6	31	31.1	6.9	0.24	0.23
19	5.1	32	30.4	4.5	0.11	0.14
20	11.0	35	48.9	5.9	0.09	0.41
21	22.8	40	69.4	7.0	0.05	0.76
22	21.0	43	52.6	5.5	0.02	0.78
23	18.8	48	82.2	9.9	0.04	0.89
24	18.9	47	105.1	14.2	0.06	1.30